

**Responses to Reviewer #1**

General comments. The authors have conducted an interesting study to investigate the influence of the Pacific-North America teleconnection (PNA) on U.S. winter aerosol concentrations using both statistical methods and a chemistry model. This work contributes to our understanding of climate patterns responsible for PM<sub>2.5</sub> variability and is appropriate for ACP. But some of the conclusions are relatively weak. So I recommend that the paper can be published only after a major revision as describe below.

1. Even though PNA is the leading circulation pattern in the North Pacific and North America in the troposphere during the wintertime, the authors should also show it is important for the aerosol variability. What is the fraction of temporal variability that can be explained by PNA? To show this, the authors can calculate the correlation coefficient between PNA and aerosol concentrations in each site.

**Response:**

Following the Reviewer's suggestion, we have calculated the correlation coefficient between PNAI and EPA-AQS surface aerosol concentrations at each site for each aerosol species (PM<sub>2.5</sub>, SO<sub>4</sub><sup>2-</sup>, NO<sub>3</sub><sup>-</sup>, NH<sub>4</sub><sup>+</sup>, OC, or BC) (auxiliary Fig. S2, see below). At most sites, positive (negative) correlation coefficients in Fig. S2 correspond to the increases (decreases) in aerosol concentration in PNA+ months relative to PNA- months shown in Fig. 3 of our manuscript. Large positive correlation coefficients are found over California, the contiguous Salt Lake, and over and near the eastern Midwest (Fig. S2). The fraction of temporal variability explained by PNA (FTVEP) can be quantified approximately by the square of correlation coefficient (<http://mathbits.com/MathBits/TISection/Statistics2/correlation.htm>) (auxiliary Fig. S3, see below). For all aerosol species, FTVEP are about 5–15% at most sites. For PM<sub>2.5</sub>, SO<sub>4</sub><sup>2-</sup>, NO<sub>3</sub><sup>-</sup> and NH<sub>4</sub><sup>+</sup> aerosols, high FTVEP values are found over and near the eastern Midwest, where the PNA teleconnection explains up to 50%, 40%, 50%, and 40% of temporal variances of surface concentrations of these aerosol species, respectively. We have added these descriptions to the end of Sect. 3.1.

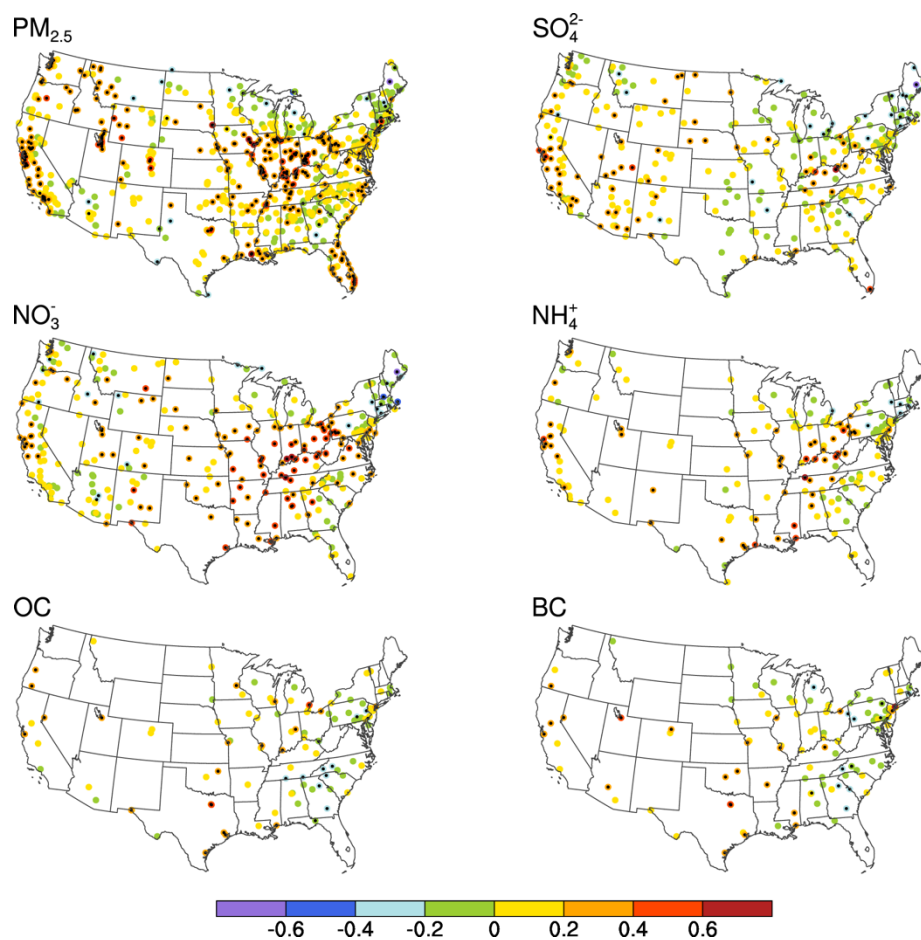


**Fig. S2.** Correlation coefficient between PNAI and EPA-AQS surface aerosol concentrations at each site for each aerosol species ( $PM_{2.5}$ ,  $SO_4^{2-}$ ,  $NO_3^-$ ,  $NH_4^+$ , BC, or OC). The measurements are the same as those used in Fig. 3. The sites with black dots are those that have passed the two-tail t-test with 90% confidence level.

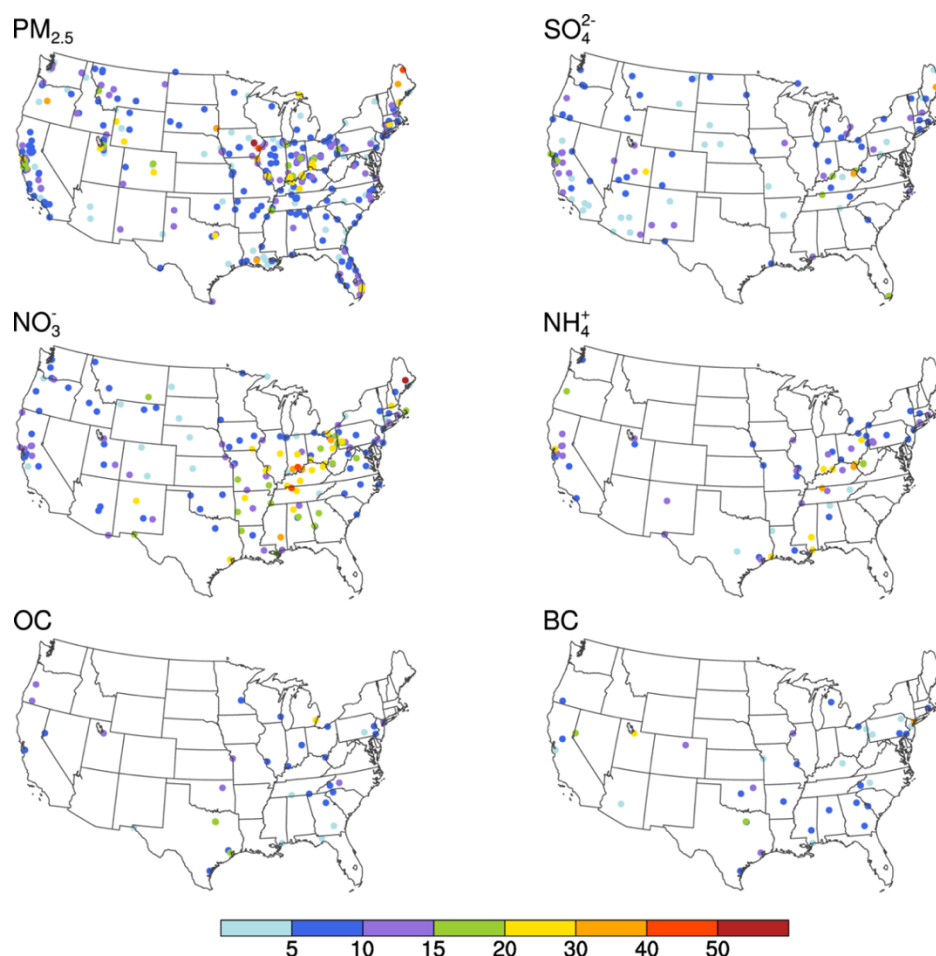


**Fig. S3.** The fraction (%) of temporal variability of EPA-AQS surface aerosol concentrations explained by PNA at each site for each aerosol species ( $PM_{2.5}$ ,  $SO_4^{2-}$ ,  $NO_3^-$ ,  $NH_4^+$ , BC, or OC). The measurements are the same as those used in Fig. 3. The sites shown here are those in Fig. S2 with the correlation coefficients passed the two-tail t-test with 90% confidence level.

2. Have the authors detrended the  $PM_{2.5}$  observations when they do a composite analysis between positive and negative PNA? The aerosol concentrations have shown a significant decreasing trend from 1999 to present in the United States. Won't this affect the conclusion?

**Response:**

This is a good point. We have redone the composite analyses for observed aerosol concentrations by detrending the observations from the EPA-AQS. The revised differences in aerosol concentrations between positive and negative PNA are similar to the results in our previous version of manuscript (those obtained without detrending); the horizontal distributions are about the same but the magnitudes of the differences in aerosol concentrations are slightly smaller. We have updated Figs. 3, 4 and Table 1, and have changed the descriptions in the text accordingly.

3. It is hasty, with just some statistical analysis, to conclude that PBL should be the most important meteorological factor that influences the concentrations of PM<sub>2.5</sub>. Maybe the authors should do a sensitivity test by fixing the PBL height in the chemistry model. If the monthly PM<sub>2.5</sub> variability is largely reduced, the major conclusion of this study should be correct.

Response:

We conclude that PBL is the most important meteorological factor that influences the concentrations of PM<sub>2.5</sub> on the basis of the magnitude of the pattern correlation coefficients (PCC). The same statistical approach was also used in previous studies (Levy et al., 2008; Jeong and Park, 2013; Allen et al., 2015). Levy et al. (2008), by simulations with the NOAA/GFDL climate model, reported that the regional pattern of changes in surface temperature did not correspond well to the regional pattern of radiative forcings of short-lived species because of the low global PCC of  $-0.172$  under the IPCC A1B scenario. Jeong and Park (2013) used the PCC values to show the impacts of variabilities in temperature, precipitation, relative humidity, mixing depth, cloud fraction, and surface wind speed on regional patterns of concentrations of O<sub>3</sub>, (NH<sub>4</sub>)<sub>2</sub>SO<sub>4</sub>, and NH<sub>4</sub>NO<sub>3</sub> in East Asia on the basis of the GEOS-Chem simulation. Allen et al. (2015) quantified the role of precipitation in the changes of aerosol burdens from the Atmospheric Chemistry and Climate Model Intercomparison Project (ACCMIP); they obtained global PCC values of  $-0.36$ ,  $-0.33$  and  $-0.30$  between precipitation and burdens of SO<sub>4</sub><sup>2-</sup>, BC, and OC, respectively.

The sensitivity test suggested by the Reviewer was carried out by Dawson et al. (2007). Dawson et al. (2007) reported, by fixing all meteorological parameters but perturbing PBLH in the Particulate Matter Comprehensive Air Quality Model with extensions (PMCAMx), that PM<sub>2.5</sub> concentrations over the Mideast in January decreased by about  $1 \mu\text{g m}^{-3}$  if PBLH decreased by 150 m. They concluded that the effect of mixing height on PM<sub>2.5</sub> concentrations is rather important, especially in polluted areas. However, such sensitivity experiment by changing one specific meteorological variable (for example, PBLH) ignored the covariance of other meteorological parameters (such as temperature and convection associated with PBLH), which could not give us realistic responses of aerosol concentrations to changes in meteorological conditions.

4. Is there a specific reason that the authors use a very old version of GEOS-Chem model? According to the info here (<http://acmg.seas.harvard.edu/geos/>), the current public release is v10-01. But the authors still use v8-2 that was released five years ago. Also their model is driven by GEOS4 for 1986-2006. Why not use updated meteorological fields? How does this model treat the Secondary Organic Aerosol (SOA) and what mechanism is used? In the wintertime, SOA might still be a very important component in the south US.

Response:

The GEOS-Chem Version 8-02-01 is used in our study, because we have evaluated this version's performance in simulating aerosol concentrations in



our previous studies (Zhu et al., 2012; Yang et al., 2015). This version has also been used by other recent studies on atmospheric chemistry (Jiang et al. 2015; Luo et al. 2015; Marlier et al. 2015).

Our simulation is driven by the GEOS-4 meteorological data, which are available for years 1986–2006. Although the relatively new MERRA meteorological fields can be used to drive the GEOS-Chem model for years 1979–2013, there is a problem of long-term inhomogeneity in MERRA reanalysis data for precipitation, humidity, and temperature in the lower troposphere due to the introduction of new observation types in different time (<http://gmao.gsfc.nasa.gov/pubs/docs/Chen480.pdf>), which would influence the decadal simulation in our study. This problem will be solved in MERRA-2 datasets (Molod et al. 2015), but unfortunately the MERRA-2 meteorological fields are currently not available.

Considering that the impacts of PNA on temperature, relative humidity, surface wind speed, and precipitation obtained from the GEOS-4 meteorological data for 1986–2006 (Fig. 7 in manuscript) are similar to those obtained from the NCEP Reanalysis and Global Precipitation Climatology Center (GPCC) data for years 1948–2010 (see Fig. D in our response to your last comment), we do not think that the use of the GEOS-4 data compromises the conclusions in our study.

Considering the large uncertainties in chemistry schemes of secondary organic aerosol (SOA), SOA in our simulation is assumed to be the 10% carbon yield of OC from biogenic terpenes (Park et al., 2003) and 2% carbon yield of OC from biogenic isoprene (van Donkelaar et al., 2007; Mu and Liao, 2014). This is now clarified in Sect. 2.2.

Observational studies have shown that SOA accounts for small fractions of OC and PM<sub>2.5</sub> in winter over the southeastern U.S. (Zheng et al. 2002; Ke et al. 2007; Zheng et al. 2007; Blanchard et al. 2008; Ding et al. 2008; Kleindienst et al., 2007, 2010; Weber, 2010). For example, Kleindienst et al. (2007) showed that SOA contributed about 0.5  $\mu\text{g C m}^{-3}$  (about 18%) to OC in January–February, 2003, by field study carried out at a research site in Research Triangle Park, North Carolina. Weber (2010) compiled SOA observations at 15 sites in the southeastern U.S. in 2007 and showed that SOA concentration averaged over sites was about 0.9  $\mu\text{g m}^{-3}$  (or about 10% of PM<sub>2.5</sub> mass) due to the low biogenic VOC emissions at low temperatures in winter.

Specific comments.

Abstract. Why do the authors just use observations over 1999–2003 when data is available from 1999 to 2013?

Response:

Thanks for pointing out this mistake. It has been changed to “1999–2013”.

Section 1. Maybe the author needs to give a literature review using more recent studies.

Response:

We have added about 10 recent studies (published in 2014 and 2015) in our Introduction section.

Section 2.1. Please specify the detrending method.

Response:

We have added the description on detrending method in Sect. 2.1: “Since the observed aerosol concentrations exhibited a significant decreasing trend from 1999 to present in the U.S. due to the reductions in emissions of aerosols and aerosol precursors (Alston et al. 2012, <http://www3.epa.gov/airtrends/aqtrends.html#comparison>), the long-term linear trend in concentrations is identified by the least-square fit and then removed from the observed concentrations for each site.”

Section 2.2. Please specify if SOA is included in the chemistry model.

Response:

We have added in Sect. 2.2 the description on SOA simulation: “Considering the large uncertainties in chemistry schemes of secondary organic aerosol (SOA), SOA in our simulation is assumed to be the 10% carbon yield of OC from terpenes and and 2% carbon yield of OC from biogenic isoprene (van Donkelaar et al. 2007; Mu and Liao 2014).”

Section 2.3. There are many other definitions of PNA. Can these different definitions affect the conclusion?

Response:

There are three commonly used definitions of PNAI: (1) PNAI defined by Leathers et al. (1991) ( $PNAI_{Leathers}$ ). This is the definition used in our manuscript. (2) PNAI defined by Wallace and Gutzler (1981) ( $PNAI_{Wallace}$ ) as:

$$PNAI_{wallace} = \frac{1}{4} [z^*(20^\circ N, 160^\circ W) - z^*(45^\circ N, 165^\circ W) + z^*(55^\circ N, 115^\circ W) - z^*(30^\circ N, 85^\circ W)]$$

, where \* denotes the normalized geopotential height at 500 hPa. (3) PNAI defined by NOAA Climate Prediction Center (CPC) ( $PNAI_{NOAA}$ , [http://www.cpc.ncep.noaa.gov/products/precip/CWlink/pna/month\\_pna\\_index\\_2.shtml](http://www.cpc.ncep.noaa.gov/products/precip/CWlink/pna/month_pna_index_2.shtml)). All these three definitions reflect the same atmospheric teleconnections over the region of North Pacific to North America region. The correlation coefficients between  $PNAI_{Leathers}$  and  $PNAI_{Wallace}$  (or between  $PNAI_{Leathers}$  and  $PNAI_{NOAA}$ ) is equal to or larger than 0.94, when we calculate PNAI for 1979–2013 by using the NCEP-2 reanalyzed meteorological data or PNAI for 1986–2006 by using the assimilated GEOS-4 data (see Fig. A below).

The different definitions of PNAI do not influence our conclusion. The differences in observed surface-layer aerosol concentrations between the PNA+ and PNA– months on the basis of  $PNAI_{Wallace}$  (Fig. B below) and  $PNAI_{NOAA}$  (Fig. C below) are similar to those on the basis of  $PNAI_{Leathers}$  (Fig. 3 in our manuscript). In Fig. B, the enhancement of  $PM_{2.5}$  reached 5–7  $\mu g m^{-3}$  (or 40–80%) in California, 3–5  $\mu g m^{-3}$  (40–80%) around the Salt Lake, 3–5  $\mu g m^{-3}$  (20–40%) over and near the eastern Midwest. Similar results are shown in Fig. C; the enhancement of  $PM_{2.5}$  reached 7–9  $\mu g m^{-3}$  (or 40–80%) in California, 5–7  $\mu g m^{-3}$  (40–80%) around the Salt Lake, 3–5  $\mu g m^{-3}$  (20–40%) over and near the eastern Midwest.

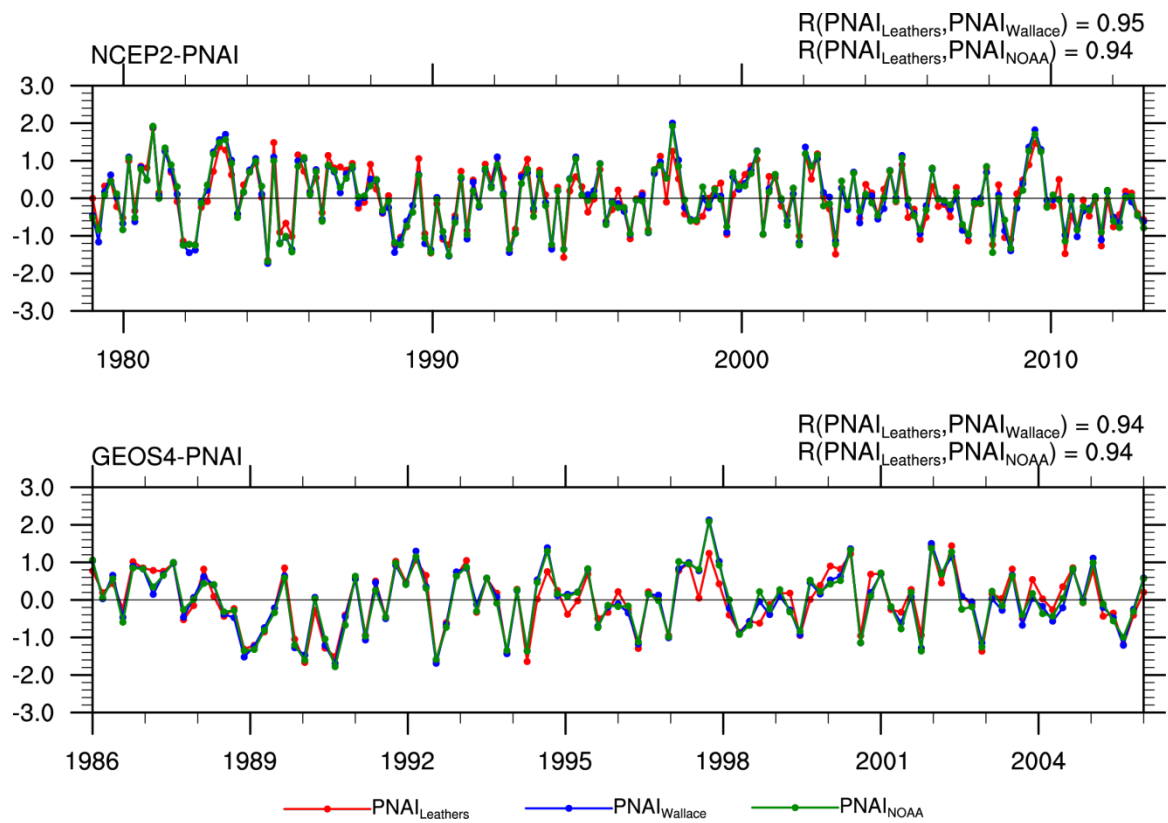


Fig. A. Top panel: Monthly PNAI in NDJFM for years of 1979–2013 calculated using the NCEP-2 data. Bottom panel: PNAI for 1986–2006 calculated using the assimilated GEOS-4 data. The correlation coefficients are marked on top right corner of each panel.

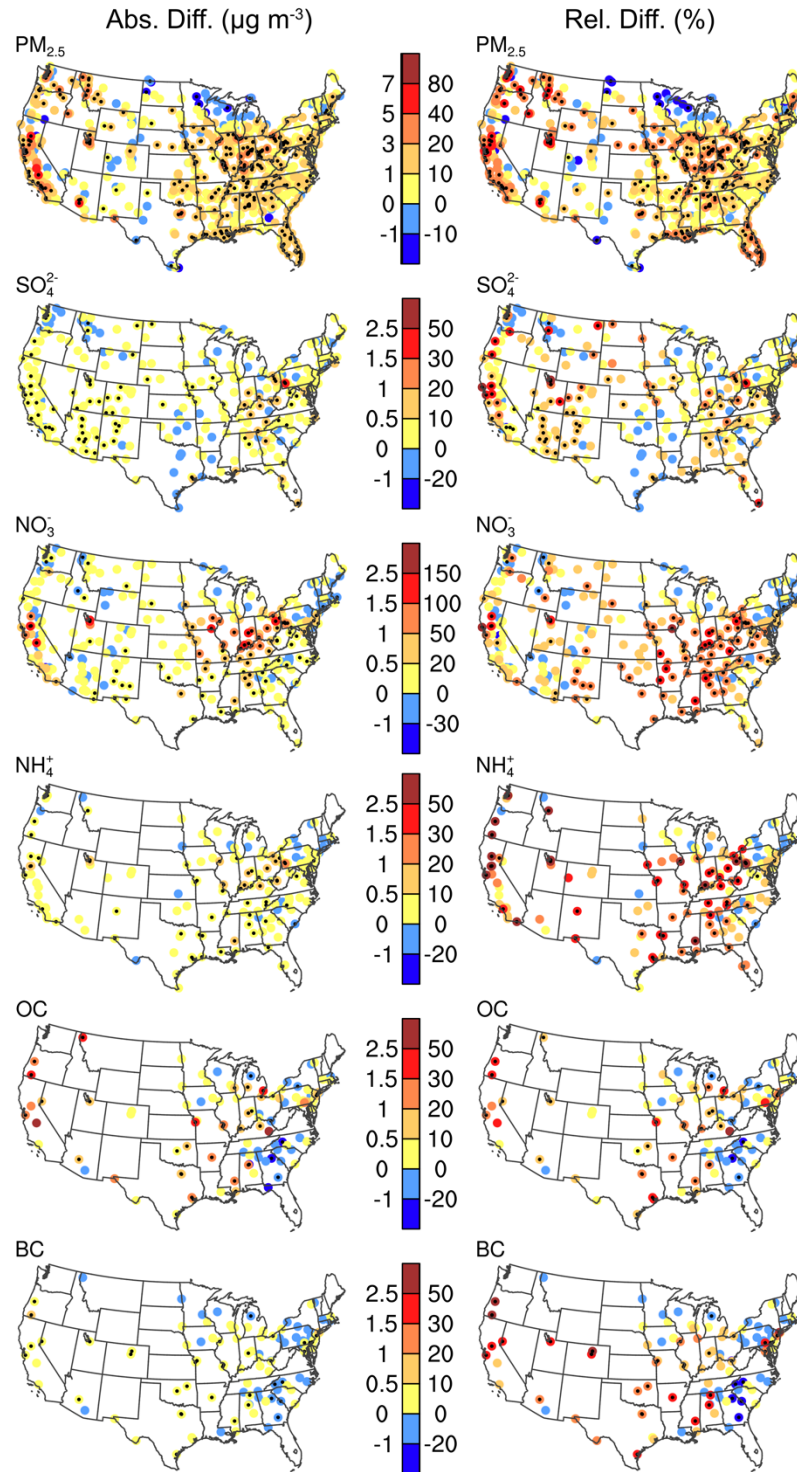


Fig. B. The same as Fig. 3 in the manuscript except that the differences in observed surface-layer aerosol concentrations between the PNA+ and PNA- months are obtained on the basis of  $\text{PNAI}_{\text{Wallace}}$ .

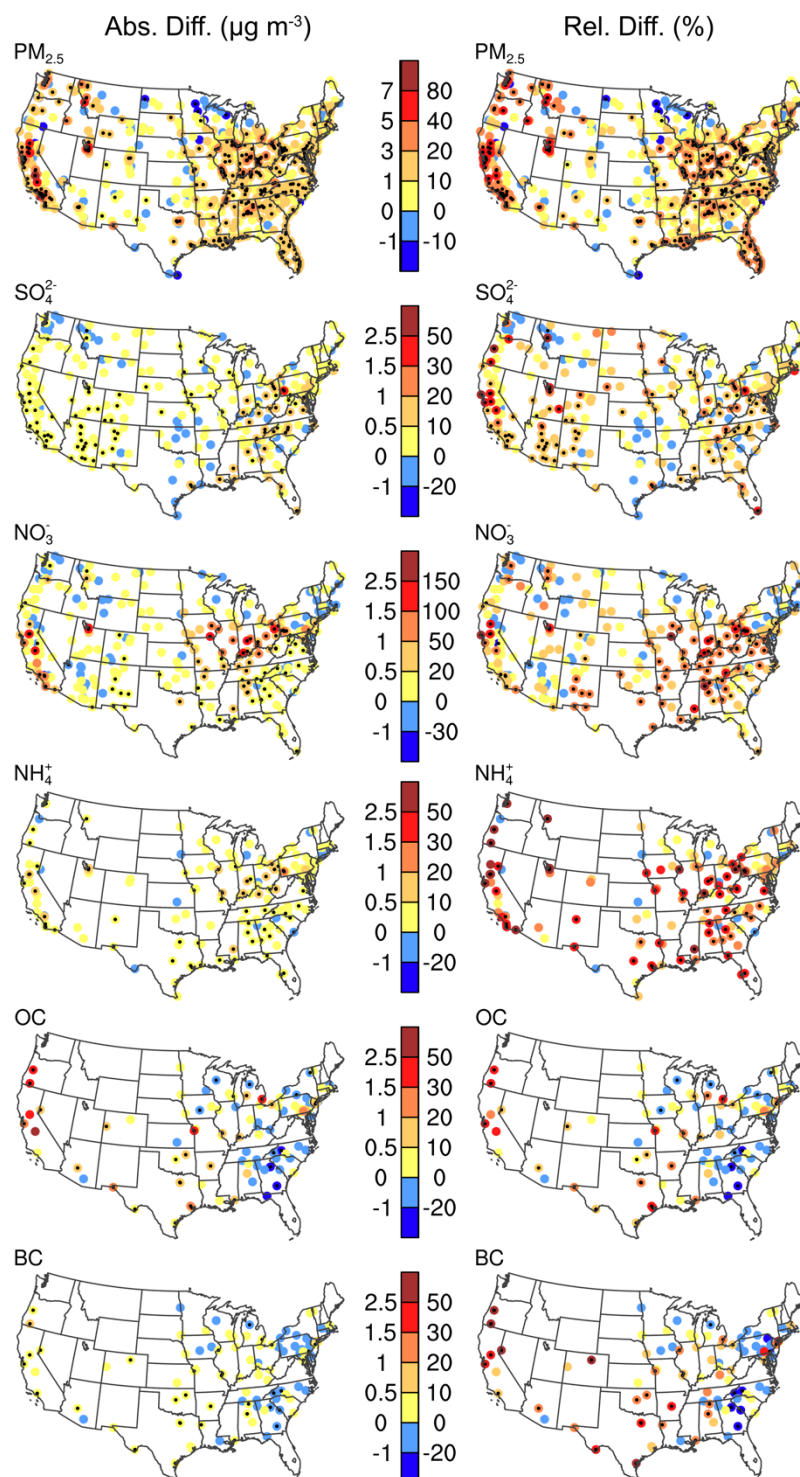


Fig. C. The same as Fig. 3 in the manuscript except that the differences in observed surface-layer aerosol concentrations between the PNA+ and PNA- months are obtained on the basis of  $PNAI_{NOAA}$ .

Section 3.1. It is very important to include the uncertainty when calculating the  $PM_{2.5}$  concentration difference between positive and negative PNA. And provide details about how you calculate the uncertainty.



Response:

We added the following sentence in Sect. 3.1: “The uncertainty associated with the differences in aerosol concentrations between PNA+ and PNA– months is represented by the two-tail Student-t test with significance level of 90%.”

Section 3.2. The decreasing emission trend should have a large effect on the conclusion about the number of exceedance days. So please show Figure 4 at different timeframes.

Response:

We have removed Sect. 3.2 following the suggestion of Reviewer #3.

Section 4.1. From Figure 5a and 5b, it seems GEOS-Chem largely underestimates the PM<sub>2.5</sub> concentrations in California. What is the reason for this? Does it improve if some updated SOA mechanisms is included in the model?

Response:

There are two reasons for the low biases in model results in California. First, the EPA-AQS network had sites in urban and suburban regions, which obtained higher concentrations than other long term networks in the U.S. (Malm et al. 2011; Rattigan et al. 2011; Hand et al. 2012; Hand et al. 2014). Hand et al. (2014) compared the concentrations of aerosols from the EPA-AQS with those from the Interagency Monitoring of Protected Visual Environments (IMPROVE) for 2008–2011, and showed that the ratios of wintertime aerosol concentrations of ammonium sulfate, ammonium nitrate, OC, and BC from the EPA-AQS to those from the IMPROVE were, respectively, 2.3, 7.7, 8.3, and 13.1, as the concentrations were averaged over the western U.S.. Liu et al. (2004) also attributed the high EPA-AQS concentrations in the western U.S. to the relative sparse urban sites that were heavily influenced by strong local sources such as automobiles and wood fires. Second, the low biases in California may also be caused by the systematic biases in emissions in the model. With a high resolution (0.5° latitude by 0.667° longitude over North America) nested-grid version of the GEOS-Chem model (version 9-01-02), Walker et al. (2012) found large underestimates of nitrate and ammonium in California, with NMB of –62% and –38%, respectively, as model results were compared with the IMPROVE and CASTNET observations.

If we update the SOA mechanism, simulated OC concentration in California might be improved slightly but the underestimates in PM<sub>2.5</sub> in this region cannot be improved, since concentrations of all aerosol species are underestimated in the western U.S.. Heo et al. (2013) showed that the measured SOA was low (about 0.2–0.3  $\mu\text{g m}^{-3}$ ) in California in winter, so improving SOA simulation should not have a large impact on simulated OC in California.



Figure 5b shows the spatial correlation between the observations and the GEOS-Chem. How about the temporal correlation in different regions? Maybe the correlation is very low. Can it affect the conclusion?

Response:

Following the reviewer's suggestion, we have calculated the temporal correlation coefficient between EPA-AQS observations and GEOS-Chem model results at each site for each aerosol species ( $\text{PM}_{2.5}$ ,  $\text{SO}_4^{2-}$ ,  $\text{NO}_3^-$ ,  $\text{NH}_4^+$ , OC, or BC) (auxiliary Fig. S4, see below). The temporal correlations are statistically significant for  $\text{PM}_{2.5}$ ,  $\text{SO}_4^{2-}$ ,  $\text{NO}_3^-$ ,  $\text{NH}_4^+$ , at most sites in the U.S., especially over and near the eastern Midwest where largest increases in aerosol concentrations are identified in the PNA+ months relative to the PNA− months. We have added these results of temporal correlation coefficients to the end of Sect. 4.1.

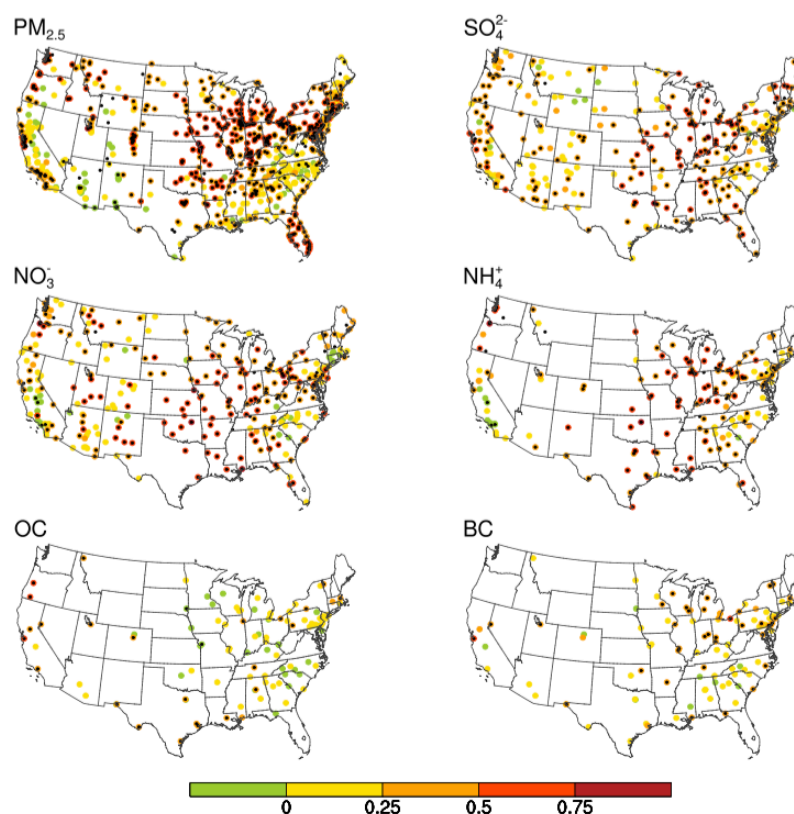


Fig. S4. The temporal correlation coefficient between EPA-AQS observations and GEOS-Chem model results at each site for each aerosol species. Datasets used here are the same as those used in Figure 4 of the manuscript. The sites with black dots are those that have passed the two-tail t-test with 90% confidence level.

Section 5.1 How important is transboundary transport of aerosols? If it contributes to a tiny amount of total  $\text{PM}_{2.5}$  mass, this section may be not important.

Response:

The monthly mean  $\text{PM}_{2.5}$  mass over the selected U.S. box was about 0.10 Tg (integration over the box from the surface to 100 hPa), and the net loss through the boundaries of the box was about  $0.32 \text{ Tg month}^{-1}$ , indicating that the transboundary transport of aerosols is very important.

Also, the authors should discuss whether the underestimate in GEOS-Chem over the west US affects the conclusion in this section.

Response:

We have added a sentence to discuss at the end of Sect. 5.1: “Note that because the GEOS-Chem model underestimates  $\text{PM}_{2.5}$  concentrations in the western U.S. (Fig. 4b), the net outflow flux from the selected box might have been underestimated, but this should not compromise our conclusions about the differences in net flux between PNA+ and PNA– phases.”

Section 5.2 I would suggest the authors to check the impact of PNA on T, RH, precipitation and surface wind speed using NCEP Reanalysis over a much longer time period, e.g. 1948-2014.

Response:

Following the reviewer’s suggestion, we have calculated the impact of PNA on T, RH and surface wind speed over 1948–2014 by using the NCEP Reanalysis and on precipitation over 1948–2010 by using Global Precipitation Climatology Center (GPCC) data (<http://www.esrl.noaa.gov/psd/data/gridded/data.gpcc.html>) (Fig. D below). The spatial patterns of the differences in meteorological parameters in Fig. D are similar to those shown in Fig. 7 (obtained for years of 1986–2006 by using the GEOS-4 data), except that more grid cells have passed the two-tail student-t test with 90% confidence level in Fig. D with more samples in a longer time period.

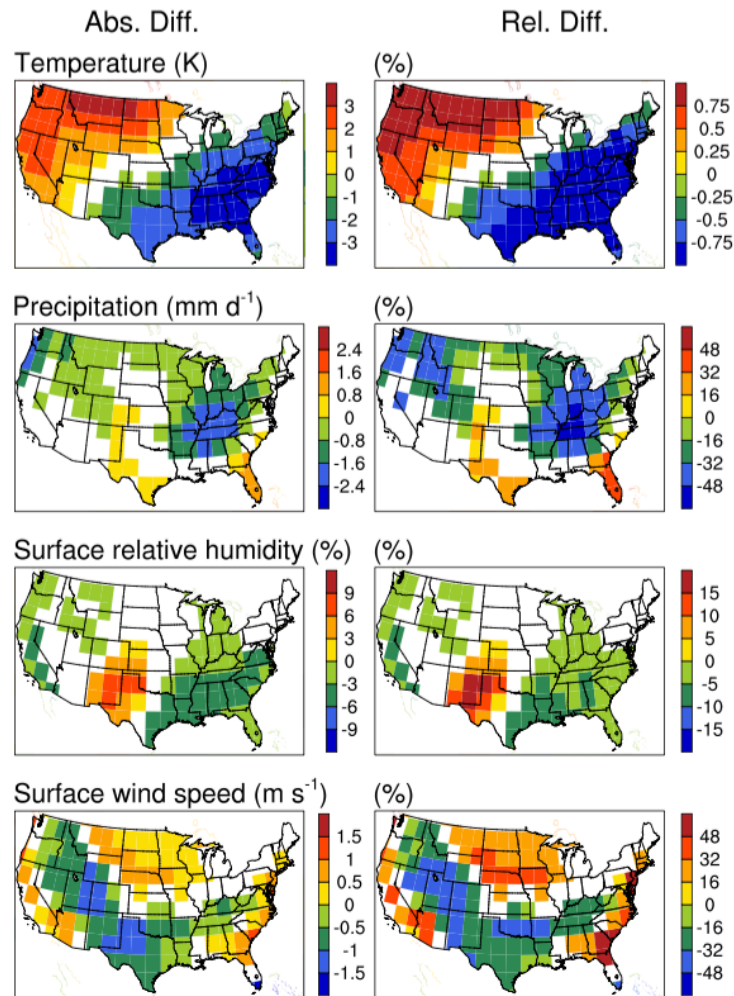


Fig. D. The same as Fig. 7 in the manuscript except that the differences in T, RH, and surface wind speed between PNA+ and PNA– months are calculated for 1948–2014 by using the NCEP Reanalysis and the differences in precipitation are calculated for 1948–2010 by using the Global Precipitation Climatology Center (GPCC) data (<http://www.esrl.noaa.gov/psd/data/gridded/data.gpcc.html>).

#### References:

- Allen, R. J., Landuyt, W. and Rumbold, S. T.: An increase in aerosol burden and radiative effects in a warmer world, *Nat. Clim. Chang.*, (OCTOBER), doi:10.1038/nclimate2827, 2015.
- Alston, E. J., Sokolik, I. N. and Kalashnikova, O. V.: Characterization of atmospheric aerosol in the US Southeast from ground- and space-based measurements over the past decade, *Atmos. Meas. Tech.*, 5(7), 1667–1682, doi:10.5194/amt-5-1667-2012, 2012.
- Blanchard, C. L., Hidy, G. M., Tanenbaum, S., Edgerton, E., Hartsell, B. and Jansen, J.: Carbon in southeastern U.S. aerosol particles: Empirical

- estimates of secondary organic aerosol formation, *Atmos. Environ.*, 42(27), 6710–6720, doi:10.1016/j.atmosenv.2008.04.011, 2008.
- Dawson, J. P., Adams, P. J. and Pandis, S. N.: Sensitivity of PM<sub>2.5</sub> to climate in the Eastern US: a modeling case study, *Atmos. Chem. Phys.*, 7(16), 4295–4309, doi:10.5194/acp-7-4295-2007, 2007.
- Ding, X., Zheng, M., Yu, L., Zhang, X., Weber, R. J., Yan, B., Russell, A. G., Edgerton, E. S. and Wang, X.: Spatial and seasonal trends in biogenic secondary organic aerosol tracers and water-soluble organic carbon in the southeastern United States., *Environ. Sci. Technol.*, 42(14), 5171–6, doi:10.1021/es7032636, 2008.
- van Donkelaar, A., Martin, R. V., Park, R. J., Heald, C. L., Fu, T. M., Liao, H. and Guenther, A.: Model evidence for a significant source of secondary organic aerosol from isoprene, *Atmos. Environ.*, 41(6), 1267–1274, doi:10.1016/j.atmosenv.2006.09.051, 2007.
- Hand, J. L., Schichtel, B. A., Malm, W. C., Pitchford, M. and Frank, N. H.: Spatial and seasonal patterns in urban influence on regional concentrations of speciated aerosols across the United States, *J. Geophys. Res. Atmos.*, 119, 12832–12849, doi:10.1002/2014JD022328.Received, 2014.
- Hand, J. L., Schichtel, B. A., Pitchford, M., Malm, W. C. and Frank, N. H.: Seasonal composition of remote and urban fine particulate matter in the United States, *J. Geophys. Res.*, 117(D5), D05209, doi:10.1029/2011JD017122, 2012.
- Heo, J., Dulger, M., Olson, M. R., McGinnis, J. E., Shelton, B. R., Matsunaga, A., Sioutas, C. and Schauer, J. J.: Source apportionments of PM<sub>2.5</sub> organic carbon using molecular marker Positive Matrix Factorization and comparison of results from different receptor models, *Atmos. Environ.*, 73, 51–61, doi:10.1016/j.atmosenv.2013.03.004, 2013.
- Jeong, J. I. and Park, R. J.: Effects of the meteorological variability on regional air quality in East Asia, *Atmos. Environ.*, 69(3), 46–55, doi:10.1016/j.atmosenv.2012.11.061, 2013.
- Jiang, Z., Jones, D. B. A., Worden, H. M. and Henze, D. K.: Sensitivity of top-down CO source estimates to the modeled vertical structure in atmospheric CO, *Atmos. Chem. Phys.*, 15(3), 1521–1537, doi:10.5194/acp-15-1521-2015, 2015.
- Ke, L., Ding, X., Tanner, R. L., Schauer, J. J. and Zheng, M.: Source contributions to carbonaceous aerosols in the Tennessee Valley Region, *Atmos. Environ.*, 41(39), 8898–8923, doi:10.1016/j.atmosenv.2007.08.024, 2007.
- Kleindienst, T. E., Jaoui, M., Lewandowski, M., Offenber, J. H., Lewis, C. W., Bhawe, P. V. and Edney, E. O.: Estimates of the contributions of biogenic and anthropogenic hydrocarbons to secondary organic aerosol at a

- southeastern US location, *Atmos. Environ.*, 41(37), 8288–8300, doi:10.1016/j.atmosenv.2007.06.045, 2007.
- Kleindienst, T. E., Lewandowski, M., Offenberg, J. H., Edney, E. O., Jaoui, M., Zheng, M., Ding, X. and Edgerton, E. S.: Contribution of Primary and Secondary Sources to Organic Aerosol and PM 2.5 at SEARCH Network Sites, *J. Air Waste Manage. Assoc.*, 60(11), 1388–1399, doi:10.3155/1047-3289.60.11.1388, 2010.
- Levy, H., Schwarzkopf, M. D., Horowitz, L., Ramaswamy, V. and Findell, K. L.: Strong sensitivity of late 21st century climate to projected changes in short-lived air pollutants, *J. Geophys. Res. Atmos.*, 113(6), 1–13, doi:10.1029/2007JD009176, 2008.
- Liu, Y., Park, R. J., Jacob, D. J., Li, Q., Kilaru, V. and Sarnat, J. A.: Mapping annual mean ground-level PM 2.5 concentrations using Multiangle Imaging Spectroradiometer aerosol optical thickness over the contiguous United States, *J. Geophys. Res.*, 109(D22), D22206, doi:10.1029/2004JD005025, 2004.
- Luo, M., Shephard, M. W., Cady-Pereira, K. E., Henze, D. K., Zhu, L., Bash, J. O., Pinder, R. W., Capps, S. L., Walker, J. T. and Jones, M. R.: Satellite observations of tropospheric ammonia and carbon monoxide: Global distributions, regional correlations and comparisons to model simulations, *Atmos. Environ.*, 106, 262–277, doi:10.1016/j.atmosenv.2015.02.007, 2015.
- Malm, W. C., Schichtel, B. A. and Pitchford, M. L.: Uncertainties in PM<sub>2.5</sub> Gravimetric and Speciation Measurements and What We Can Learn from Them, *J. Air Waste Manage. Assoc.*, 61(11), 1131–1149, doi:10.1080/10473289.2011.603998, 2011.
- Marlier, M. E., Defries, R. S., Kim, P. S., Kopplitz, S. N. and Jacob, D. J.: Fire emissions and regional air quality impacts from fires in oil palm, timber, and logging concessions in Indonesia, *Environ. Res. Lett.*, 10(8), 85005, doi:10.1088/1748-9326/10/8/085005, 2015.
- Molod, A., Takacs, L., Suarez, M. and Bacmeister, J.: Development of the GEOS-5 atmospheric general circulation model: Evolution from MERRA to MERRA2, *Geosci. Model Dev.*, 8(5), 1339–1356, doi:10.5194/gmd-8-1339-2015, 2015.
- Mu, Q. and Liao, H.: Simulation of the interannual variations of aerosols in China: role of variations in meteorological parameters, *Atmos. Chem. Phys.*, 14, 11177–11219, doi:10.5194/acp-14-9597-2014, 2014.
- Park, R. J., Jacob, D. J., Chin, M., Martin, R. V.: Sources of carbonaceous aerosols over the United States and implications for natural visibility, *J. Geophys. Res.*, 108(D12), 4355, doi:10.1029/2002JD003190, 2003.
- Rattigan, O. V., Felton, H. D., Bae, M.-S., Schwab, J. J. and Demerjian, K. L.: Comparison of long-term PM<sub>2.5</sub> carbon measurements at an urban and

- rural location in New York, *Atmos. Environ.*, 45(19), 3228–3236, doi:10.1016/j.atmosenv.2011.03.048, 2011.
- Walker, J. M., Philip, S., Martin, R. V. and Seinfeld, J. H.: Simulation of nitrate, sulfate, and ammonium aerosols over the United States, *Atmos. Chem. Phys.*, 12(22), 11213–11227, doi:10.5194/acp-12-11213-2012, 2012.
- Weber, R.: Secondary organic aerosol in the Southeastern United States : A summary of findings from ambient studies, in 12th Conference on Atmospheric Chemistry: Field and Laboratory Studies of Air Quality II. [online] Available from: <https://ams.confex.com/ams/90annual/webprogram/Paper164747.html>, 2010.
- Yang, Y., Liao, H. and Lou, S.: Decadal trend and interannual variation of outflow of aerosols from East Asia: Roles of variations in meteorological parameters and emissions, *Atmos. Environ.*, 100, 141–153, doi:10.1016/j.atmosenv.2014.11.004, 2015.
- Zheng, M., Cass, G. R., Ke, L., Wang, F., Schauer, J. J., Edgerton, E. S. and Russell, A. G.: Source apportionment of daily fine particulate matter at Jefferson Street, Atlanta, GA, during summer and winter, *J Air Waste Manag Assoc*, 57(2), 228–242, doi:10.1080/10473289.2007.10465322, 2007.
- Zheng, M., Cass, G. R., Schauer, J. J. and Edgerton, E. S.: Source apportionment of PM<sub>2.5</sub> in the southeastern United States using solvent-extractable organic compounds as tracers, *Environ. Sci. Technol.*, 36(11), 2361–2371, doi:10.1021/es011275x, 2002.
- Zhu, J., Liao, H. and Li, J.: Increases in aerosol concentrations over eastern China due to the decadal-scale weakening of the East Asian summer monsoon, *Geophys. Res. Lett.*, 39(9), L09809, doi:10.1029/2012GL051428, 2012.



## Manuscript # ACP-2015-804

### Responses to Reviewer #2

#### Overview

This study relates winter variability of particulate matter (PM) to changes in the Pacific-North America climate index. The authors use both observations and model simulations of PM. A statistically significant difference in PM is identified between the positive and negative phases of the PNA, particularly in the US Midwest. The authors provide some statistical evidence that changes in meteorology attributable to the PNA is the cause.

Overall the paper is generally clear. I think the research fits well within the scope of ACP and that the results would be well-received by the community. However, I have a number of concerns. I believe the authors can ease these concerns with additional work. I recommend the manuscript for major revision.

#### General Comments

I have some concern about the definition of the PNA index. It is not clear why the geopotential height in three grid boxes is sufficient. I recommend using a more standard index. For example, the NOAA Climate Prediction Center provides monthly values of the PNA index using the more common EOF loading approach. Also, just looking by eye, the NOAA CPC PNA data appears to differ from the PNAI presented here.

#### Response:

There are three commonly used definitions of PNAI: (1) PNAI defined by Leathers et al. (1991) ( $PNAI_{Leathers}$ ). This is the definition used in our manuscript. (2) PNAI defined by Wallace and Gutzler (1981) ( $PNAI_{Wallace}$ ) as:

$$PNAI_{Wallace} = \frac{1}{4} [z^*(20^\circ N, 160^\circ W) - z^*(45^\circ N, 165^\circ W) + z^*(55^\circ N, 115^\circ W) - z^*(30^\circ N, 85^\circ W)]$$
, where \* denotes the normalized geopotential height at 500 hPa. (3) PNAI defined by NOAA Climate Prediction Center (CPC) ( $PNAI_{NOAA}$ , [http://www.cpc.ncep.noaa.gov/products/precip/CWlink/pna/month\\_pna\\_index\\_2.shtml](http://www.cpc.ncep.noaa.gov/products/precip/CWlink/pna/month_pna_index_2.shtml)). All these three definitions reflect the same atmospheric teleconnections over the region of North Pacific to North America region. The correlation coefficients between  $PNAI_{Leathers}$  and  $PNAI_{Wallace}$  (or between  $PNAI_{Leathers}$  and  $PNAI_{NOAA}$ ) is equal to or larger than 0.94, when we calculate PNAI for 1979–2013 by using the NCEP-2 reanalyzed meteorological data or PNAI for 1986–2006 by using the assimilated GEOS-4 data (see Fig. A below). Therefore it is sufficient to use  $PNAI_{Leathers}$  in our study.

By using the PNAI defined by geopotential heights in 3 grid boxes ( $PNAI_{Leathers}$ ) and in 4 grid boxes ( $PNAI_{Wallace}$ ), many previous studies examined the variation and mechanism of PNA as well as the relationship between PNA and surface weather over the U.S. (Yarnal and Diaz, 1986; Carleton et al., 1990; Leathers et al., 1991; Leathers and Palecki, 1992;

Trenberth and Hurrell, 1994; Rodionov and Assel, 2001; Schoof and Pryor, 2006).

There are three reasons for the differences between PNAI shown in our Fig. 2 and that shown by NOAA CPC ([http://www.cpc.ncep.noaa.gov/products/precip/CWlink/pna/month\\_pna\\_index.shtml](http://www.cpc.ncep.noaa.gov/products/precip/CWlink/pna/month_pna_index.shtml)). First, the calculation depends strongly on the length of samples. The NOAA CPC PNAI has the samples covering all months throughout the year over 1950–present, with the mean value and variance of the time series different from what we have in our calculation of PNAI (in our work we are only concerned with the PNAI for the months of NDJFM over 1986–2013). Second, the NOAA CPC PNAI has been smoothed by a 3-month running mean method. Third, the NOAA CPC PNAI is calculated by using the geopotential height with seasonal cycle, but the PNAI in our work is calculated by using the deseasonalized geopotential height to isolate the monthly variation.

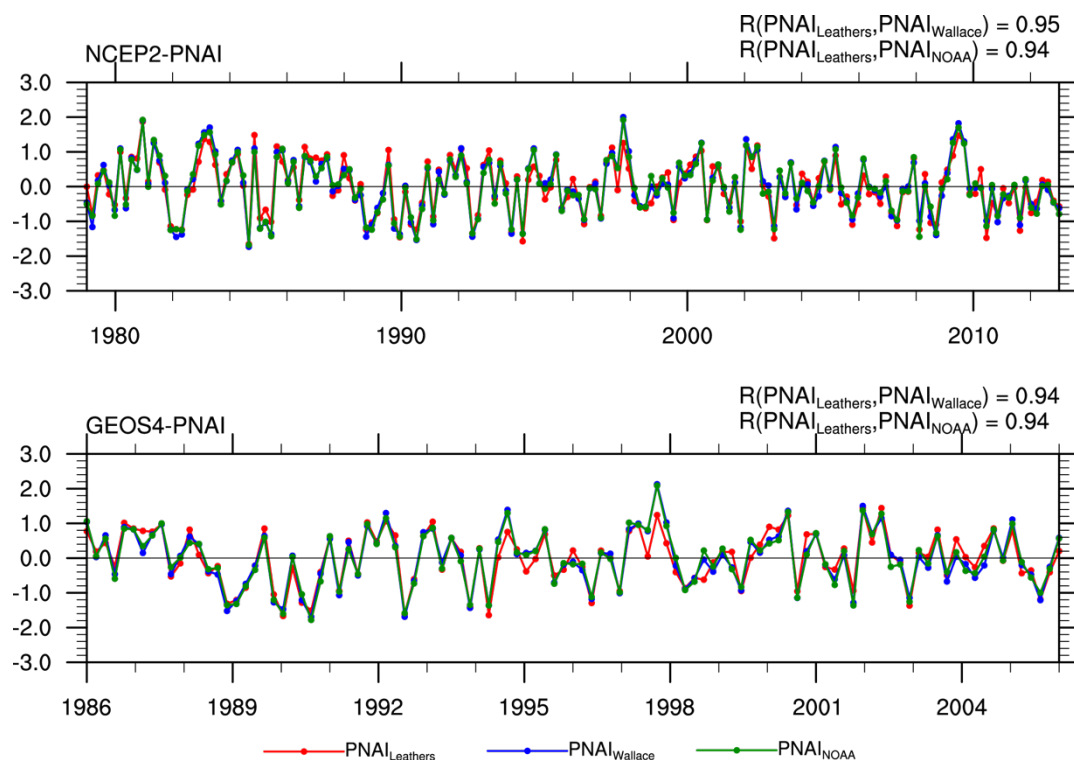


Fig. A. Top panel: Monthly PNAI in NDJFM for years of 1979–2013 calculated using the NCEP-2 data. Bottom panel: PNAI for 1986–2006 calculated using the assimilated GEOS-4 data. The correlation coefficients are marked on top right corner of each panel.

- Most of the analysis focuses on differences between the positive and negative phases of the PNA. It is generally most constructive to isolate the impacts of each phase from neutral conditions. If the authors have motivation to compare positive vs. negative phases, they should include those thoughts in the manuscript.

Response:

The method of compositing the differences between the positive and negative phases of one atmospheric circulation index (ACI) is a commonly

used approach to analyze the impact of the ACI on a specific phenomenon. Most importantly, the composite differences can show the magnitude of the influence of ACI. Such approach has been used in many studies to examine the impact of climate variability on concentrations of aerosols (Di Pierro et al., 2011; Singh and Palazoglu, 2012; Zhu et al., 2012; Jerez et al., 2013; Qu et al., 2015) and on concentrations of tracer gases (Eckhardt et al., 2003; Liang et al., 2005; Jerez et al., 2013; Yang et al., 2014).

- The definition of the PNAI appears to have a significant flaw. I think this may just be a mistake in how the equation is written. By my calculation the denominator of  $Z'^*_{i,j}$  is always 0. The summation can be disturbed across the parentheses (since the terms are simply subtracted). The first term generates the average value of  $Z'$  (which should be 0 anyway, see below). Summing the second term is trivial since there is no dependence on  $i$  or  $j$ , so it is multiplied by  $N \times 5$  and then divided by  $N \times 5$ . Thus both terms give the average value of  $Z'$ :  $Z' - Z' = 0$ .

The second term of the numerator, by my calculation, should also be 0. The summation of anomalies from a mean will always be equal to 0, if the period used for estimation of the mean and period of anomalies are the same.

This equation needs correction; it is clearly not the algorithm used to produce the data in Fig. 2. Perhaps this is an issue with notation. See additional comment about these equations below.

Response:

Thanks for pointing out the typographic errors. We now have the following corrected equation in the revised manuscript:

$$Z'_{i,j} = \frac{Z'_{i,j}}{\sqrt{\frac{1}{n \times 5} \sum_{i=1}^n \sum_{j=1}^5 Z'^2_{i,j}}}$$

- There are significant trends in PM2.5 and aerosol composition over this time period (hints of this can be seen in Fig. 5c). The EPA AQS data should be detrended (in addition to removing seasonality) in order to best detect interannual variability. It needs to be shown that differences arise from true variability and not other factors (emission regulations). Indeed, just by eye, most of the positive phase months are in the early part of the period and negative at the end. This could introduce an artifact of emission regulations.

Response:

This is a good point. We have redone the composite analyses for observed aerosol concentrations by detrending the observations from the EPA-AQS. The revised differences in aerosol concentrations between positive and negative PNA are similar to the results in our previous version of manuscript (those obtained without detrending); the horizontal distributions are about the same but the magnitudes of the differences in aerosol concentrations are slightly smaller. We have updated Figs. 3, 4 and Table 1, and have changed the descriptions in the text accordingly.

- How are regional averages performed? A US-scale average will generally be more heavily weighted by the East Coast since there are more sites in that region. Some of the regional average numbers presented (US, western US, eastern US) should be reassessed.

Response:

We agree with the Reviewer. We have added a sentence in Sect. 3 to clarify this: "It should be noted that, in our analyses above, the locations of measurements and the numbers of samples were different for different aerosol species. The regional averages were also influenced by the uneven distributions of observational sites in different regions. Therefore, model results from the GEOS-Chem simulation will be used to further analyze the impacts of PNA on aerosols in the U.S., as presented in the subsequent sections."

- The figures are very hard to view. I recommend breaking up some of them to allow larger maps. Figures 3, 5, and 6 are particularly hard to read. The data in the maps is useful and necessary.

Response:

The original figures are not so small. The current very small figures were caused by the landscape pages of ACPD. It is expected that the figures will be easier to view when each of these figures can take up a whole portrait page in its ACP version.

**Specific Comments** - Page 33210, Line 6: "...Air Quality System of Environ- mental . . ." should be ". . .Air Quality System of the Environmental. . ."

Response:

Changed.

- Page 33215, Line 4: It is unclear if 5 days of observations are required or 5 observational periods. A single observational period could be 5 days long.

Response:

We have clarified this as "... there were at least 5 observation records within each month."

- Page 33217, Line 14: The notation here is confusing. The equation defining  $Z'$  should not have two references to  $i$  ( $i$  is listed as an input and the summation variable).

Response:

Corrected.

- Page 33218, Line 2: "PANI" should be "PNAI".

Response:

Changed.

- Page 33218, Line18: I do think contiguous Salt Lake is an identifiable location.

Response:

We have changed “the contiguous Salt Lake” to “the contiguous Salt Lake (northern Utah)”.

- Page 33219, Line 9: Why is 90th percentile used? 95th percentile is more standard.

Response:

The 90% confidence level for t-test is also commonly used in previous studies to examine the impacts of atmospheric circulation on aerosols (Schultz et al., 2007; Wu et al., 2008, 2013; Gong et al., 2010; Hirdman et al., 2010; Qian et al., 2011; Jerez et al., 2013; Huang et al., 2014; Gettelman et al., 2015).

- Figure 2: The difference between Figure 2a and 2b is not clear. The panels have slightly different labels, but the data and highlighted +/- points appear identical.

Response:

The Fig. 2a (Fig. 2b) was the PNAI for analyzing observed PM<sub>2.5</sub> (individual aerosol species) over 1999–2013 (2000–2013). Figs. 2a and 2b are almost identical for the highlighted +/- points except for those in year 1999. See Sect. 2.3 for our definitions of PNA+ and PNA–.

- Page 33222, Line 23: Again, you cannot use the variable *i* in the summation notation since its already used to denote the month of interest.

Response:

We have changed *i* to *m*, *n* to *M*, and the revised equation is:

$$DM_m = (C_m - \frac{1}{M} \sum_{m=1}^M C_m) / \frac{1}{M} \sum_{m=1}^M C_m$$

- Table 3 – The mass flux values seem a little low. I recommend double-checking the calculation.

Response:

We have checked our calculation and the results are right.

## References

Carleton, A. M., Carpenter, D. a. and Weser, P. J.: Mechanisms of Interannual Variability of the Southwest United States Summer Rainfall Maximum, J. Clim., 3, 999–1015, doi:10.1175/1520-0442(1990)003<0999:MOIVOT>2.0.CO;2, 1990.

- Eckhardt, S., Stohl, a., Beirle, S., Spichtinger, N., James, P., Forster, C., Junker, C., Wagner, T., Platt, U. and Jennings, S. G.: The North Atlantic Oscillation controls air pollution transport to the Arctic, *Atmos. Chem. Phys. Discuss.*, 3(3), 3222–3240, doi:10.5194/acpd-3-3222-2003, 2003.
- Gottelman, A., Shindell, D. T. and Lamarque, J. F.: Impact of aerosol radiative effects on 2000-2010 surface temperatures, *Clim. Dyn.*, doi:10.1007/s00382-014-2464-2, 2015.
- Gong, S. L., Zhao, T. L., Sharma, S., Toom-Saunty, D., Lavoué, D., Zhang, X. B., Leaitch, W. R. and Barrie, L. a.: Identification of trends and interannual variability of sulfate and black carbon in the Canadian High Arctic: 1981–2007, *J. Geophys. Res.*, 115(D7), D07305, doi:10.1029/2009JD012943, 2010.
- Hirdman, D., Burkhardt, J. F., Sodemann, H., Eckhardt, S., Jefferson, a., Quinn, P. K., Sharma, S., Ström, J. and Stohl, a.: Long-term trends of black carbon and sulphate aerosol in the Arctic: changes in atmospheric transport and source region emissions, *Atmos. Chem. Phys.*, 10(19), 9351–9368, doi:10.5194/acp-10-9351-2010, 2010.
- Huang, L., Fu, R. and Jiang, J. H.: Impacts of fire emissions and transport pathways on the interannual variation of CO in the tropical upper troposphere, *Atmos. Chem. Phys.*, 14(8), 4087–4099, doi:10.5194/acp-14-4087-2014, 2014.
- Jerez, S., Jimenez-Guerrero, P., Montávez, J. P. and Trigo, R. M.: Impact of the North Atlantic Oscillation on European aerosol ground levels through local processes: a seasonal model-based assessment using fixed anthropogenic emissions, *Atmos. Chem. Phys.*, 13(22), 11195–11207, doi:10.5194/acp-13-11195-2013, 2013.
- Leathers, D. J. and Palecki, M. A.: The Pacific/North American Teleconnection Pattern and United States Climate. Part II: Temporal Characteristics and Index Specification, *J. Clim.*, 5(7), 707–716, doi:10.1175/1520-0442(1992)005<0707:TPATPA>2.0.CO;2, 1992.
- Leathers, D. J., Yarnal, B. and Palecki, M. A.: The Pacific/North American Teleconnection Pattern and United States Climate. Part I: Regional Temperature and Precipitation Associations, *J. Clim.*, 4(5), 517–528, doi:10.1175/1520-0442(1991)004<0517:TPATPA>2.0.CO;2, 1991.
- Liang, Q., Jaegle, L. and Wallace, J. M.: Meteorological indices for Asian outflow and transpacific transport on daily to interannual timescales, *J. Geophys. Res.*, 110(D18), D18308, doi:10.1029/2005JD005788, 2005.
- Di Pierro, M., Jaeglé, L. and Anderson, T. L.: Satellite observations of aerosol transport from East Asia to the Arctic: three case studies, *Atmos. Chem. Phys.*, 11(5), 2225–2243, doi:10.5194/acp-11-2225-2011, 2011.
- Qian, Y., Flanner, M. G., Leung, L. R. and Wang, W.: Sensitivity studies on the impacts of Tibetan Plateau snowpack pollution on the Asian hydrological cycle and monsoon climate, *Atmos. Chem. Phys.*, 11(5), 1929–1948, doi:10.5194/acp-11-1929-2011, 2011.
- Qu, W., Wang, J., Zhang, X., Yang, Z. and Gao, S.: Effect of cold wave on winter visibility over eastern China, *J. Geophys. Res. Atmos.*, 120(6), 2394–2406, doi:10.1002/2014JD021958, 2015.



- Rodionov, S. and Assel, R.: A new look at the Pacific/North American Index, *Geophys. Res. Lett.*, 28(8), 1519–1522, doi:10.1029/2000GL012185, 2001.
- Schoof, J. T. and Pryor, S. C.: An evaluation of two GCMs: simulation of North American teleconnection indices and synoptic phenomena, *Int. J. Climatol.*, 26(2), 267–282, doi:10.1002/joc.1242, 2006.
- Schultz, D. M., Mikkonen, S., Laaksonen, A. and Richman, M. B.: Weekly precipitation cycles? Lack of evidence from United States surface stations, *Geophys. Res. Lett.*, 34(22), L22815, doi:10.1029/2007GL031889, 2007.
- Singh, A. and Palazoglu, A.: Climatic variability and its influence on ozone and PM pollution in 6 non-attainment regions in the United States, *Atmos. Environ.*, 51, 212–224, doi:10.1016/j.atmosenv.2012.01.020, 2012.
- Trenberth, K. E. and Hurrell, J. W.: Decadal atmosphere-ocean variations in the Pacific, *Clim. Dyn.*, 9(6), 303–319, doi:10.1007/BF00204745, 1994.
- Wallace, J. M. and Gutzler, D. S.: Teleconnections in the Geopotential Height Field during the Northern Hemisphere Winter, *Mon. Weather Rev.*, 109(4), 784–812, doi:10.1175/1520-0493(1981)109<0784:TITGHF>2.0.CO;2, 1981.
- Wu, J., Fu, C., Xu, Y., Tang, J. P., Wang, W. and Wang, Z.: Simulation of direct effects of black carbon aerosol on temperature and hydrological cycle in Asia by a Regional Climate Model, *Meteorol. Atmos. Phys.*, 100, 179–193, doi:10.1007/s00703-008-0302-y, 2008.
- Wu, R., Wen, Z. and He, Z.: ENSO Contribution to Aerosol Variations over the Maritime Continent and the Western North Pacific during 2000–10, *J. Clim.*, 26(17), 6541–6560, doi:10.1175/JCLI-D-12-00253.1, 2013.
- Yang, Y., Liao, H. and Li, J.: Impacts of the East Asian summer monsoon on interannual variations of summertime surface-layer ozone concentrations over China, *Atmos. Chem. Phys.*, 14(13), 6867–6879, doi:10.5194/acp-14-6867-2014, 2014.
- Yarnal, B. and Diaz, H. F.: Relationships between extremes of the Southern oscillation and the winter climate of the Anglo-American Pacific Coast, *J. Climatol.*, 6(2), 197–219, doi:10.1002/joc.3370060208, 1986.
- Zhu, J., Liao, H. and Li, J.: Increases in aerosol concentrations over eastern China due to the decadal-scale weakening of the East Asian summer monsoon, *Geophys. Res. Lett.*, 39(9), L09809, doi:10.1029/2012GL051428, 2012.

This manuscript examines the correlation between the Pacific-North America (PNA) phases and the wintertime surface-layer aerosol concentrations at the United States (US) on monthly scale. It uses the observation (1999-2013) from the Air Quality System of Environmental Protection Agency (EPA-AQS) and the simulation (1986-2006) from Goddard Earth Observing System chemical transport model (GEOS-Chem). Both the observation and simulation are composite to months with positive and negative PNA phases. The mean aerosol loadings are found to be higher for PNA+ months. The authors tried to understand the mechanisms for the PNA impacts on aerosol concentrations with the chemical transport model (CTM). Cross-boundary fluxes are found to be responsible for the PM<sub>2.5</sub> increase in PNA+ months. With the pattern correlation coefficients (PCCs), they quantified the relative influence on local aerosol abundances from temperature, precipitation, relative humidity, wind, and boundary layer height.

The manuscript is well organized, and within the scope of ACP. Overall, I found that the observation-based analysis on the PNA impact on aerosol was more valuable than the model-based attempt on understanding the driving mechanisms. It can be published after addressing the following questions/comments.

1. Although it is mentioned that chemical reactions affect the aerosol concentrations, it seems assumed that large-scale circulation and/or meteorological factors dominate the chemical factors. Some references showing the relative contributions of dynamics, physics, and chemical impacts on aerosols are helpful.

Response:

The meteorological parameters influence the concentrations of aerosols by both physical and chemical processes. The second paragraph of our introduction section reviews mainly the impacts of meteorological parameters (such as temperature and relative humidity) on chemical reactions, and the third paragraph of this section is focused on the impacts of atmospheric circulation on aerosols. Since the impacts of meteorological parameters on physical and chemical processes are coupled, few studies have quantified the relative contributions of dynamics, physics, and chemical impacts.

2. It is known for years that the GEOS-Chem model has high biases in OH (chemistry is too “hot”, resulting for example too short methane lifetime). Is this problem improved in the GEOS-Chem version used here? What is the CH<sub>4</sub> lifetime in the model? The oxidizing capacity of the troposphere is largely determined by OH, which is a chemical sink for the aerosols studied here. It is

hard to represent aerosols correctly in the model without reasonable OH, unless the chemical impact is trivial. In fact, the biases in the chemistry simulation may explain some of the model-obs differences denoted in Sect. 4.1.

Response:

Wu et al. (2007) simulated methane lifetime by using the GEOS-Chem version 7-04-02 and reported a methane lifetime of 10.3 yr. Holmes et al. (2013) examined methane lifetime on the basis of the GEOS-Chem (version 9-01-02) simulation and reported a lifetime of 9.4–10.2 yr. Therefore, methane lifetime from the GEOS-Chem agrees closely with the lifetime of  $11.2 \pm 1.3$  yr constrained by methyl chloroform observations by Prather et al. (2012). For the version 8-02-01 of the GEOS-Chem model used in our study, the 1 yr benchmark run obtained an annual and tropospheric mean OH concentrations of  $1.18 \times 10^6$  molec  $\text{cm}^{-3}$  ([http://wiki.seas.harvard.edu/geos-chem/index.php/Mean\\_OH\\_concentration](http://wiki.seas.harvard.edu/geos-chem/index.php/Mean_OH_concentration)), which is less than the OH concentration ( $1.22 \times 10^6$  molec  $\text{cm}^{-3}$ ) from the version 9-01-02 by Holmes et al. (2013) and the OH concentration ( $1.24 \times 10^6$  molec  $\text{cm}^{-3}$ ) from version 7-04-02 by Wu et al. (2007).

The aerosol concentrations are not so sensitive to OH concentrations in model simulations. Rae et al. (2007) examined the sensitivity of sulfate to oxidant concentration and climate, and found that the global sulfate burden would decrease by about 3% with an 11.7% reduction in OH burden over 1990–2100. However, sulfate burden would increase by 9% owing to climate change alone over 1990–2100. Heald et al. (2012) found that a reduction in OH levels by 25% did not influence the simulated nitrate levels (within 5% of the baseline concentrations), because a reduction in nitric acid formation was somewhat compensated by an increase in lifetime. Hence the biases in simulated OH concentrations should not be the key reason for the model-obs differences presented in Sect. 4.1.

2. Sect. 5.2 uses the PCC to quantify the relative contribution of different meteorological variables to the aerosol changes due to different PNA phases. It finds some correlations. But more sophisticated analysis is required to infer the driving mechanisms.

Response:

These are three commonly used methods to quantify the relative contribution of different meteorological variables: the multi linear regression (MLR) (Tai et al, 2010, 2012), the sensitivity experiments (SE) (Aw and Kleeman, 2003; Dawson et al, 2007; Kleeman, 2007), and the pattern correlation coefficients (PCC) (Levy et al., 2008; Jeong and Park, 2013; Allen et al., 2015). MLR quantifies the relative contribution of different meteorological variables by establishing the temporal empirical relationship between aerosol concentrations and the meteorological variables, but it does not concern with the spatial distribution of the influence of meteorological variables. SE, by changing one specific meteorological variable (for example, PBLH) ignores the covariance of other meteorological parameters (such as temperature and convection associated with PBLH), which cannot give us a realistic responses of aerosol concentrations to changes in meteorological

conditions. PCC quantifies the relationship between meteorology and aerosol concentrations both spatially and temporally.

We use the magnitude of the pattern correlation coefficients (PCC) to quantify the relative contribution of different meteorological variables to the changes in aerosols. The same statistical approach was also used in previous studies (Levy et al., 2008; Jeong and Park, 2013; Allen et al., 2015). Levy et al. (2008), by simulations with the NOAA/GFDL climate model, reported that the regional pattern of changes in surface temperature did not correspond well to the regional pattern of radiative forcings of short-lived species because of the low global PCC of  $-0.172$  under the IPCC A1B scenario. Jeong and Park (2013) used the PCC values to show the impacts of variabilities in temperature, precipitation, relative humidity, mixing depth, cloud fraction, and surface wind speed on regional patterns of concentrations of  $O_3$ ,  $(NH_4)_2SO_4$ , and  $NH_4NO_3$  in East Asia on the basis of the GEOS-Chem simulation. Allen et al. (2015) quantified the role of precipitation in the changes of aerosol burdens from the Atmospheric Chemistry and Climate Model Intercomparison Project (ACCMIP); they obtained global PCC values of  $-0.36$ ,  $-0.33$  and  $-0.30$  between precipitation and burdens of  $SO_4^{2-}$ , BC, and OC, respectively.

Specific comments:

1. Sect. 2.2, besides noting the methane (or other species that can infer OH concentration) lifetime, it is worth mentioning how many layers are in the PBL as the focus of the study is the aerosols in the surface layer, which is largely impacted by the presentation of PBL structure in the model.

Response:

We have added the following sentence in Sect. 2.2: “The instantaneous vertical mixing in the planetary boundary layer (PBL) is accounted for by the TURBDAY mixing scheme (Bey et al., 2001). The PBL occupies the lowest 3–6 vertical model layers over the U.S..”

2. P33218, L24, what are the numbers if restrict to the sites that pass the t test? Are they significantly different from current ones? Try to get a sense on how different sampling changes the results.

Response:

Following the suggestion, we have recalculated the average differences between PNA+ and PNA– phases by using the sites that pass the t test. The results are shown in Table A (see below). The differences were larger than those calculated with the sites that both pass and do not pass the t-test with 90% confidence level.

Table A. The absolute ( $\mu g\ m^{-3}$ ) and relative (%) differences in observed aerosol concentrations between the PNA+ and PNA– months (PNA+ minus PNA–). The observed concentrations are averaged over the sites that have passed the two-tail student-t test with 90% confidence level in the whole of U.S., in the western U.S., or in the eastern U.S.. The measurements are from the EPA-AQS data. The \*\* and \* indicate the differences that have passed the two-tail student-t test with 95% and 90% significance levels, respectively.

	Whole U.S.	Western U.S.	Eastern U.S
PM <sub>2.5</sub>	1.9 (17.6%)**	2.7 (30.5%)**	1.7 (14.9%)**
SO <sub>4</sub> <sup>2-</sup>	0.1 (6.3%)	0.2 (20.3%)**	0.2 (5.4%)
NO <sub>3</sub> <sup>-</sup>	0.6 (68.8%)**	0.5 (67.2%)**	0.7 (71.6%)**
NH <sub>4</sub> <sup>+</sup>	0.3 (27.2%)*	0.5 (72.0%)**	0.3 (22.7%)**
OC	0.5 (11.3%)**	0.6 (13.0%)**	0.4 (10.5%)**
BC	0.3 (44.3%)**	0.3 (39.3%)**	0.3 (47.4%)**

3. Sect. 3.2 can be removed. It is very short and does not add much, if any, to the paper. The results shown in Fig. 4 are mostly numbers close to 0. No significance test is done for those numbers, so I am not sure statistically how significant those numbers are. If the authors would like to keep this section, I'd highly recommend the significance test. The tools used for extreme weather/climate can be borrowed, which often rely on shifted (towards high tail) probability distribution functions.

Response:

We have removed Sect. 3.2 following your suggestion.

4. P33222, L10-18: How much of the underestimated modeling PM<sub>2.5</sub>, SO<sub>4</sub>, NO<sub>3</sub>, etc. is caused by “too hot” chemistry in the model as mentioned above? The authors seem believe that it is mainly because of the observational uncertainties. Even it is the case, a factor of up to 13 differences in different measurements is worrisome. Such large error bars of the observations bring up the question if those observations are suitable for scientific applications.

Response:

We think that the biases in simulated OH concentrations should not be the key reason for the model-obs differences (see our response to #2 of your general comments).

There are two reasons for the low biases in model results. First, the EPA-AQS network had sites in urban and suburban regions, which obtained higher concentrations than other long term networks in the U.S. (Malm et al. 2011; Rattigan et al. 2011; Hand et al. 2012; Hand et al. 2014). Hand et al. (2014) compared the concentrations of aerosols from the EPA-AQS with those from the Interagency Monitoring of Protected Visual Environments (IMPROVE) for 2008–2011, and showed that the ratios of wintertime aerosol concentrations of ammonium sulfate, ammonium nitrate, OC, and BC from the EPA-AQS to those from the IMPROVE were, respectively, 2.3, 7.7, 8.3, and 13.1, as the concentrations were averaged over the western U.S.. Liu et al. (2004) also attributed the high EPA-AQS concentrations in the western U.S. to the relative sparse urban sites that were heavily influenced by strong local sources such as automobiles and wood fires. Second, the low biases may also be caused by the systematic biases in emissions in the model. With a high resolution (0.5° latitude by 0.667° longitude over North America) nested-grid version of the GEOS-Chem model (version 9-01-02), Walker et al. (2012) found large underestimates of nitrate and ammonium in California, with NMB

of -62% and -38%, respectively, as model results were compared with the IMPROVE and CASTNET observations.

The EPA observations together with the GEOS-Chem simulation were used by previous studies (for example, Liu et al., 2004; van Donkelaar et al., 2006; Drury et al., 2010; Tai et al., 2010, 2012). Even though there were biases in EPA observations, the statistically significant differences in aerosol concentrations between PNA+ and PNA- months (Fig. 3 of our manuscript) still provide valuable information for the purpose of our study.

5. P33223, L5-10: I understand why the GFED OC and BC lines are added to those plots. I suggest adding one or two sentences explaining the reason for it, so it would read logically smoother.

Response:

We have added a sentence here: "Since the biomass burning emissions, which contribute largely to carbonaceous aerosols, have large interannual variations (Duncan et al., 2003; Generoso et al., 2003; van der Werf et al., 2006), we also show in Fig. 4c the time series of DMs of biomass burning emissions of OC and BC by using biomass burning emissions in NDJFM over 2000–2006 from GFED v2."

6. Sect. 4.2: Figures 3 and 6 are compared extensively. It would be better if the corresponding panels (abs and relative differences) use the same color bars. Otherwise, it is difficult to see some of the features noted in the text.

Response:

Thanks for the suggestion. We now use the same color bars for relative differences in Figs. 3 and 6 of the revised manuscript. We have tried to use same color bars for absolute differences but decided to keep using different color bars in these two figures. Otherwise it will be difficult to see spatial distributions of the absolute differences between PNA+ and PNA- phases due to the low biases in simulated concentrations.

7. Table 4: There is no point to show the numbers that fail the significance test. I'd suggest changing them to NaNs or dashes.

Response:

To be consistent with Tables 1 and 2, we think it is better to keep the PCC numbers passed or failed the significant test in Table 3. All correlation coefficients were presented in the studies of effects of meteorology or atmospheric circulations on pollutants (Gong et al., 2006; Liang et al., 2005; Vukovich, 1995; Liu et al., 2013; Wu et al., 2013).

8. Figure 2: It is redundant showing panels (a) and (b) only because different years of PNA phases are marked. I suggest that either (a) or (b) be deleted, but marking the PNA+/- months for the whole period (1986-2013). It will allow comparing the NCEP2- PNAI and GEOS4-PNAI for more years than the current form.

Response:



The PNAI are shown in those panels because of our definition of the PNAI phases: the positive PNA months (PNA+) were 25% of the  $n \times 5$  PNAI months with the highest positive PNAI values, the negative PNA months (PNA-) were 25% of the  $n \times 5$  PNAI months with the highest negative PNAI values, and the rest months were referred to as the transitional months (see Sect. 2.3). The Fig. 2a (Fig. 2b) was the PNAI for analyzing observed PM<sub>2.5</sub> (individual aerosol species) over 1999–2013 (2000–2013). Figs. 2a and 2b are almost identical for the highlighted +/- points except for those in year 1999.

9. Figure 3: The caption should mention the results are for monthly averages (it says in the text, but should be clear in the caption as well). Also, the test is to confirm if the two averages (PNA+/-) are significantly different. The caption should be revised to be more specific about this.

Response:

We have revised the figure caption as: “The absolute ( $\mu\text{g m}^{-3}$ , left column) and relative differences (% , right column) in observed monthly mean aerosol concentrations between PNA+ and PNA- months (PNA+ minus PNA-). The measurements of PM<sub>2.5</sub> were carried out over 1999–2013, in which there were 18 PNA+ months and 18 PNA- months as shown in Fig. 2a. The measurements of speciated aerosols were taken during 2000–2013, in which there were 17 PNA+ and 17 PNA- months (Fig. 2b). The sites with black dots were the differences that passed the two-tail t-test with 90% confidence level.”

10. Figure 5(b): Many panels show clearly two regimes. Does it make sense to fit a single line? Maybe two lines are better?

Response:

Following the suggestion, we now show fits for the eastern, western, and whole of U.S., as represented by red, blue, and black lines, respectively.

11. Figure 5 caption: Space is missing “DMof”

Response:

Corrected.

Reference:

- Allen, R. J., Landuyt, W. and Rumbold, S. T.: An increase in aerosol burden and radiative effects in a warmer world, *Nat. Clim. Chang.*, (OCTOBER), doi:10.1038/nclimate2827, 2015.
- Aw, J. and Kleeman, M. J.: Evaluating the first-order effect of intraannual temperature variability on urban air pollution, *J. Geophys. Res.*, 108(D12), 4365, doi:10.1029/2002JD002688, 2003.
- Bey, I., Jacob, D. J., Yantosca, R. M., Logan, J. a., Field, B. D., Fiore, A. M., Li, Q., Liu, H. Y., Mickley, L. J. and Schultz, M. G.: Global modeling of tropospheric chemistry with assimilated meteorology: Model description and evaluation, *J. Geophys. Res.*, 106(D19), 23073, doi:10.1029/2001JD000807, 2001.

- Dawson, J. P., Adams, P. J. and Pandis, S. N.: Sensitivity of PM<sub>2.5</sub> to climate in the Eastern US: a modeling case study, *Atmos. Chem. Phys.*, 7(16), 4295–4309, doi:10.5194/acp-7-4295-2007, 2007.
- van Donkelaar, A., Martin, R. V., Park, R. J. and Donkelaar, A. Van: Estimating ground-level PM 2.5 using aerosol optical depth determined from satellite remote sensing, *J. Geophys. Res.*, 111(D21), D21201, doi:10.1029/2005JD006996, 2006.
- Drury, E., Jacob, D. J., Spurr, R. J. D., Wang, J., Shinozuka, Y., Anderson, B. E., Clarke, A. D., Dibb, J., McNaughton, C. and Weber, R.: Synthesis of satellite (MODIS), aircraft (ICARTT), and surface (IMPROVE, EPA-AQS, AERONET) aerosol observations over eastern North America to improve MODIS aerosol retrievals and constrain surface aerosol concentrations and sources, *J. Geophys. Res.*, 115(D14), D14204, doi:10.1029/2009JD012629, 2010.
- Duncan, B. N., Martin, R. V., Staudt, A. C., Yevich, R. and Logan, J. A.: Interannual and seasonal variability of biomass burning emissions constrained by satellite observations, *J. Geophys. Res.*, 108(D2), 4100, doi:10.1029/2002JD002378, 2003.
- Generoso, S., Bréon, F.-M., Balkanski, Y., Boucher, O. and Schulz, M.: Improving the seasonal cycle and interannual variations of biomass burning aerosol sources, *Atmos. Chem. Phys.*, 3(4), 1211–1222, doi:10.5194/acp-3-1211-2003, 2003.
- Gong, S. L., Zhang, X. Y., Zhao, T. L., Zhang, X. B., Barrie, L. A., McKendry, I. G. and Zhao, C. S.: A Simulated Climatology of Asian Dust Aerosol and Its Trans-Pacific Transport. Part II: Interannual Variability and Climate Connections, *J. Clim.*, 19(1), 104–122, doi:10.1175/JCLI3606.1, 2006.
- Hand, J. L., Schichtel, B. A., Pitchford, M., Malm, W. C. and Frank, N. H.: Seasonal composition of remote and urban fine particulate matter in the United States, *J. Geophys. Res.*, 117(D5), D05209, doi:10.1029/2011JD017122, 2012.
- Hand, J. L., Schichtel, B. A., Malm, W. C., Pitchford, M. and Frank, N. H.: Spatial and seasonal patterns in urban influence on regional concentrations of speciated aerosols across the United States, *J. Geophys. Res. Atmos.*, 119, 12832–12849, doi:10.1002/2014JD022328, Received, 2014.
- Heald, C. L., J. L. Collett Jr., Lee, T., Benedict, K. B., Schwandner, F. M., Li, Y., Clarisse, L., Hurtmans, D. R., Van Damme, M., Clerbaux, C., Coheur, P.-F., Philip, S., Martin, R. V. and Pye, H. O. T.: Atmospheric ammonia and particulate inorganic nitrogen over the United States, *Atmos. Chem. Phys.*, 12(21), 10295–10312, doi:10.5194/acp-12-10295-2012, 2012.
- Holmes, C. D., Prather, M. J., Søvde, O. A. and Myhre, G.: Future methane, hydroxyl, and their uncertainties: key climate and emission parameters for future predictions, *Atmos. Chem. Phys.*, 13(1), 285–302, doi:10.5194/acp-13-285-2013, 2013.
- Jeong, J. I. and Park, R. J.: Effects of the meteorological variability on regional air quality in East Asia, *Atmos. Environ.*, 69(3), 46–55, doi:10.1016/j.atmosenv.2012.11.061, 2013.
- Kleeman, M. J.: A preliminary assessment of the sensitivity of air quality in California to global change, *Clim. Change*, 87(S1), 273–292, doi:10.1007/s10584-007-9351-3, 2007.

- Levy, H., Schwarzkopf, M. D., Horowitz, L., Ramaswamy, V. and Findell, K. L.: Strong sensitivity of late 21st century climate to projected changes in short-lived air pollutants, *J. Geophys. Res. Atmos.*, 113(6), 1–13, doi:10.1029/2007JD009176, 2008.
- Liang, Q., Jaegle, L. and Wallace, J. M.: Meteorological indices for Asian outflow and transpacific transport on daily to interannual timescales, *J. Geophys. Res.*, 110(D18), D18308, doi:10.1029/2005JD005788, 2005.
- Liu, Y., Park, R. J., Jacob, D. J., Li, Q., Kilaru, V. and Sarnat, J. A.: Mapping annual mean ground-level PM<sub>2.5</sub> concentrations using Multiangle Imaging Spectroradiometer aerosol optical thickness over the contiguous United States, *J. Geophys. Res.*, 109(D22), D22206, doi:10.1029/2004JD005025, 2004.
- Liu, Y., Liu, J. and Tao, S.: Interannual variability of summertime aerosol optical depth over East Asia during 2000–2011: a potential influence from El Niño Southern Oscillation, *Environ. Res. Lett.*, 8(4), 044034, doi:10.1088/1748-9326/8/4/044034, 2013.
- Malm, W. C., Schichtel, B. A. and Pitchford, M. L.: Uncertainties in PM<sub>2.5</sub> Gravimetric and Speciation Measurements and What We Can Learn from Them, *J. Air Waste Manage. Assoc.*, 61(11), 1131–1149, doi:10.1080/10473289.2011.603998, 2011.
- Prather, M., Holmes, C., and Hsu, J.: Reactive greenhouse gas scenarios: Systematic exploration of uncertainties and the role of atmospheric chemistry, *Geophys. Res. Lett.*, 39, doi:10.1029/2012GL051440, 2012.
- Rae, J. G. L., Bellouin, N., Jones, a., Johnson, C. E., Boucher, O. and Haywood, J. M.: Sensitivity of global sulphate aerosol production to changes in oxidant concentrations and climate, *J. Geophys. Res.*, 112(D10), D10312, doi:10.1029/2006JD007826, 2007.
- Rattigan, O. V., Felton, H. D., Bae, M.-S., Schwab, J. J. and Demerjian, K. L.: Comparison of long-term PM<sub>2.5</sub> carbon measurements at an urban and rural location in New York, *Atmos. Environ.*, 45(19), 3228–3236, doi:10.1016/j.atmosenv.2011.03.048, 2011.
- Tai, a. P. K., Mickley, L. J., Jacob, D. J., Leibensperger, E. M., Zhang, L., Fisher, J. a. and Pye, H. O. T.: Meteorological modes of variability for fine particulate matter (PM<sub>2.5</sub>) air quality in the United States: implications for PM<sub>2.5</sub> sensitivity to climate change, *Atmos. Chem. Phys.*, 12(6), 3131–3145, doi:10.5194/acp-12-3131-2012, 2012.
- Tai, A. P. K., Mickley, L. J. and Jacob, D. J.: Correlations between fine particulate matter (PM<sub>2.5</sub>) and meteorological variables in the United States: Implications for the sensitivity of PM<sub>2.5</sub> to climate change, *Atmos. Environ.*, 44(32), 3976–3984, doi:10.1016/j.atmosenv.2010.06.060, 2010.
- Vukovich, F. M.: Regional-scale boundary layer ozone variations in the eastern United States and their association with meteorological variations, *Atmos. Environ.*, 29(17), 2259–2273, doi:10.1016/1352-2310(95)00146-P, 1995.
- Walker, J. M., Philip, S., Martin, R. V. and Seinfeld, J. H.: Simulation of nitrate, sulfate, and ammonium aerosols over the United States, *Atmos. Chem. Phys.*, 12(22), 11213–11227, doi:10.5194/acp-12-11213-2012, 2012.
- van der Werf, G. R., Randerson, J. T., Giglio, L., Collatz, G. J., Kasibhatla, P. S. and Arellano, a. F.: Interannual variability of global biomass burning emissions from 1997 to 2004, *Atmos. Chem. Phys. Discuss.*, 6(2), 3175–3226, doi:10.5194/acpd-6-3175-2006, 2006.

- Wu, R., Wen, Z. and He, Z.: ENSO Contribution to Aerosol Variations over the Maritime Continent and the Western North Pacific during 2000–10, *J. Clim.*, 26(17), 6541–6560, doi:10.1175/JCLI-D-12-00253.1, 2013.
- Wu, S., Mickley, L. J., Jacob, D. J., Logan, J. A., Yantosca, R. M. and Rind, D.: Why are there large differences between models in global budgets of tropospheric ozone?, *J. Geophys. Res.*, 112(D5), D05302, doi:10.1029/2006JD007801, 2007.

The Impact of Monthly Variation of the Pacific-North America (PNA) Teleconnection  
Pattern on Wintertime Surface-layer Aerosol Concentrations in the United States

Jin Feng<sup>1,2</sup>, Hong Liao<sup>1,\*</sup>, Jianping Li<sup>3</sup>

<sup>1</sup>State key Laboratory of Atmospheric Boundary Layer Physics and Atmospheric  
Chemistry, Institute of Atmospheric Physics, Chinese Academy of Sciences, Beijing,  
China

<sup>2</sup>University of Chinese Academy of Science, Beijing, China

<sup>3</sup>College of Global Change and Earth System Science of Beijing Normal University,  
Beijing, China

\*Corresponding author address:

Prof. Hong Liao  
LAPC, Institute of Atmospheric Physics  
Chinese Academy of Sciences  
Beijing 100029, China  
E-mail: hongliao@mail.iap.ac.cn

## Abstract

The Pacific-North America teleconnection (PNA) is the leading general circulation pattern in the troposphere over the region of North Pacific to North America during wintertime. This study examined the impacts of monthly variation of the PNA phase (positive or negative phase) on wintertime surface-layer aerosol concentrations in the U.S. by analyzing observations during 1999–2013 from the **Air Quality System of the Environmental Protection Agency** (EPA-AQS) and the model results for 1986–2006 from the global three-dimensional Goddard Earth Observing System (GEOS) chemical transport model (GEOS-Chem). The composite analyses on the EPA-AQS observations over 1999–2013 showed that the average concentrations of  $\text{PM}_{2.5}$ , sulfate, nitrate, ammonium, organic carbon, and black carbon aerosols over the U.S. were higher in the PNA positive phases than in the PNA negative phases by  $1.0 \mu\text{g m}^{-3}$  (8.7%),  $0.01 \mu\text{g m}^{-3}$  (0.5%),  $0.3 \mu\text{g m}^{-3}$  (29.1%),  $0.1 \mu\text{g m}^{-3}$  (11.9%),  $0.6 \mu\text{g m}^{-3}$  (13.5%), and  $0.2 \mu\text{g m}^{-3}$  (27.8%), respectively. The simulated geographical patterns of the differences in concentrations of all aerosol species between the PNA positive and negative phases were similar to observations. Based on the GEOS-Chem simulation driven by the assimilated meteorological fields, the PNA-induced variation in planetary boundary layer height was found to be the most dominant meteorological factor that influenced the concentrations of  $\text{PM}_{2.5}$ , sulfate, ammonium, organic carbon, and black carbon, and the PNA-induced variation in temperature was the most important parameter that influenced nitrate aerosol. Results from this work have important implications for understanding and prediction of air quality in the United States.



## 1 Introduction

Aerosols are the major air pollutants that have adverse effects on human health, reduce atmospheric visibility, and influence climate through aerosol-radiation and aerosol-cloud interactions (IPCC, 2013). Aerosol concentrations are high over the industrialized regions such as the U.S., Europe, and East Asia, which are driven by emissions of aerosols and aerosol precursors (Dutkiewicz et al. 2000; Vestreng et al. 2007; Hand et al. 2012a; Mijling et al. 2013) and regional meteorological conditions.

Previous studies have shown that aerosol concentrations are very sensitive to meteorological parameters (Aw and Kleeman 2003; Wise and Comrie 2005; Dawson et al. 2007; Kleeman 2008; Jacob and Winner 2009; Tai et al. 2010; Tai et al. 2012a; Allen et al. 2015; Markakis et al. 2015; Megaritis et al. 2014; Porter et al. 2015). Aw and Kleeman (2003) examined the sensitivity of  $PM_{2.5}$  (aerosol particles which diameter  $\leq 2.5 \mu m$ ) concentration to temperature by performing sensitivity studies in the California Institute of Technology/UC Davis (CIT/UCD) air quality model. A cross-board increase in temperature by 5 K in Southern California on September 25, 1996, led to decreases in peak  $PM_{2.5}$  concentrations by up to  $30.7 \mu g m^{-3}$  (~30%). Wise and Comrie (2005) reported, by statistical analyses of observational datasets obtained from Air Quality System of U.S. Environmental Protection Agency (EPA-AQS), that the variations in meteorological parameters accounted for 20–50% of the variability in aerosol levels over 1990–2003 in five metropolitan areas in the southwestern U.S.. They found that aerosols in these five cities were most sensitive to relative humidity. Dawson et al. (2007) found, by sensitivity studies in the Particulate Matter Comprehensive Air Quality Model with extensions (PMCAMx), that  $PM_{2.5}$  concentrations in summer had a small sensitivity to temperature increases ( $-16 ng m^{-3} K^{-1}$  on average) because the increases in sulfate offset the decreases in

nitrate and organics, while PM<sub>2.5</sub> concentrations in winter decreased significantly with temperature ( $-170 \text{ ng m}^{-3} \text{ K}^{-1}$  on average) because the increases in temperature led to large reductions in nitrate and organics. Dawson et al. (2007) also showed that PM<sub>2.5</sub> concentrations increased with humidity in both winter and summer. Jacob and Winner (2009) summarized by literature review that the regional stagnation, mixing depth, and precipitation are the most important meteorological parameters that influence surface-layer aerosol concentrations. Future climate change was also simulated to influence aerosol levels over the U.S. by about  $1 \text{ } \mu\text{g m}^{-3}$  (Jacob and Winner 2009), as a result of the climate-induced changes in atmospheric oxidants, transport, deposition, and the shift of gas-particle equilibria (Liao et al. 2006; Unger et al. 2006; Bauer et al. 2007; Jacob and Winner 2009; Pye et al. 2009; Lam et al. 2011; Day and Pandis 2011; Juda-Rezler et al. 2012; Tai et al. 2012b).

Previous studies have also reported that the changes in atmospheric circulation pattern and climate systems, such as the East Asian Summer Monsoon (EASM), North Atlantic Oscillation (NAO), El Nino-South Oscillation (ENSO), Atlantic Multidecadal Oscillation (AMO), and Arctic sea ice (ASI), can modulate distributions and concentrations of aerosols (Moulin et al. 1997; Singh and Palazoglu 2012; Zhu et al. 2012; Jerez et al. 2013; Liu et al. 2013; Xiao et al. 2014; Wang et al. 2015). Zhu et al. (2012) found, by simulation of aerosol concentrations over years 1986–2006 with the global chemical transport model GEOS-Chem, that the decadal-scale weakening of the EASM led to increases in aerosol concentrations in eastern China, and summertime surface aerosol concentrations in the weakest EASM years were larger than those in the strongest EASM years by approximately 20%. Moulin et al. (1997) showed that the variations in NAO could influence mineral dust aerosol transported to the North Atlantic Ocean and the Mediterranean Sea, since the mean aerosol optical

depth (AOD) of dust in summer correlated with the NAO index during 1983–1994 with a correlation coefficient of 0.50. Jerez et al. (2013) found, by simulations of aerosols for years 1970–1999 with the CHIMERE chemistry transport model driven by the BCMWF ERA40 reanalysis data, that the concentrations of  $PM_{10}$  and  $PM_{2.5}$  in the southern European regions in winter differed by 10 and 20  $\mu g\ m^{-3}$ , respectively, between the positive and negative NAO phases. By using the multi-angle imaging spectroradiometer satellite (MISR) datasets of AOD during 2000–2011, Liu et al. (2013) found a period of 3–4 years in observed summertime AOD over the North China Plain (NCP), and the peak of summertime AOD in NCP occurred four months later after the rapidly transition of El Nino from a warm phase to a cold phase because of the associated cyclone anomaly and maritime inflow over the NCP. Singh and Palazoglu (2012) found correlations between PDO and ENSO and the aerosol exceedance days (defined as the days with  $PM_{2.5}$  concentrations larger than the U.S. National Ambient Air Quality Standard) at 6 regions in the U.S. by using the EPA-AQS  $PM_{2.5}$  wintertime datasets during 1950–2008.

The Pacific-North America teleconnection pattern (PNA) is one of the most recognized, influential climate patterns in the mid-latitudes over the region of North Pacific to North America during wintertime with monthly variations (Wallace and Gutzler 1981; Blackmon et al. 1984; Liang et al. 2005; Athanasiadis and Ambaum 2009). The PNA phase is defined by the geopotential height anomalies in the middle troposphere over the vicinity of Hawaii, the south of the Aleutian Islands, the intermountain region of North America, and the Gulf Coast region in the U.S. (Wallace and Gutzler 1981). A positive (negative) PNA phase is characterized by positive (negative) geopotential height anomalies over the vicinity of Hawaii and the northwestern North America, while negative (positive) geopotential height anomalies

over south of the Aleutian Islands and the Gulf Coast region (see Fig. S1 in the auxiliary material).

The PNA has large impacts on surface-layer meteorological variables in the U.S. during wintertime. Previous studies have reported strong positive (negative) correlation between PNA and surface ambient temperature in the northwestern (southeastern) U.S. (Leathers et al. 1991; Redmond and Koch 1991; Liu et al. 2015), and negative correlation between PNA and precipitation rate (Leathers et al. 1991; Coleman and Rogers 2003; Ning and Bradley 2014; 2015) and moisture (Coleman and Rogers 2003) in the contiguous Ohio River Valley. These variations in meteorological parameters in the U.S. are associated with the PNA-induced anomalies in jet stream position, activities of cold fronts, and synoptic cyclones (Leathers et al. 1991; Notaro et al. 2006; Myoung and Deng 2009).

Several studies have examined the impacts of PNA on aerosols. Gong et al. (2006) studied the interannual variations in the trans-Pacific transport of Asian dust during 1960–2003 by using the Northern Aerosol Regional Climate Model (NARCM). They found a negative correlation (with a correlation coefficient of  $-0.55$ ) between the PNA and the ratio of dust mass that reached the North American continent to that exported from Asia because of the strong westerly jet in the East Pacific during the negative PNA phases. Di Pierro et al. (2011), by using satellite retrieval of aerosol optical depth (AOD) from Cloud-Aerosol Lidar with Orthogonal Polarization (CALIOP), identified 11 events of Asian aerosol transport to the Arctic during 2007 to 2009, in which 4 events were associated with the negative PNA phases. These studies, however, were focused on the impact of PNA on the transport of aerosols due to the variations in westerly jet stream and blocking activity. Furthermore, these studies were limited to aerosols in the regions of North America and the Arctic.

We examine in this work the impacts of monthly variations in PNA phase on aerosol concentrations in the U.S. during wintertime, by analyses of the observed aerosol concentrations during 1999–2013 from EPA-AQS and also by simulations of aerosol concentrations for years 1986–2006 using the global chemical transport model GEOS-Chem. The scientific goals of this work are (1) to quantify the differences in wintertime concentrations of sulfate ( $\text{SO}_4^{2-}$ ), nitrate ( $\text{NO}_3^-$ ), ammonium ( $\text{NH}_4^+$ ), black carbon (BC), organic carbon (OC), and  $\text{PM}_{2.5}$  in the U.S. between different PNA phases, and (2) to understand the roles of PNA-induced variations in meteorology (for example, surface air temperature, wind speed, planetary boundary layer height, precipitation, and relative humidity) in influencing the wintertime aerosol concentrations. The definition of the PNA index, the EPA-AQS observation data used in this work, and the numerical simulation with the GEOS-Chem model are described in Sect. 2. Sections 3 and 4 present the impacts of the PNA on wintertime aerosol concentrations in the U.S. obtained from the EPA-AQS observations and the GEOS-Chem simulation, respectively. The mechanisms for the impacts of PNA on aerosols are examined in Sect. 5.

## **2 Data, simulation, and methodology**

### **2.1 Observed aerosol concentrations**

Observed concentrations of aerosols are obtained from the Air Quality System of the U.S. Environmental Protection Agency (EPA-AQS, <http://www.epa.gov/airquality/airdata/>). The EPA-AQS daily  $\text{PM}_{2.5}$  mass concentrations are available over 1999–2013 at about 1200 sites, and the speciated aerosol concentrations, including those of  $\text{SO}_4^{2-}$ ,  $\text{NO}_3^-$ ,  $\text{NH}_4^+$ , BC and OC, are available for 2000–2013 at about 300 sites.

The measurements of aerosol concentrations from the EPA-AQS were carried out at various time intervals (for example, with measurements every one, three or six days) at different sites, and there were plenty of missing values at many sites. The observed concentrations are pre-processed following the **three** steps: (1) For a specific site, the observations are used in our analyses if the site had at least 5 months of observations and **there were at least 5 observation records within each month**. (2) The mean seasonal cycle in aerosol concentrations in the months of November-March is removed by using the similar approach to that used for PNA index (see Sect. 2.3 below). Such deseasonality approach was used in previous studies that examined the monthly variations in mineral dust aerosol (Cakmur et al. 2001; Mahowald et al. 2003), the decreasing trends in observed PM<sub>2.5</sub> concentrations and satellite AOD in the southeastern U.S. over 2000–2009 (Alston et al. 2012), and the monthly variations in global AOD (Li et al. 2013). (3) **Since the observed aerosol concentrations exhibited a significant decreasing trend from 1999 to present in the U.S. due to the reductions in emissions of aerosols and aerosol precursors (Alston et al. 2012, <http://www3.epa.gov/airtrends/aqtrends.html#comparison>), the long-term linear trend in concentrations is identified by the least-square fit and then removed from the observed concentrations for each site**. The EPA-AQS sites with measurements that meet the criteria described in (1) are shown in Fig. 1.

## **2.2 GEOS-Chem Simulation**

We also examine the impacts of PNA on simulated aerosol concentrations in the U.S. by using the GEOS-Chem model (version 8-2-1, <http://acmg.seas.harvard.edu/geos>). The GEOS-Chem model is a global chemical transport model driven by the assimilated meteorological fields from the Goddard Earth Observing System (GEOS) of the NASA Global Modeling and Assimilation Office (GMAO). The version of the



model we use has a horizontal resolution of  $2^\circ \times 2.5^\circ$  and 30 hybrid sigma-P layers from the surface to 0.01 hPa altitude. The model has a fully coupled simulation of tropospheric  $\text{O}_3$ - $\text{NO}_x$ -VOC chemistry and aerosols including  $\text{SO}_4^{2-}$ ,  $\text{NO}_3^-$ ,  $\text{NH}_4^+$ , BC, OC (Park et al. 2003; Park et al. 2004), mineral dust (Fairlie et al. 2007), and sea salt (Alexander et al. 2005). Considering the large uncertainties in chemistry schemes of secondary organic aerosol (SOA), SOA in our simulation is assumed to be the 10% carbon yield of OC from biogenic terpenes (Park et al., 2003) and 2% carbon yield of OC from biogenic isoprene (van Donkelaar et al., 2007; Mu and Liao, 2014). We mainly examine simulated anthropogenic aerosols from the GEOS-Chem simulation, since mineral dust concentrations in winter are very small (Malm et al. 2004; Zhang et al. 2013) and sea salt is not a major aerosol species in the U.S. (Malm et al. 2004).

The model uses the advection scheme of Lin and Rood (1996), the deep convective scheme of Zhang and McFarlane (1995), the shallow convection scheme of Hack (1994), the wet deposition scheme of Liu et al. (2001), and the dry deposition scheme of Wesely (1989) and Wang et al. (1998). The instantaneous vertical mixing in the planetary boundary layer (PBL) is accounted for by the TURBDAY mixing scheme (Bey et al., 2001). The PBL occupies the lowest 3–6 vertical model layers over the U.S..

We simulate aerosols for years of 1986–2006 driven by the GEOS-4 reanalysis data. The years of 1986–2006 are chosen for chemistry-aerosol simulation because these are the years that the GEOS-4 datasets are available. Global anthropogenic emissions are from the Global Emissions Inventory Activity (GEIA) (Park et al. 2004; Park et al. 2006; Zhu et al. 2012; Yang et al. 2015). Anthropogenic emissions over the U.S. are overwritten by the U.S. EPA National Emission Inventory for 1999 (NEI99), which have monthly variations in emissions of precursors including  $\text{SO}_2$ ,  $\text{NO}_x$ , and

NH<sub>3</sub>. Monthly biomass burning emissions are taken from the Global Fire Emissions Database version 2 (GFED-2) (Giglio et al. 2006; van der Werf et al. 2006). During the simulation of aerosols for years of 1986–2006, the global anthropogenic and biomass burning emissions of aerosols and aerosol precursors are fixed at year 2005 levels, so that the variations in aerosol concentrations are caused by variations in meteorological parameters (PNA phases) alone.

Natural emissions of O<sub>3</sub> precursors, including biogenic NMVOCs and NO<sub>x</sub> from lightning and soil, are allowed to vary over 1986–2006 following the variations in the GEOS-4 meteorological parameters. Biogenic NMVOC emissions are calculated using the module of Model of Emissions of Gases and Aerosols from Nature (Guenther et al. 2006). Lightning NO<sub>x</sub> emissions are described by Sauvage et al. (2007) and Murray et al. (2012). Soil NO<sub>x</sub> emissions are calculated using the algorithm proposed by Yienger and Levy (1995).

The GEOS-Chem simulation of aerosols in the U.S. have been evaluated extensively by previous studies (Park et al. 2003; Park et al. 2004; Park et al. 2005; Heald et al. 2006; van Donkelaar et al. 2006; Liao et al. 2007; Heald et al. 2008; van Donkelaar et al. 2008; Fu et al. 2009; Drury et al. 2010; Leibensperger et al. 2011; Zhang et al. 2012). These studies have shown that the GEOS-Chem model can capture the magnitudes and distributions of aerosols in the U.S..

### **2.3 PNA index**

The PNA index (PNAI) is commonly used to quantify the changes in PNA phase (Wallace and Gutzler 1981; Leathers et al. 1991). This study follows the definition of PNAI by Leathers et al. (1991). In order to examine the monthly variations in PNA, the mean seasonal cycle of geopotential height at 700 hPa is removed for the months of November, December, January, February, and March (NDJFM) in the studied years.

Such deseasonality approach has been used in the analyses of the growth and decay of PNA phase in NDJFM (Feldstein 2002), the development of NAO (Feldstein 2003), the influence of NAO on precipitation in Europe (Qian et al. 2000), and the variations in Madden–Julian oscillation (Wheeler and Hendon 2004). If we are concerned with the PNAI during  $n$  years, the monthly PNAI in month  $j$  ( $j$  is one of the 5 months of NDJFM) of year  $i$  is calculated by:

$$PNAI = \frac{1}{3} [-Z_{i,j}^*(47.9^\circ N, 170^\circ W) + Z_{i,j}^*(47.9^\circ N, 110^\circ W) - Z_{i,j}^*(29.7^\circ N, 86.3^\circ W)] \quad (1)$$

where  $Z_{i,j}^* = \frac{Z'_{i,j}}{\sqrt{\frac{1}{n \times 5} \sum_{i=1}^n \sum_{j=1}^5 Z_{i,j}'^2}}$  and  $Z'_{i,j} = Z_{i,j} - \frac{1}{n} \sum_{i=1}^n Z_{i,j}$ . Therefore,  $Z'_{i,j}$  denotes the removal of seasonal cycle, and  $Z_{i,j}^*$  denotes the standardized anomaly of geopotential height at 700 hPa in month  $j$  of year  $i$  with seasonal-cycle removed.

The PNAI is calculated by using both the National Center of Environmental Prediction-Department of Energy Atmospheric Model Inter-comparison Project Reanalysis data (NCEP-2, horizontal resolution  $2.5^\circ \times 2.5^\circ$  globally, <http://www.esrl.noaa.gov/psd/data/gridded/data.ncep.reanalysis2.html>) for years of 1986–2013 (referred to as NCEP2-PNAI) and the GEOS-4 assimilated meteorological data (referred to as GEOS4-PNAI) for 1986–2006 (Fig. 2). Both series of PNA index show strong monthly variations (Fig. 2), and the GEOS4-PNAI agrees with NCEP2-PNAI over 1986–2006 with a high correlation coefficient of 0.99, indicating that the NCEP-2 and GEOS-4 datasets are consistent in representing the monthly variations of PNAI.

There are  $n \times 5$  PNAI values for  $n$  years, since we calculate PNAI for the months of NDJFM of each year. These  $n \times 5$  PNAI values are classified into 3 categories for our composite analyses of aerosol concentrations and meteorological parameters: the positive PNA months (PNA+) that are 25% of the  $n \times 5$  PNAI months with the highest

positive PNAI values, the negative PNA months (PNA–) that are 25% of the  $n \times 5$  PNAI months with the highest negative PNAI values, and the rest months that are referred to as the transitional months (Fig. 2).

### 3 Impacts of PNA on observed aerosol concentrations

The measurements of  $PM_{2.5}$  are available over 1999–2013, in which there were 18 PNA+ months and 18 PNA– months as shown in Fig. 2a. Figure 3 shows the differences in observed surface-layer  $PM_{2.5}$  concentrations between the PNA+ and PNA– months (concentrations averaged over the 18 PNA+ months minus those averaged over the 18 PNA– months). The uncertainty associated with the differences in aerosol concentrations between PNA+ and PNA– months is represented by the two-tail Student-t test with significance level of 90%. Among 1044 sites with  $PM_{2.5}$  concentrations (Fig.1), 42% of which had statistically significant differences in  $PM_{2.5}$  between PNA+ and PNA– months. Relative to the PNA– months,  $PM_{2.5}$  concentrations in PNA+ months were higher in California, the contiguous Salt Lake (northern Utah), and over and near the eastern Midwest. The enhancement of  $PM_{2.5}$  reached 7–9  $\mu g m^{-3}$  (or 40–80%) in California, 7–9  $\mu g m^{-3}$  (80–100%) around the Salt Lake, 3–5  $\mu g m^{-3}$  (40–80%) over and near the eastern Midwest. At sites in North Dakota, Wisconsin, Michigan, Minnesota, Montana, Texas and Maine, the  $PM_{2.5}$  concentrations were lower by up to 2  $\mu g m^{-3}$  (–10 to –20%) in PNA+ months than in PNA– months. As the concentrations are averaged over all sites (including the sites that pass and do not pass the t-test with 90% confidence level) in the U.S., the western U.S. (west of 100°W, Fig.1), and the eastern U.S. (east of 100°W, Fig. 1),  $PM_{2.5}$  concentrations were higher by 1.0  $\mu g m^{-3}$  (8.7%), 1.3  $\mu g m^{-3}$  (14.3%), and 0.8  $\mu g m^{-3}$  (7.2%), respectively, in the PNA+ months than in PNA– months (Table 1).

298 The measurements of speciated aerosols are available during 2000–2013, in  
 299 which there were 17 PNA+ and 17 PNA– months (Fig. 2b). Figure 3 also shows the  
 300 differences in observed surface-layer concentrations of individual aerosol species  
 301 between the PNA+ and PNA– months. The differences in concentrations of  $\text{SO}_4^{2-}$ ,  
 302  $\text{NO}_3^-$  and  $\text{NH}_4^+$  show statistically significant positive values at most sites. Among the  
 303 355, 343, and 194 sites with measurements of  $\text{SO}_4^{2-}$ ,  $\text{NO}_3^-$  and  $\text{NH}_4^+$ , 30%, 44%, and  
 304 39% of which pass the two-tail t-test with 90% confidence level, respectively. While  
 305 the absolute differences in concentrations of  $\text{SO}_4^{2-}$ ,  $\text{NO}_3^-$  and  $\text{NH}_4^+$  between PNA+  
 306 and PNA– were in the range of 0–1  $\mu\text{g m}^{-3}$  at most sites, the maximum differences  
 307 reached 1.5–2.5  $\mu\text{g m}^{-3}$  (30–50%) for  $\text{SO}_4^{2-}$  in Pennsylvania, 1.5–2.5  $\mu\text{g m}^{-3}$  (150–  
 308 200%) for  $\text{NO}_3^-$  in Illinois, Indiana and Ohio, and 1.5–2.5  $\mu\text{g m}^{-3}$  (50–70%) for  $\text{NH}_4^+$  in  
 309 Pennsylvania. Averaged over the sites with measurements, the absolute differences  
 310 in concentrations of  $\text{SO}_4^{2-}$  and  $\text{NO}_3^-$  between PNA+ and PNA– months were larger in  
 311 the eastern U.S. than in the western U.S.. As shown in Table 1, the differences in the  
 312 averaged concentrations of  $\text{SO}_4^{2-}$ ,  $\text{NO}_3^-$  and  $\text{NH}_4^+$  were, respectively, 0.1  $\mu\text{g m}^{-3}$   
 313 (3.7%), 0.4  $\mu\text{g m}^{-3}$  (36.5%), and 0.1  $\mu\text{g m}^{-3}$  (10.5%) in the eastern U.S., 0.03  $\mu\text{g m}^{-3}$   
 314 (3.2%), 0.2  $\mu\text{g m}^{-3}$  (23.8%), and 0.2  $\mu\text{g m}^{-3}$  (31.6%) in the western U.S., as well as  
 315 0.01  $\mu\text{g m}^{-3}$  (0.5%), 0.3  $\mu\text{g m}^{-3}$  (29.1%), and 0.1  $\mu\text{g m}^{-3}$  (11.9%) in the whole of U.S..

316 With regard to carbonaceous aerosols, among the 105 and 104 sites with  
 317 measurements of OC and BC, 39% and 31% of which pass the two-tail t-test with 90%  
 318 confidence, respectively. The differences in concentrations of these two species  
 319 between PNA+ and PNA– months show similar geographical pattern, with positive  
 320 values at most sites but negative values in Michigan, New York, and the South  
 321 Atlantic States. The maximum differences between the PNA+ and PNA– months  
 322 reached 2.5–3  $\mu\text{g m}^{-3}$  (50–70%) in Kentucky for OC. Averaged over sites with

measurements available, the absolute differences in OC and BC concentrations between the PNA+ and PNA– months were larger in the western U.S. than in the eastern U.S. (Table 1). Among all aerosol species listed in Table 1, OC exhibited the largest absolute differences between the PNA phases in the western U.S., because OC accounts for 25–65% of  $PM_{2.5}$  in the western U.S. (Malm et al. 2004) and the OC observed by EPA-AQS network, which are located in urban and suburban settings, were higher than the observations by other long term networks in U.S. (Malm et al. 2011, Rattigan et al. 2011, Hand et al. 2012b, 2014).

Observations from EPA-AQS datasets indicate the large impacts of PNA phase on aerosol concentrations in the U.S.. It should be noted that, in our analyses above, the locations of measurements and the numbers of samples were different for different aerosol species. The regional averages were also influenced by the uneven distributions of observational sites in different regions. Therefore, model results from the GEOS-Chem simulation will be used to further analyze the impacts of PNA on aerosols in the U.S., as presented in the subsequent sections.

We have also calculated the correlation coefficient between PNAI and EPA-AQS surface aerosol concentrations at each site for each aerosol species ( $PM_{2.5}$ ,  $SO_4^{2-}$ ,  $NO_3^-$ ,  $NH_4^+$ , OC, or BC) (see auxiliary Fig. S2). At most sites, positive (negative) correlation coefficients in Fig. S2 corresponded to the increases (decreases) in aerosol concentration in PNA+ months relative to PNA– months shown in Fig. 3. Positive correlation coefficients were large over California, the contiguous Salt Lake, and over and near the eastern Midwest. The fraction of temporal variability explained by PNA (FTVEP) can be quantified approximately by the square of correlation coefficient (<http://mathbits.com/MathBits/TISection/Statistics2/correlation.htm>) (see auxiliary Fig. S3). For all aerosol species, FTVEP were about 5–15% at most sites.



For  $\text{PM}_{2.5}$ ,  $\text{SO}_4^{2-}$ ,  $\text{NO}_3^-$  and  $\text{NH}_4^+$  aerosols, FTVEP values were high over and near the eastern Midwest, where the PNA teleconnection explained up to 50%, 40%, 50%, and 40% of temporal variances of surface concentrations of these aerosol species, respectively.

## 4 Impacts of PNA on simulated aerosol concentrations

### 4.1 Simulated aerosol concentrations and model evaluation

Fig. 4a shows the simulated surface-layer concentrations of  $\text{PM}_{2.5}$  (the sum of  $\text{SO}_4^{2-}$ ,  $\text{NO}_3^-$ ,  $\text{NH}_4^+$ , BC, and OC) and each aerosol species averaged over NDJFM of 1999–2006. These years are selected because they are the common years of model results and EPA-AQS observation datasets. The simulated  $\text{PM}_{2.5}$  concentrations were higher in the eastern U.S. than in the western U.S.. The maximum surface  $\text{PM}_{2.5}$  concentrations reached 14–16  $\mu\text{g m}^{-3}$  in Ohio and Pennsylvania.  $\text{PM}_{2.5}$  concentrations in the western U.S. were generally less than 4  $\mu\text{g m}^{-3}$ , except for California where  $\text{PM}_{2.5}$  concentrations were 2–6  $\mu\text{g m}^{-3}$ . The distribution of  $\text{SO}_4^{2-}$  was similar to that of  $\text{PM}_{2.5}$ , with higher concentrations in the eastern U.S. (1–8  $\mu\text{g m}^{-3}$ ) than in the western U.S. (0–3  $\mu\text{g m}^{-3}$ ) due to the coal-fired power plants in the Midwest (Park et al. 2006). The concentrations of  $\text{NO}_3^-$  and  $\text{NH}_4^+$  were the highest over and near the eastern Midwest, with values of 3–4 and 2–3  $\mu\text{g m}^{-3}$ , respectively. The maximum OC concentrations were simulated to be 2–3  $\mu\text{g m}^{-3}$  in two regions, from Ohio to Massachusetts and from Alabama to South Carolina. The simulated BC concentrations in the U.S. were 0–1  $\mu\text{g m}^{-3}$ , except for the contiguous New York where BC concentrations reached 1–2  $\mu\text{g m}^{-3}$ . The magnitudes and geographic distributions of  $\text{SO}_4^{2-}$ ,  $\text{NO}_3^-$ ,  $\text{NH}_4^+$  concentrations simulated in our work are similar to

those simulated by Park et al. (2006) and Pye et al. (2009), and our simulated OC and BC were similar to those reported by Park et al. (2003).

Figure 4b presents the scatter plots of the simulated concentrations versus the EPA-AQS observations. The simulated PM<sub>2.5</sub> concentrations had normalized mean bias (  $NMB = \sum_{m=1}^M (S_m - O_m) / \sum_{m=1}^M (O_m) \times 100\%$  , where  $S_m$  and  $O_m$  are the simulated and observed aerosol concentrations in month  $m$ , respectively.  $M$  is the total number of winter months examined) of -30% over the U.S., and the correlation coefficient between simulated and observed PM<sub>2.5</sub> concentrations was 0.57. The simulated wintertime SO<sub>4</sub><sup>2-</sup>, NO<sub>3</sub><sup>-</sup> and NH<sub>4</sub><sup>+</sup> had NMBs of 37%, 4%, and 26%, respectively. Similar bias in simulated SO<sub>4</sub><sup>2-</sup> in December-January-February (DJF) was reported Park et al. (2006), as the GEOS-Chem model results were compared with observations from the Clean Air Status and Trends Network (CASTNET). The high bias in our simulated NH<sub>4</sub><sup>+</sup> was associated with the overestimation of SO<sub>4</sub><sup>2-</sup>. Our model underestimates PM<sub>2.5</sub>, SO<sub>4</sub><sup>2-</sup>, NO<sub>3</sub><sup>-</sup>, NH<sub>4</sub><sup>+</sup>, OC and BC in the western U.S. (Fig. 4b), which can be explained in part by the relatively high aerosol concentrations observed for this region from the EPA-AQS. Hand et al. (2014) compared the observed concentrations of aerosols from the EPA-AQS with those from the Interagency Monitoring of Protected Visual Environments (IMPROVE) for 2008–2011, and showed that the ratios of wintertime aerosol concentrations of ammonium sulfate, ammonium nitrate, OC, and BC from the EPA-AQS to those from the IMPROVE were, respectively, 2.3, 7.7, 8.3, and 13.1, as the concentrations were averaged over the western U.S.. Liu et al. (2004) also attributed the high EPA-AQS concentrations in the western U.S. to the relative sparse urban sites that were heavily influenced by strong local sources such as automobiles and wood fires. The low model biases in the western U.S. may also be caused by the biases in emissions in the model.

Since this study is dedicated to examine the influence of PNA phase on the month-to-month variations of aerosol concentrations during wintertime, Fig. 4c compares, for each aerosol species, the deviation from the mean (DM) of observed concentration with that of simulated concentration for each winter month. The DM is defined as  $DM_m = (C_m - \frac{1}{M} \sum_{m=1}^M C_m) / \frac{1}{M} \sum_{m=1}^M C_m$ , where  $C_m$  is the simulated average aerosol concentration over the U.S. in month  $m$ , and  $M$  is the number of winter months examined (we consider the months of NDJFM over 1999–2006 for PM<sub>2.5</sub>, and the months of NDJFM over 2000–2006 for SO<sub>4</sub><sup>2-</sup>, NO<sub>3</sub><sup>-</sup>, NH<sub>4</sub><sup>+</sup>, BC, and OC). The model captures fairly well the peaks and troughs of DMs for PM<sub>2.5</sub>, SO<sub>4</sub><sup>2-</sup>, NO<sub>3</sub><sup>-</sup> and NH<sub>4</sub><sup>+</sup>, with correlation coefficients of 0.61, 0.45, 0.33, and 0.65, respectively. The model does not capture well the monthly variations of DMs of concentrations of OC and BC, because both anthropogenic and biomass burning emissions are fixed at year 2005 levels during our simulation over 1986–2006 to isolate the impacts of variations in meteorological parameters (PNA phases) on aerosols (see Sect. 2.2). Since the biomass burning emissions, which contribute largely to carbonaceous aerosols, have large interannual variations (Duncan et al., 2003; Generoso et al., 2003; van der Werf et al., 2006), we also show in Fig. 4c the time series of DMs of biomass burning emissions of OC and BC by using biomass burning emissions in NDJFM over 2000–2006 from GFED v2. The correlation coefficients between biomass burning emissions and observed concentrations of OC and BC were 0.36 and 0.34, respectively, indicating that the observed variations in OC and BC were influenced by monthly and interannual variations in biomass burning. We have also calculated the temporal correlation coefficient between EPA-AQS observations and GEOS-Chem model results at each site for each aerosol species (auxiliary Fig. S4). The temporal correlations were statistically significant for PM<sub>2.5</sub>, SO<sub>4</sub><sup>2-</sup>, NO<sub>3</sub><sup>-</sup>, NH<sub>4</sub><sup>+</sup> at

most sites in the U.S., especially over and near the eastern Midwest where largest increases in aerosol concentrations were identified in the PNA+ months relative to the PNA– months.

## 4.2 Impact of PNA on simulated surface-layer aerosol concentrations

We have performed the GEOS-Chem simulation for years 1986–2006, in which there were 35 PNA+ and 35 PNA– months (Fig. 2). Figure 5a shows the concentrations of  $PM_{2.5}$  and each aerosols species ( $SO_4^{2-}$ ,  $NO_3^-$ ,  $NH_4^+$ , BC, and OC) averaged over the PNA– months of 1986–2006. The magnitudes and geographic distributions of aerosol concentrations in PNA– months were similar to those averaged over NDJFM of years 1999–2006 in Fig. 4.

The simulated absolute and relative differences in aerosol concentrations between PNA+ and PNA– months are shown in Figs. 5b and 5c. The  $PM_{2.5}$  concentrations over the U.S. are simulated to increase in PNA+ relative to PNA– months. The maximum enhancement in  $PM_{2.5}$  concentrations in PNA+ months was  $1.8\text{--}2.4\ \mu\text{g m}^{-3}$  (20–40%), located in the juncture of Tennessee and Arkansas. Note that the pattern of simulated differences in  $PM_{2.5}$  between PNA+ and PNA– months was similar to that of observations (Fig. 3), except that the simulated differences were not large in California, mainly due to the underestimation of OC in California as compared to EPA-AQS data (Fig. 4b). The simulated  $PM_{2.5}$  concentrations were higher by  $0.6\ \mu\text{g m}^{-3}$  (12.2%),  $0.3\ \mu\text{g m}^{-3}$  (14.0%), and  $0.9\ \mu\text{g m}^{-3}$  (10.8%) over the whole of, western, and eastern U.S., respectively, in the PNA+ months than in PNA– months (Table 2). The simulated relative difference in  $PM_{2.5}$  was close to that from observations (Table 1) in the western U.S., but the simulated relative differences in  $PM_{2.5}$  were larger than those from observations in the eastern and whole of U.S..

Fig. 5 also shows the differences in simulated surface-layer concentrations of  $\text{SO}_4^{2-}$ ,  $\text{NO}_3^-$  and  $\text{NH}_4^+$  between the PNA+ and the PNA- months. The differences in concentrations of  $\text{SO}_4^{2-}$  were larger in the western than in the eastern U.S., with maximum enhancements of 0.4–0.8  $\mu\text{g m}^{-3}$  (30–50%) over the West North Central States (South Dakota, Nebraska, Minnesota, Iowa, and Missouri). The differences in concentrations of  $\text{NO}_3^-$  and  $\text{NH}_4^+$  between PNA+ and PNA- months had similar geographical patterns, with increases in concentrations in a large fraction of the eastern U.S. and over a belt region along the Rocky Mountain in the western U.S.. The increases in concentrations of  $\text{NO}_3^-$  and  $\text{NH}_4^+$  over the eastern U.S. in PNA+ months relative to PNA- months agreed very well with those seen in observations (Fig. 3). The differences in concentrations of  $\text{SO}_4^{2-}$ ,  $\text{NO}_3^-$  and  $\text{NH}_4^+$  in the eastern U.S. between the PNA+ and PNA- months were 0.2  $\mu\text{g m}^{-3}$  (4.0%), 0.4  $\mu\text{g m}^{-3}$  (33.5%), and 0.2  $\mu\text{g m}^{-3}$  (13.2%), respectively (Table 2).

The differences in concentrations of OC and BC between PNA+ and PNA- months had similar geographical patterns, with large increases in concentrations over and near the eastern Midwest and the region from northwestern U.S. to Texas. The maximum differences reached 0.2–0.4  $\mu\text{g m}^{-3}$  (10–20%) and 0.1–0.2  $\mu\text{g m}^{-3}$  (20–30%) in Illinois, Indiana and Ohio for OC and BC, respectively. The magnitudes of the differences in OC and BC were statistically significant but were smaller than the observations (Tables 1 and 2). The absolute differences in OC were less than 0.1  $\mu\text{g m}^{-3}$  in the western, eastern and whole of U.S due to the underestimation of OC in the simulation.

In summary, model results agreed with observations in that the concentrations of all aerosol species of  $\text{SO}_4^{2-}$ ,  $\text{NO}_3^-$ ,  $\text{NH}_4^+$ , BC, and OC averaged over the U.S. were higher in PNA+ months than in PNA- months. Relative to the PNA- months, the

average concentration of  $PM_{2.5}$  over the U.S. was higher by about 8.7% (12.2%) based on observed (simulated) concentrations. Furthermore, simulated geographical patterns of the differences in  $PM_{2.5}$  and each aerosol species between the PNA+ and PNA– months were similar to those seen in observations, with the largest increases in aerosol concentrations in PNA+ months over and near the eastern Midwest.

## **5 Mechanisms for the impact of PNA on aerosol concentrations**

### **5.1 The impact of PNA on transboundary transport of aerosols**

The transboundary transport of pollutants to and from the U.S. depends largely on winds in the free troposphere (Liang et al. 2004). Figure 6 shows the horizontal winds at 700 hPa averaged over the winter months of NDJFM of 1986–2006 and the corresponding differences between PNA+ and PNA– months on the basis of the GEOS-4 meteorological fields. Strong westerlies prevailed over the U.S. in wintertime (Fig. 6a). Relative to the PNA– months, anomalous northeasterlies occurred over a large fraction of U.S. in the PNA+ months. Anomalous anti-cyclonic circulation occurred near the northwestern U.S. and anomalous cyclonic circulation occurred near the southeastern U.S. (Fig. 6b), corresponding to the large positive and negative differences in geopotential height in these two regions (see auxiliary Fig. S1), respectively.

We also calculate mass fluxes of  $PM_{2.5}$  at the four lateral boundaries (from the surface to 100 hPa) of the U. S. for different PNA phases (Table 3). The domain of the box to represent the U. S. is (75–120°W, 28–49°N), as shown in Fig. 6b. For  $PM_{2.5}$  in wintertime, the inflow from the west boundary and the outflow from the east boundary had the largest absolute values (Table 3). Relative to the PNA– months, the inflow from the west boundary and the outflow from the east boundary in PNA+ months



exhibited reductions of  $17.1 \text{ kg s}^{-1}$  and  $12.8 \text{ kg s}^{-1}$ , respectively (Table 3). The inflow flux from south boundary decreased by  $19.3 \text{ kg s}^{-1}$ , and the inflow flux from north boundary increased by  $37.6 \text{ kg s}^{-1}$ , leading to a net increase of inflow flux of  $14.0 \text{ kg s}^{-1}$  in PNA+ months. Therefore, the transboundary transport has an overall effect of increasing  $\text{PM}_{2.5}$  aerosols in the U.S. in PNA+ months relative to PNA– months. The relative change in net flux was 11.4%  $((\text{PNA+ minus PNA-}) \times 100\% / \text{PNA-})$  (Table 3), coinciding well with the enhancement of 12.2% in surface-layer  $\text{PM}_{2.5}$  concentration averaged over the U.S. (Table 2). Note that because the GEOS-Chem model underestimates  $\text{PM}_{2.5}$  concentrations in the western U.S. (Fig. 4b), the net outflow flux from the selected box might have been underestimated, but this should not compromise our conclusions about the differences in net flux between PNA+ and PNA– phases.

## 5.2 Local changes in aerosol concentrations caused by the PNA

The PNA pattern is also associated with variations in meteorological variables such as temperature (Leathers et al. 1991; Konrad II 1998; Notaro et al. 2006; Knight et al. 2008; Liu et al. 2015; Ning and Bradley 2014, 2015), precipitation (Leathers et al. 1991; Henderson and Robinson 1994; Coleman and Rogers 2003; Notaro et al. 2006; Archambault et al. 2008; Myoung and Deng 2009; Ning and Bradley 2014, 2015; Wise et al. 2015) and humidity (Sheridan 2003; Coleman and Rogers 2003; Knight et al. 2008) in U.S., which are expected to influence aerosol concentrations within the U.S. through chemical reactions, transport, and deposition.

Figure 7 shows the composite differences, between the PNA+ and PNA– months, in surface air temperature (T), precipitation rate (PR), relative humidity (RH), surface wind speed (WS), and planetary boundary layer height (PBLH), based on the reanalyzed GEOS-4 datasets. Relative to PNA– months, temperatures were higher

522 by 1–3 K over the northwestern U.S. and lower by 1–4 K in the southeastern region.  
 523 Such geographic distributions of temperature anomalies were attributed to the  
 524 maritime warm air in the northwestern U.S. accompanied by the enhanced  
 525 tropospheric geopotential height in North America (Leathers et al. 1991; Sheridan  
 526 2003; Liu et al. 2015; Ning and Bradley 2015) (see also auxiliary Fig. 1d) and the  
 527 more frequent outbreak of cold air in southeastern U.S. accompanied by the  
 528 depressed geopotential height (Konrad II 1998; Liu et al. 2015) (see also auxiliary Fig.  
 529 1d). The differences in precipitation between PNA+ and PNA– months reached –1.6  
 530 to –2.4 mm day<sup>–1</sup> (–32 to –48%) over and near the eastern Midwest, –2.4 to –3.2 mm  
 531 day<sup>–1</sup> (–48 to –64%) in the northwestern U.S., and 1.6–2.4 mm day<sup>–1</sup> (16–32%) in the  
 532 southeastern U.S.. These effects of PNA on precipitation were similar to those  
 533 obtained from wintertime station data by Leathers et al. (1991), Coleman and Rogers  
 534 (2003) and Wise et al. (2015). With respect to RH, the values in the eastern U.S. were  
 535 generally lower in the PNA+ months than in PNA– months, as a result of the reduced  
 536 moisture flux from the Gulf of Mexico to the eastern U.S. (Coleman and Rogers 2003),  
 537 where RH showed maximum reduction of –3 to –9%. The enhancement of RH of up  
 538 to 6–9% in Texas, Oklahoma and New Mexico was due to the anomalous easterlies  
 539 over the south central U.S. (see Fig. 7), which diminished the influence of the dry air  
 540 from the deserts of the southwestern U.S. and northwestern Mexico in PNA+ months  
 541 (Sheridan 2003). The surface WS showed reductions in PNA+ months relative to  
 542 PNA– months in two regions, one was the belt region along the Rocky Mountain from  
 543 the northwestern U.S. to Texas (with the maximum reductions of 1.5–2.0 m s<sup>–1</sup> (48–  
 544 64%)) and the other region, with a northeast-southwest orientation, was from Ohio to  
 545 Louisiana (with maximum reductions of 0.5–1.0 m s<sup>–1</sup> (16–32%) ). The differences in  
 546 PBLH between PNA+ and PNA– months were statistically significant in the western

U.S. and in the belt region from the northeastern U.S. to the eastern Midwest, with the maximum reductions in PBLH of 75–100 m (15–20%) and 75–100 m (10–15%), respectively.

The comparisons of Fig. 5b with Fig. 7a indicate that the increases in  $PM_{2.5}$  concentrations over and near the eastern Midwest in PNA+ months relative to the PNA– months can be attributed to the decreases in PR, WS and PBLH in these locations, since the changes in these three variables depressed wet deposition, local horizontal diffusion, and vertical diffusion of the surface aerosols, respectively. The increases in  $SO_4^{2-}$  in the western U.S. (Fig. 5b) corresponded to the decreases in PR and PBLH and the increased temperature. The increases in temperature enhance chemical reaction rates (Aw and Kleeman 2003; Dawson et al. 2007; Kleeman 2008). In the eastern U.S., although PR, WS, and PBLH decreased over and near the eastern Midwest, the cooling in the eastern U.S. might have offset the effects by PR, WS, and PBLH, inducing practically no changes in  $SO_4^{2-}$  in the eastern U.S.. The large increases in  $NO_3^-$  and  $NH_4^+$  in the southeastern U.S. (Fig. 5b) can be attributed to the reduced surface temperature, which was favorable to the wintertime formation of  $NO_3^-$  and  $NH_4^+$  (Dawson et al. 2007). The differences in concentrations of OC and BC between PNA+ and PNA– corresponded well with the reduced PR, WS and PBLH.

In order to quantify the impacts of anomalies in meteorological parameters driven by PNA on concentrations of different aerosol species, the pattern correlation coefficients (PCC, [http://glossary.ametsoc.org/wiki/Pattern\\_correlation](http://glossary.ametsoc.org/wiki/Pattern_correlation)) are calculated and shown in Table 4. These pattern correlation coefficients denote the relationship between the geographical distribution of anomalies of each of T, PR, RH, WS, and PBLH (Fig. 7b) and that of the differences in concentration of each aerosol

species between PNA+ and PNA– months (Fig. 5c). As shown in Table 4, over the whole U.S., the PNA influenced  $\text{SO}_4^{2-}$  concentrations mainly through changes PBLH, PR, and T, with the highest PCC values of –0.43, –0.38, and +0.26, respectively. For  $\text{NO}_3^-$ , the PNA-induced variations in temperature had a strong negative correlation (PCC=–0.59) with the PNA-induced differences in concentrations, indicating that surface temperature was the dominant meteorological factor to influence  $\text{NO}_3^-$  concentrations. For  $\text{NH}_4^+$ , OC, and BC, PR and PBLH were the two variables that had the largest negative PCC values (Table 4). Note that PBLH was the most important meteorological variable for  $\text{SO}_4^{2-}$ ,  $\text{NH}_4^+$ , OC and BC, which contributed to the high correlation between PBLH and  $\text{PM}_{2.5}$ .

## 6 Conclusions

This study examined the impacts of monthly variation in the PNA phase on wintertime surface-layer aerosol concentrations in the U.S. by the analyses of EPA-AQS observations over 1999–2013 and model results for 1986–2006 from the global chemical transport model GEOS-Chem.

The composite analyses on the EPA-AQS observations showed that the average concentrations of  $\text{PM}_{2.5}$ ,  $\text{SO}_4^{2-}$ ,  $\text{NO}_3^-$ ,  $\text{NH}_4^+$ , OC, and BC aerosols over the U.S. were higher in the PNA+ months than in the PNA– months by  $1.0 \mu\text{g m}^{-3}$  (8.7%),  $0.01 \mu\text{g m}^{-3}$  (0.5%),  $0.3 \mu\text{g m}^{-3}$  (29.1%),  $0.1 \mu\text{g m}^{-3}$  (11.9%),  $0.6 \mu\text{g m}^{-3}$  (13.5%), and  $0.2 \mu\text{g m}^{-3}$  (27.8%), respectively. Regionally, the observed  $\text{PM}_{2.5}$  concentrations were higher by  $3\text{--}5 \mu\text{g m}^{-3}$  (40–80%) over the Midwest, and by  $7\text{--}9 \mu\text{g m}^{-3}$  (80–100%) around the Salt Lake, as the concentrations in PNA+ months were compared to those in PNA– months.

The impacts of PNA phase on aerosol concentrations were reproduced fairly well by the GEOS-Chem simulation with fixed anthropogenic emissions (the variations of aerosols concentrations were driven by changes in meteorological fields alone). Concentrations of  $\text{SO}_4^{2-}$ ,  $\text{NO}_3^-$ ,  $\text{NH}_4^+$ , BC, and OC averaged over the U.S. were simulated to be higher in the PNA+ months than in PNA– months. The average concentration of  $\text{PM}_{2.5}$  over the U.S. was simulated to be 12.2% higher in the PNA+ months relative to the PNA– months, in close agreement with the observations. Simulated geographical patterns of the differences in  $\text{PM}_{2.5}$  and each aerosol species between the PNA+ and PNA– months were similar to those seen in observations. The largest increases in aerosol concentrations in the PNA+ months were simulated to be over and near the eastern Midwest, but the model results showed small PNA-induced changes in aerosol concentrations in the western U.S..

The mechanisms for the impacts of PNA on aerosol concentrations were examined. The transboundary transport was found to have an overall effect of increasing  $\text{PM}_{2.5}$  aerosols in the U.S. in the PNA+ months relative to PNA– months. Compared to the PNA– months, anomalous northeasterlies occurred over a large fraction of U.S., which led to a net increase in inflow flux of  $\text{PM}_{2.5}$  of  $14.0 \text{ Kg s}^{-1}$  in PNA+ months. Regionally within the U.S., the PNA influenced aerosol concentrations through changes in precipitation rate (PR), planetary boundary layer height (PBLH), surface wind speed (WS), surface air temperature (T) and relative humidity (RH), as represented by the pattern correlation coefficients (PCCs). The PNA influenced  $\text{SO}_4^{2-}$  concentration mainly through changes PBLH, PR, and T, with the highest PCC values of  $-0.43$ ,  $-0.38$ , and  $+0.26$ , respectively. For  $\text{NO}_3^-$ , the PNA-induced variations in temperature had a strong negative correlation ( $\text{PCC}=-0.59$ ) with the PNA-induced differences in concentrations. For  $\text{NH}_4^+$ , OC, and BC, PR and PBLH were the two

variables that had the largest negative PCC values. Because PBLH was the most important meteorological variable for  $\text{SO}_4^{2-}$ ,  $\text{NH}_4^+$ , OC and BC, which led to a high correlation between PBLH and  $\text{PM}_{2.5}$ .

Conclusions from this study have important implications for air quality in the U.S.. Leathers and Palechi (1992) showed that the PNAI were generally low in 1947–1957 but consistently high in 1958–1987. The PNAI during 1948–2010 exhibited an increasing trend for positive phases and a decreasing trend for negative phases (Liu et al. 2015; Ning et al. 2015; [http://research.jisao.washington.edu/data\\_sets/pna/#djf](http://research.jisao.washington.edu/data_sets/pna/#djf)), indicating that wintertime particulate matter pollution in most areas of U.S. deteriorated due to variations in PNA phase alone. Climate models projected that positive PNA phases would increase in the future because of the global warming (Kachi and Nitta, 1997; Müller and Roeckner 2008; Zhou 2014). Therefore, the trend in PNA pattern underlies the necessity of strict emission reduction strategies for greenhouse gases, aerosols, and aerosol precursors.

*Acknowledgements.* This work was supported by the National Basic Research Program of China (973 program, Grant 2014CB441202), the Strategic Priority Research Program of the Chinese Academy of Sciences Strategic Priority Research Program Grant No. XDA05100503, and the National Natural Science Foundation of China under grants 91544219, 41475137, and 41321064.

## References

- Alexander, B., Park, R.J., Jacob, D.J., Li, Q.B., Yantosca, R.M., Savarino, J., Lee, C.C.W., Thiemens, M.H.: Sulfate formation in sea-salt aerosols: Constraints from oxygen isotopes, *J. Geophys. Res.*, 110(D10), D10307, doi:10.1029/2004JD005659, 2005.
- Allen, R. J., Landuyt, W. and Rumbold, S. T.: An increase in aerosol burden and radiative effects in a warmer world, *Nat. Clim. Chang.*, (OCTOBER), doi:10.1038/nclimate2827, 2015.
- Alston, E. J., Sokolik, I. N. and Kalashnikova, O. V.: Characterization of atmospheric aerosol in the US Southeast from ground- and space-based measurements over the past decade, *Atmos. Meas. Tech.*, 5(7), 1667–1682, doi:10.5194/amt-5-1667-2012, 2012.
- Archambault, H. M., Bosart, L. F., Keyser, D. and Aiyyer, A. R.: Influence of Large-Scale Flow Regimes on Cool-Season Precipitation in the Northeastern United States, *Mon. Weather Rev.*, 136(8), 2945–2963, doi:10.1175/2007MWR2308.1, 2008.
- Athanasiadis, P. J. and Ambaum, M. H. P.: Linear Contributions of Different Time Scales to Teleconnectivity, *J. Clim.*, 22(13), 3720–3728, doi:10.1175/2009JCLI2707.1, 2009.
- Aw, J. and Kleeman, M. J.: Evaluating the first-order effect of intraannual temperature variability on urban air pollution, *J. Geophys. Res.*, 108(D12), 4365, doi:10.1029/2002JD002688, 2003.
- Bauer, S. E., Koch, D., Unger, N., Metzger, S. M., Shindell, D. T. and Streets, D. G.: Nitrate aerosols today and in 2030: a global simulation including aerosols and tropospheric ozone, *Atmos. Chem. Phys.*, 7(19), 5043–5059, doi:10.5194/acp-7-5043-2007, 2007.
- Bey, I., Jacob, D. J., Yantosca, R. M., Logan, J. a., Field, B. D., Fiore, A. M., Li, Q., Liu, H. Y., Mickley, L. J. and Schultz, M. G.: Global modeling of tropospheric chemistry with assimilated meteorology: Model description and evaluation, *J. Geophys. Res.*, 106(D19), 23073, doi:10.1029/2001JD000807, 2001.
- Blackmon, M. L., Lee, Y.-H. and Wallace, J. M.: Horizontal Structure of 500 mb Height Fluctuations with Long, Intermediate and Short Time Scales, *J. Atmos. Sci.*, 41(6), 961–980, doi:10.1175/1520-0469(1984)041<0961:HSOMHF>2.0.CO;2, 1984.
- Cakmur, R. V., Miller, R. L. and Tegen, I.: A comparison of seasonal and interannual variability of soil dust aerosols over the Atlantic Ocean as inferred by the TOMS AI and AVHRR AOT retrievals, *J. Geophys. Res.*, 106(D16), 18287, doi:10.1029/2000JD900525, 2001.
- Chen, J., Vaughan, J., Avise, J., O'Neill, S. and Lamb, B.: Enhancement and evaluation of the AIRPACT ozone and PM<sub>2.5</sub> forecast system for the Pacific Northwest, *J. Geophys. Res. Atmos.*, 113(14), 1–20, doi:10.1029/2007JD009554, 2008.
- Coleman, J. S. M. and Rogers, J. C.: Ohio River Valley Winter Moisture Conditions Associated with the Pacific–North American Teleconnection Pattern, *J. Clim.*,



687 16(6), 969–981, doi:10.1175/1520-0442(2003)016<0969:ORVWMC>2.0.CO;2,  
688 2003.

689 Dawson, J. P., Adams, P. J. and Pandis, S. N.: Sensitivity of PM<sub>2.5</sub> to climate in the  
690 Eastern US: a modeling case study, *Atmos. Chem. Phys.*, 7(16), 4295–4309,  
691 doi:10.5194/acp-7-4295-2007, 2007.

692 Day, M. C. and Pandis, S. N.: Predicted changes in summertime organic aerosol  
693 concentrations due to increased temperatures, *Atmos. Environ.*, 45(36), 6546–  
694 6556, doi:10.1016/j.atmosenv.2011.08.028, 2011.

695 Di Pierro, M., Jaeglé, L. and Anderson, T. L.: Satellite observations of aerosol  
696 transport from East Asia to the Arctic: three case studies, *Atmos. Chem. Phys.*,  
697 11(5), 2225–2243, doi:10.5194/acp-11-2225-2011, 2011.

698 Drury, E., Jacob, D. J., Spurr, R. J. D., Wang, J., Shinozuka, Y., Anderson, B. E.,  
699 Clarke, A. D., Dibb, J., McNaughton, C. and Weber, R.: Synthesis of satellite  
700 (MODIS), aircraft (ICARTT), and surface (IMPROVE, EPA-AQS, AERONET)  
701 aerosol observations over eastern North America to improve MODIS aerosol  
702 retrievals and constrain surface aerosol concentrations and sources, *J. Geophys.*  
703 *Res.*, 115(D14), D14204, doi:10.1029/2009JD012629, 2010.

704 Duncan, B. N., Martin, R. V., Staudt, A. C., Yevich, R. and Logan, J. A.: Interannual  
705 and seasonal variability of biomass burning emissions constrained by satellite  
706 observations, *J. Geophys. Res.*, 108(D2), 4100, doi:10.1029/2002JD002378,  
707 2003.

708 Dutkiewicz, V. A., Das, M. and Husain, L.: The relationship between regional SO<sub>2</sub>  
709 emissions and downwind aerosol sulfate concentrations in the northeastern US,  
710 *Atmos. Environ.*, 34(11), 1821–1832, doi:10.1016/S1352-2310(99)00334-9,  
711 2000.

712 Fairlie, D. T., Jacob, D. J. and Park, R. J.: The impact of transpacific transport of  
713 mineral dust in the United States, *Atmos. Environ.*, 41(6), 1251–1266,  
714 doi:10.1016/j.atmosenv.2006.09.048, 2007.

715 Feldstein, S. B.: Fundamental mechanisms of the growth and decay of the PNA  
716 teleconnection pattern, *Q. J. R. Meteorol. Soc.*, 128(581), 775–796,  
717 doi:10.1256/0035900021643683, 2002.

718 Feldstein, S. B.: The dynamics of NAO teleconnection pattern growth and decay, *Q. J.*  
719 *R. Meteorol. Soc.*, 129(589), 901–924, doi:10.1256/qj.02.76, 2003.

720 Fu, T.-M., Jacob, D. J. and Heald, C. L.: Aqueous-phase reactive uptake of  
721 dicarbonyls as a source of organic aerosol over eastern North America, *Atmos.*  
722 *Environ.*, 43(10), 1814–1822, doi:10.1016/j.atmosenv.2008.12.029, 2009.

723 Generoso, S., Bréon, F.-M., Balkanski, Y., Boucher, O. and Schulz, M.: Improving the  
724 seasonal cycle and interannual variations of biomass burning aerosol sources,  
725 *Atmos. Chem. Phys.*, 3(4), 1211–1222, doi:10.5194/acp-3-1211-2003, 2003.

726 Giglio, L., van der Werf, G. R., Randerson, J. T., Collatz, G. J. and Kasibhatla, P.:  
727 Global estimation of burned area using MODIS active fire observations, *Atmos.*  
728 *Chem. Phys.*, 6(4), 957–974, doi:10.5194/acp-6-957-2006, 2006.

729 Gong, S. L., Zhang, X. Y., Zhao, T. L., Zhang, X. B., Barrie, L. A., McKendry, I. G. and  
730 Zhao, C. S.: A Simulated Climatology of Asian Dust Aerosol and Its Trans-Pacific

- 731 Transport. Part II: Interannual Variability and Climate Connections, *J. Clim.*,  
732 19(1), 104–122, doi:10.1175/JCLI3606.1, 2006.
- 733 Guenther, A., Karl, T., Harley, P., Wiedinmyer, C., Palmer, P. I. and Geron, C.:  
734 Estimates of global terrestrial isoprene emissions using MEGAN (Model of  
735 Emissions of Gases and Aerosols from Nature), *Atmos Chem Phys* 6:3181-3210.  
736 doi: 10.5194/acp-6-3181-2006, 2006.
- 737 Hack, J. J.: Parameterization of moist convection in the National Center for  
738 Atmospheric Research community climate model (CCM2), *J. Geophys. Res.*,  
739 99(D3), 5551, doi:10.1029/93JD03478, 1994.
- 740 Hand, J. L., Schichtel, B. A., Malm, W. C. and Pitchford, M. L.: Particulate sulfate ion  
741 concentration and SO<sub>2</sub> emission trends in the United States from the early 1990s  
742 through 2010, *Atmos. Chem. Phys.*, 12(21), 10353–10365,  
743 doi:10.5194/acp-12-10353-2012, 2012a.
- 744 Hand, J. L., Schichtel, B. A., Pitchford, M., Malm, W. C. and Frank, N. H.: Seasonal  
745 composition of remote and urban fine particulate matter in the United States, *J.*  
746 *Geophys. Res.*, 117(D5), D05209, doi:10.1029/2011JD017122, 2012b.
- 747 Hand, J. L., Schichtel, B. A., Malm, W. C., Pitchford, M. and Frank, N. H.: Spatial and  
748 seasonal patterns in urban influence on regional concentrations of speciated  
749 aerosols across the United States, *J. Geophys. Res. Atmos.*, 119, 12832–  
750 12849, doi:10.1002/2014JD022328. Received, 2014.
- 751 Heald, C. L., Jacob, D. J., Park, R. J., Alexander, B., Fairlie, T. D., Yantosca, R. M. and  
752 Chu, D. A.: Transpacific transport of Asian anthropogenic aerosols and its impact  
753 on surface air quality in the United States, *J. Geophys. Res. D Atmos.*, 111, 1–13,  
754 doi:10.1029/2005JD006847, 2006.
- 755 Heald, C. L., Henze, D. K., Horowitz, L. W., Feddema, J., Lamarque, J.-F., Guenther,  
756 A., Hess, P. G., Vitt, F., Seinfeld, J. H., Goldstein, A. H. and Fung, I.: Predicted  
757 change in global secondary organic aerosol concentrations in response to future  
758 climate, emissions, and land use change, *J. Geophys. Res. Atmos.*, 113(D5),  
759 D05211, doi:10.1029/2007JD009092, 2008.
- 760 Henderson, K. G. and Robinson, P. J.: Relationships between the pacific/north  
761 american teleconnection patterns and precipitation events in the south-eastern  
762 USA, *Int. J. Climatol.*, 14(3), 307–323, doi:10.1002/joc.3370140305, 1994.
- 763 IPCC: Climate Change 2013 The Physical Science Basis: Working Group I  
764 Contribution to the Fifth Assessment Report of the Intergovernmental Panel on  
765 Climate Change, 1st ed., Cambridge University Press, New York. [online]  
766 Available from:  
767 [http://www.climatechange2013.org/images/report/WG1AR5\\_ALL\\_FINAL.pdf](http://www.climatechange2013.org/images/report/WG1AR5_ALL_FINAL.pdf)  
768 The last access date was November 20, 2015.
- 769 Jacob, D. J. and Winner, D. A.: Effect of climate change on air quality, *Atmos. Environ.*,  
770 43(1), 51–63, doi:10.1016/j.atmosenv.2008.09.051, 2009.
- 771 Jaffe, D., Tamura, S. and Harris, J.: Seasonal cycle and composition of background  
772 fine particles along the west coast of the US, *Atmos. Environ.*, 39(2), 297–306,  
773 doi:10.1016/j.atmosenv.2004.09.016, 2005.
- 774 Jerez, S., Jimenez-Guerrero, P., Montávez, J. P. and Trigo, R. M.: Impact of the North  
775 Atlantic Oscillation on European aerosol ground levels through local processes:

776 a seasonal model-based assessment using fixed anthropogenic emissions,  
 777 Atmos. Chem. Phys., 13(22), 11195–11207, doi:10.5194/acp-13-11195-2013,  
 778 2013.

779 Juda-Rezler, K., Reizer, M., Huszar, P., Krüger, B., Zanis, P., Syrakov, D., Katragkou,  
 780 E., Trapp, W., Melas, D., Chervenkov, H., Tegoulis, I. and Halenka, T.:  
 781 Modelling the effects of climate change on air quality over Central and Eastern  
 782 Europe: concept, evaluation and projections, Clim. Res., 53(3), 179–203,  
 783 doi:10.3354/cr01072, 2012.

784 Kachi, M. and Nitta, T.: Decadal variations of the global atmosphere-ocean system, J.  
 785 Meteorol. Soc. Japan, 75(3), 657–675, 1997.

786 Kleeman, M. J.: A preliminary assessment of the sensitivity of air quality in California to  
 787 global change, Clim. Change, 87(1), 273–292, doi:10.1007/s10584-007-9351-3,  
 788 2008.

789 Knight, D. B., Davis, R. E., Sheridan, S. C., Hondula, D. M., Sitka, L. J., Deaton, M.,  
 790 Lee, T. R., Gawtry, S. D., Stenger, P. J., Mazzei, F. and Kenny, B. P.: Increasing  
 791 frequencies of warm and humid air masses over the conterminous United States  
 792 from 1948 to 2005, Geophys. Res. Lett., 35(10), L10702,  
 793 doi:10.1029/2008GL033697

794 Konrad II, C. E.: Persistent planetary scale circulation patterns and their relationship  
 795 with cold air outbreak activity over the Eastern United States, Int. J. Climatol.,  
 796 18(11), 1209–1221,  
 797 doi:10.1002/(SICI)1097-0088(199809)18:11<1209::AID-JOC301>3.0.CO;2-K,  
 798 1998.

799 Lam, Y. F., Fu, J. S., Wu, S. and Mickley, L. J.: Impacts of future climate change and  
 800 effects of biogenic emissions on surface ozone and particulate matter  
 801 concentrations in the United States, Atmos. Chem. Phys., 11(10), 4789–4806,  
 802 doi:10.5194/acp-11-4789-2011, 2011.

803 Leathers, D. J. and Palecki, M. A.: The Pacific/North American Teleconnection Pattern  
 804 and United States Climate. Part II: Temporal Characteristics and Index  
 805 Specification, J. Clim., 5(7), 707–716,  
 806 doi:10.1175/1520-0442(1992)005<0707:TPATPA>2.0.CO;2, 1992.

807 Leathers, D. J., Yarnal, B. and Palecki, M. A.: The Pacific/North American  
 808 Teleconnection Pattern and United States Climate. Part I: Regional Temperature  
 809 and Precipitation Associations, J. Clim., 4(5), 517–528,  
 810 doi:10.1175/1520-0442(1991)004<0517:TPATPA>2.0.CO;2, 1991.

811 Leibensperger, E. M., Mickley, L. J., Jacob, D. J. and Barrett, S. R. H.: Intercontinental  
 812 influence of NO<sub>x</sub> and CO emissions on particulate matter air quality, Atmos.  
 813 Environ., 45(19), 3318–3324, doi:10.1016/j.atmosenv.2011.02.023, 2011.

814 Li, J., Carlson, B. E. and Lacis, A. A.: Application of spectral analysis techniques in the  
 815 intercomparison of aerosol data: 1. An EOF approach to analyze the  
 816 spatial-temporal variability of aerosol optical depth using multiple remote sensing  
 817 data sets, J. Geophys. Res. Atmos., 118(15), 8640–8648,  
 818 doi:10.1002/jgrd.50686, 2013.

819 Liang, Q., Jaeglé, L., Jaffe, D. A., Weiss-Penzias, P., Heckman, A. and Snow, J. A.:  
 820 Long-range transport of Asian pollution to the northeast Pacific: Seasonal

821 variations and transport pathways of carbon monoxide, *J. Geophys. Res. D*  
822 *Atmos.*, 109, 1–16, doi:10.1029/2003JD004402, 2004.

823 Liang, Q., Jaeglé, L. and Wallace, J. M.: Meteorological indices for Asian outflow and  
824 transpacific transport on daily to interannual timescales, *J. Geophys. Res.*,  
825 110(D18), D18308, doi:10.1029/2005JD005788, 2005.

826 Liao, H., Chen, W. T. and Seinfeld, J. H.: Role of climate change in global predictions  
827 of future tropospheric ozone and aerosols, *J. Geophys. Res. Atmos.*, 111, 1–18,  
828 doi:10.1029/2005JD006852, 2006.

829 Liao, H., Henze, D. K., Seinfeld, J. H., Wu, S. and Mickley, L. J.: Biogenic secondary  
830 organic aerosol over the United States: Comparison of climatological simulations  
831 with observations, *J. Geophys. Res.*, 112(D6), D06201,  
832 doi:10.1029/2006JD007813, 2007.

833 Lin, S.-J. and Rood, R. B.: Multidimensional Flux-Form Semi-Lagrangian Transport  
834 Schemes, *Mon. Weather Rev.*, 124(9), 2046–2070,  
835 doi:10.1175/1520-0493(1996)124<2046:MFFSLT>2.0.CO;2, 1996.

836 Liu, H.-Y., Jacob, D. J., Bey, I. and Yantosca, R. M.: Constraints Pb-210 and Be-7 on  
837 Wet Deposition and Transport in a Global Three-Dimensional Chemical Tracer  
838 Model Driven by Assimilated Meteorological Fields, *J. Geophys. Res. Atmos.*,  
839 106(D11), doi:10.1029/2000JD900839, 2001.

840 Liu, Y., Park, R. J., Jacob, D. J., Li, Q., Kilaru, V. and Sarnat, J. A.: Mapping annual  
841 mean ground-level PM<sub>2.5</sub> concentrations using Multiangle Imaging  
842 Spectroradiometer aerosol optical thickness over the contiguous United States, *J.*  
843 *Geophys. Res.*, 109(D22), D22206, doi:10.1029/2004JD005025, 2004.

844 Liu, Y., Liu, J. and Tao, S.: Interannual variability of summertime aerosol optical depth  
845 over East Asia during 2000–2011: a potential influence from El Niño Southern  
846 Oscillation, *Environ. Res. Lett.*, 8(4), 044034,  
847 doi:10.1088/1748-9326/8/4/044034, 2013.

848 Liu, Z., Jian, Z., Yoshimura, K., Buening, N. H., Poulsen, C. J. and Bowen, G. J.:  
849 Recent contrasting winter temperature changes over North America linked to  
850 enhanced positive Pacific-North American pattern, *Geophys. Res. Lett.*, 42, 1–8,  
851 doi:10.1002/2015GL065656, 2015.

852 Mahowald, N., Luo, C., del Corral, J., Zender, C.S.: Interannual variability in  
853 atmospheric mineral aerosols from a 22-year model simulation and  
854 observational data, *J. Geophys. Res.*, 108(D12), 4352,  
855 doi:10.1029/2002JD002821, 2003.

856 Malm, W. C.: Spatial and monthly trends in speciated fine particle concentration in the  
857 United States, *J. Geophys. Res.*, 109(D3), D03306, doi:10.1029/2003JD003739,  
858 2004.

859 Malm, W. C., Schichtel, B. A. and Pitchford, M. L.: Uncertainties in PM<sub>2.5</sub> Gravimetric  
860 and Speciation Measurements and What We Can Learn from Them, *J. Air Waste*  
861 *Manage. Assoc.*, 61(11), 1131–1149, doi:10.1080/10473289.2011.603998,  
862 2011.

863 Markakis, K., Valari, M., Perrussel, O., Sanchez, O. and Honore, C.: Climate-forced  
864 air-quality modeling at the urban scale: sensitivity to model resolution, emissions

865 and meteorology, *Atmos. Chem. Phys.*, 15(13), 7703–7723,  
 866 doi:10.5194/acp-15-7703-2015, 2015.

867 Megaritis, a. G., Fountoukis, C., Charalampidis, P. E., Denier van der Gon, H. a. C.,  
 868 Pilinis, C. and Pandis, S. N.: Linking climate and air quality over Europe: effects  
 869 of meteorology on PM<sub>2.5</sub> concentrations, *Atmos. Chem. Phys.*, 14(18), 10283–  
 870 10298, doi:10.5194/acp-14-10283-2014, 2014.

871 Mijling, B., van der A, R. J. and Zhang, Q.: Regional nitrogen oxides emission trends in  
 872 East Asia observed from space, *Atmos. Chem. Phys.*, 13, 12003–12012, doi:  
 873 10.5194/acp-13-12003-2013, 2013.

874 Moulin, C. and Lambert, C. E., Dulac, F., Dayan, U.: Control of atmospheric export of  
 875 dust from North Africa by the North Atlantic Oscillation, *Nature*, 387(June), 691–  
 876 694, 1997.

877 Mu, Q. and Liao, H.: Simulation of the interannual variations of aerosols in China: role  
 878 of variations in meteorological parameters, *Atmos. Chem. Phys.*, 14, 11177–  
 879 11219, doi:10.5194/acp-14-9597-2014, 2014.

880 Müller, W. A. and Roeckner, E.: ENSO teleconnections in projections of future climate  
 881 in ECHAM5/MPI-OM, *Clim. Dyn.*, 31(5), 533–549,  
 882 doi:10.1007/s00382-007-0357-3, 2008.

883 Murray, L. T., Jacob, D. J., Logan, J. A., Hudman, R. C. and Koshak, W. J.: Optimized  
 884 regional and interannual variability of lightning in a global chemical transport  
 885 model constrained by LIS/OTD satellite data, *J. Geophys. Res. Atmos.*,  
 886 117(D20), D20307, doi:10.1029/2012JD017934, 2012.

887 Myoung, B. and Deng, Y.: Interannual Variability of the Cyclonic Activity along the U.S.  
 888 Pacific Coast: Influences on the Characteristics of Winter Precipitation in the  
 889 Western United States, *J. Clim.*, 22(21), 5732–5747,  
 890 doi:10.1175/2009JCLI2889.1, 2009.

891 Ning, L. and Bradley, R. S.: Winter precipitation variability and corresponding  
 892 teleconnections over the northeastern United States, *J. Geophys. Res. Atmos.*,  
 893 119(13), 7931–7945, doi:10.1002/2014JD021591, 2014.

894 Ning, L. and Bradley, R. S.: Winter Climate Extremes over the Northeastern United  
 895 States and Southeastern Canada and Teleconnections with Large-Scale Modes  
 896 of Climate Variability, *J. Clim.*, 28(6), 2475–2493,  
 897 doi:10.1175/JCLI-D-13-00750.1, 2015.

898 Notaro, M., Wang, W.-C. and Gong, W.: Model and Observational Analysis of the  
 899 Northeast U.S. Regional Climate and Its Relationship to the PNA and NAO  
 900 Patterns during Early Winter, *Mon. Weather Rev.*, 134(11), 3479–3505,  
 901 doi:10.1175/MWR3234.1, 2006.

902 Park, R. J., Jacob, D. J., Chin, M., Martin, R. V.: Sources of carbonaceous aerosols  
 903 over the United States and implications for natural visibility, *J. Geophys. Res.*,  
 904 108(D12), 4355, doi:10.1029/2002JD003190, 2003.

905 Park, R. J., Jacob, D. J., Field, B. D., Yantosca, R. M., Chin, M.: Natural and  
 906 transboundary pollution influences on sulfate-nitrate-ammonium aerosols in the  
 907 United States: Implications for policy, *J. Geophys. Res.*, 109(D15), D15204,  
 908 doi:10.1029/2003JD004473, 2004.

909 Park, R. J., Jacob, D. J., Palmer, P. I., Clarke, A. D., Weber, R. J., Zondlo, M. A.,  
 910 Eisele, F. L., Bandy, A. R., Thornton, D. C., Sachse, G. W. and Bond, T. C.:  
 911 Export efficiency of black carbon aerosol in continental outflow: Global  
 912 implications, *J. Geophys. Res. Atmos.*, 110, 1–7, doi:10.1029/2004JD005432,  
 913 2005.

914 Park, R. J., Jacob, D. J., Kumar, N. and Yantosca, R. M.: Regional visibility statistics in  
 915 the United States: Natural and transboundary pollution influences, and  
 916 implications for the Regional Haze Rule, *Atmos. Environ.*, 40(28), 5405–5423,  
 917 doi:10.1016/j.atmosenv.2006.04.059, 2006.

918 Porter, W. C., Heald, C. L., Cooley, D. and Russell, B.: Investigating the observed  
 919 sensitivities of air-quality extremes to meteorological drivers via quantile  
 920 regression, *Atmos. Chem. Phys.*, 15(18), 10349–10366,  
 921 doi:10.5194/acp-15-10349-2015, 2015.

922 Pye, H. O. T., Liao, H., Wu, S., Mickley, L. J., Jacob, D. J., Henze, D. K. and Seinfeld,  
 923 J. H.: Effect of changes in climate and emissions on future  
 924 sulfate-nitrate-ammonium aerosol levels in the United States, *J. Geophys. Res.*,  
 925 114(D1), D01205, doi:10.1029/2008JD010701, 2009.

926 Qian, B., Corte-Real, J. and Xu, H.: Is the North Atlantic Oscillation the most important  
 927 atmospheric pattern for precipitation in Europe?, *J. Geophys. Res.*, 105(D9),  
 928 11901, doi:10.1029/2000JD900102, 2000.

929 Rattigan, O. V., Felton, H. D., Bae, M.-S., Schwab, J. J. and Demerjian, K. L.:  
 930 Comparison of long-term PM<sub>2.5</sub> carbon measurements at an urban and rural  
 931 location in New York, *Atmos. Environ.*, 45(19), 3228–3236,  
 932 doi:10.1016/j.atmosenv.2011.03.048, 2011.

933 Redmond, K. T. and Koch, R. W.: Surface Climate and Streamflow Variability in the  
 934 Western United States and Their Relationship to Large-Scale Circulation Indices,  
 935 *Water Resour. Res.*, 27(9), 2381–2399, doi:10.1029/91WR00690, 1991.

936 Sauvage, B., Martin, R. V., van Donkelaar, A., Liu, X., Chance, K., Jaeglé, L., Palmer,  
 937 P. I., Wu, S. and Fu, T.-M.: Remote sensed and in situ constraints on processes  
 938 affecting tropical tropospheric ozone, *Atmos. Chem. Phys.*, 7(3), 815–838,  
 939 doi:10.5194/acp-7-815-2007, 2007.

940 Sheridan, S. C.: North American weather-type frequency and teleconnection indices,  
 941 *Int. J. Climatol.*, 23(1), 27–45, doi:10.1002/joc.863, 2003.

942 Singh, A. and Palazoglu, A.: Climatic variability and its influence on ozone and PM  
 943 pollution in 6 non-attainment regions in the United States, *Atmos. Environ.*, 51,  
 944 212–224, doi:10.1016/j.atmosenv.2012.01.020, 2012.

945 Tai, A. P. K., Mickley, L. J., Jacob, D. J., Leibensperger, E. M., Zhang, L., Fisher, J. A.  
 946 and Pye, H. O. T.: Meteorological modes of variability for fine particulate matter  
 947 (PM<sub>2.5</sub>) air quality in the United States: implications for PM<sub>2.5</sub> sensitivity to climate  
 948 change, *Atmos. Chem. Phys.*, 12(6), 3131–3145,  
 949 doi:10.5194/acp-12-3131-2012, 2012a.

950 Tai, A. P. K., Mickley, L. J. and Jacob, D. J.: Correlations between fine particulate  
 951 matter (PM<sub>2.5</sub>) and meteorological variables in the United States: Implications for  
 952 the sensitivity of PM<sub>2.5</sub> to climate change, *Atmos. Environ.*, 44(32), 3976–3984,  
 953 doi:10.1016/j.atmosenv.2010.06.060, 2010.



954 Tai, A. P. K., Mickley, L. J. and Jacob, D. J.: Impact of 2000–2050 climate change on  
 955 fine particulate matter (PM<sub>2.5</sub>) air quality inferred from a multi-model analysis of  
 956 meteorological modes, *Atmos. Chem. Phys.*, 12(23), 11329–11337,  
 957 doi:10.5194/acp-12-11329-2012, 2012b.

958 Unger, N., Shindell, D. T., Koch, D. M., Amann, M., Cofala, J. and Streets, D. G.:  
 959 Influences of man-made emissions and climate changes on tropospheric ozone,  
 960 methane, and sulfate at 2030 from a broad range of possible futures, *J. Geophys.*  
 961 *Res.*, 111(D12), D12313, doi:10.1029/2005JD006518, 2006.

962 van der Werf, G. R., Randerson, J. T., Giglio, L., Collatz, G. J., Kasibhatla, P. S. and  
 963 Arellano, A. F.: Interannual variability of global biomass burning emissions from  
 964 1997 to 2004, *Atmos. Chem. Phys.*, 6, 3423–3441, doi:  
 965 10.5194/acpd-6-3175-2006, 2006.

966 van Donkelaar, A., Martin, R. V., Park, R. J.: Estimating ground-level PM<sub>2.5</sub> using  
 967 aerosol optical depth determined from satellite remote sensing, *J. Geophys. Res.*,  
 968 111(D21), D21201, doi:10.1029/2005JD006996, 2006.

969 van Donkelaar, A., Martin, R. V., Park, R. J., Heald, C. L., Fu, T. M., Liao, H. and  
 970 Guenther, A.: Model evidence for a significant source of secondary organic  
 971 aerosol from isoprene, *Atmos. Environ.*, 41(6), 1267–1274,  
 972 doi:10.1016/j.atmosenv.2006.09.051, 2007.

973 van Donkelaar, A., Martin, R. V., Leaitch, W. R., Macdonald, A. M., Walker, T. W.,  
 974 Streets, D. G., Zhang, Q., Dunlea, E. J., Jimenez, J. L., Dibb, J. E., Huey, L. G.,  
 975 Weber, R. and Andreae, M. O.: Analysis of aircraft and satellite measurements  
 976 from the Intercontinental Chemical Transport Experiment (INTEX-B) to quantify  
 977 long-range transport of East Asian sulfur to Canada, *Atmos. Chem. Phys.*, 8(11),  
 978 2999–3014, doi:10.5194/acp-8-2999-2008, 2008.

979 Vestreng, V., Myhre, G., Fagerli, H., Reis, S. and Tarrasón, L.: Twenty-five years of  
 980 continuous sulphur dioxide emission reduction in Europe, *Atmos. Chem. Phys.*,  
 981 7(13), 3663–3681, doi:10.5194/acp-7-3663-2007, 2007.

982 Wallace, J. M. and Gutzler, D. S.: Teleconnections in the Geopotential Height Field  
 983 during the Northern Hemisphere Winter, *Mon. Weather Rev.*, 109(4), 784–812,  
 984 doi:10.1175/1520-0493(1981)109<0784:TITGHF>2.0.CO;2, 1981.

985 Wang H, Chen H and Liu J: Arctic Sea Ice Decline Intensified Haze Pollution in  
 986 Eastern China, *Atmospheric and Oceanic Science Letters*, 8(1), 1–9,  
 987 doi:10.3878/AOSL20140081, 2015.

988 Wang, Y., Logan, J. A. and Jacob, D. J.: Global simulation of tropospheric O<sub>3</sub>  
 989 -NO<sub>x</sub>-hydrocarbon chemistry: 2. Model evaluation and global ozone budget, *J.*  
 990 *Geophys. Res.*, 103(D9), 10727, doi:10.1029/98JD00157, 1998.

991 Wesely, M. L.: Parameterization of surface resistances to gaseous dry deposition in  
 992 regional-scale numerical models, *Atmos. Environ.*, 23(6), 1293–1304,  
 993 doi:10.1016/0004-6981(89)90153-4, 1989.

994 Wheeler, M. C. and Hendon, H. H.: An all-season real-time multivariate MJO index:  
 995 Development of an index for monitoring and prediction, *Mon. Weather Rev.*,  
 996 132(8), 1917–1932,  
 997 doi: 10.1175/1520-0493(2004)132<1917:AARMMI>2.0.CO;2,, 2004.



998 Wise, E. K. and Comrie, A. C.: Meteorologically adjusted urban air quality trends in the  
999 Southwestern United States, *Atmos. Environ.*, 39(16), 2969–2980,  
1000 doi:10.1016/j.atmosenv.2005.01.024, 2005.

1001 Xiao, D., Li, Y., Fan, S., Zhang, R., Sun, J. and Wang, Y.: Plausible influence of  
1002 Atlantic Ocean SST anomalies on winter haze in China, *Theor. Appl. Climatol.*,  
1003 doi:10.1007/s00704-014-1297-6, 2014.

1004 Yang, Y., Liao, H. and Lou, S.: Decadal trend and interannual variation of outflow of  
1005 aerosols from East Asia: Roles of variations in meteorological parameters and  
1006 emissions, *Atmos. Environ.*, 100, 141–153, doi:10.1016/j.atmosenv.2014.11.004,  
1007 2015.

1008 Yienger, J. J. and Levy, H.: Empirical model of global soil-biogenic NO<sub>x</sub> emissions, *J.*  
1009 *Geophys. Res.*, 100(D6), 11447, doi:10.1029/95JD00370, 1995.

1010 Zhang, G. J. and McFarlane, N. A.: Sensitivity of climate simulations to the  
1011 parameterization of cumulus convection in the Canadian climate centre general  
1012 circulation model, *Atmosphere-Ocean*, 33(3), 407–446,  
1013 doi:10.1080/07055900.1995.9649539, 1995.

1014 Zhang, L., Jacob, D. J., Knipping, E. M., Kumar, N., Munger, J. W., Carouge, C. C.,  
1015 van Donkelaar, A., Wang, Y. X. and Chen, D.: Nitrogen deposition to the United  
1016 States: distribution, sources, and processes, *Atmos. Chem. Phys.*, 12(10),  
1017 4539–4554, doi:10.5194/acp-12-4539-2012, 2012.

1018 Zhang, L., Kok, J. F., Henze, D. K., Li, Q. and Zhao, C.: Improving simulations of fine  
1019 dust surface concentrations over the western United States by optimizing the  
1020 particle size distribution, *Geophys. Res. Lett.*, 40(12), 3270–3275,  
1021 doi:10.1002/grl.50591, 2013.

1022 Zhou, Z.-Q., Xie, S.-P., Zheng, X.-T., Liu, Q. and Wang, H.: Global Warming–Induced  
1023 Changes in El Niño Teleconnections over the North Pacific and North America, *J.*  
1024 *Clim.*, 27(24), 9050–9064, doi:10.1175/JCLI-D-14-00254.1, 2014.

1025 Zhu, J., Liao, H. and Li, J.: Increases in aerosol concentrations over eastern China due  
1026 to the decadal-scale weakening of the East Asian summer monsoon, *Geophys.*  
1027 *Res. Lett.*, 39(9), L09809, doi:10.1029/2012GL051428, 2012.

1028

**Table 1.** The absolute ( $\mu\text{g m}^{-3}$ ) and relative (%) differences in observed aerosol concentrations between the PNA+ and PNA– months (PNA+ minus PNA–). The observed concentrations are averaged over all the sites in the whole of U.S., in the western U.S., or in the eastern U.S.. See Fig 1 for locations of the sites. The measurements are from the EPA-AQS data. The \*\* and \* indicate the differences that have passed the two-tail student-t test with 95% and 90% significance levels, respectively.

	Whole U.S.	Western U.S.	Eastern U.S
PM <sub>2.5</sub>	1.0 (8.7%)**	1.3 (14.3%)**	0.8 (7.2%)**
SO <sub>4</sub> <sup>2-</sup>	0.01 (0.5%)	0.03 (3.2%)	0.1 (3.7%)
NO <sub>3</sub> <sup>-</sup>	0.3 (29.1%)**	0.2 (23.8%)**	0.4 (36.5%)**
NH <sub>4</sub> <sup>+</sup>	0.1 (11.9%)*	0.2 (31.6%)**	0.1 (10.5%)
OC	0.6 (13.5%)**	0.9 (17.7%)**	0.3 (8.0%)**
BC	0.2 (27.8%)**	0.2 (25.0%)**	0.1 (25.2%)**

**Table 2.** The absolute ( $\mu\text{g m}^{-3}$ ) and relative (%) differences in simulated aerosol concentrations between the PNA+ and PNA– months (PNA+ minus PNA–). The simulated concentrations are averaged over the whole of U.S., the western U.S. (west of  $100^\circ\text{W}$ ), or the eastern U.S. (east of  $100^\circ\text{W}$ ). The concentrations are from the GEOS-Chem simulation for 1986–2006. The \*\* and \* indicate the differences that have passed the two-tail student-t test with 95% and 90% significance levels, respectively.

	Whole U.S.	Western U.S.	Eastern U.S.
PM <sub>2.5</sub>	0.6 (12.2%)**	0.3 (14.0%)**	0.9 (10.8%)**
SO <sub>4</sub> <sup>2-</sup>	0.2 (7.1%)	0.1 (13.5%) **	0.2 (4.0%)
NO <sub>3</sub> <sup>-</sup>	0.2 (30.3%) **	0.1 (28.5%) **	0.4 (33.5%)**
NH <sub>4</sub> <sup>+</sup>	0.2 (14.4%)**	0.1 (15.4%)**	0.2 (13.2%)**
OC	0.05 (6.5%)**	0.03 (8.6%)**	0.08 (5.9%)**
BC	0.03 (10.2%)**	0.01 (8.6%)**	0.05 (11.0%)**

**Table 3.** The composite analyses of horizontal mass fluxes ( $\text{kg s}^{-1}$ ) of  $\text{PM}_{2.5}$  for the selected box of (75–120°W, 28–49°N, from the surface to 100 hPa) in the PNA+ and PNA– months of 1986–2006. The positive values at the four boundaries indicate eastward or northward transport, and negative values indicate westward or southward transport. The positive (negative) value of net flux indicates the net gain (loss) of  $\text{PM}_{2.5}$  in the selected box. All the fluxes are from the GEOS-Chem simulation.

	Boundaries and total	Mass Flux
PNA+	West	89.7
	East	259.3
	South	24.4
	North	–36.2
	Net flux	–109.0
PNA–	West	106.8
	East	272.1
	South	43.7
	North	1.4
	Net flux	–123.0
Diff. (PNA+ minus PNA–)	West	–17.1
	East	–12.8
	South	–19.3
	North	–37.6
	Net flux	14.0

**Table 4.** The pattern correlation coefficients between the composite differences in aerosol concentrations (Fig. 5c) and the corresponding composite differences in meteorological parameters (Fig. 7b). The \* denotes the correlations that have passed the two-tail t-test with 95% confidence level.

	PM <sub>2.5</sub>	SO <sub>4</sub> <sup>2-</sup>	NO <sub>3</sub> <sup>-</sup>	NH <sub>4</sub> <sup>+</sup>	OC	BC
T	-0.13	0.26*	-0.59*	-0.22*	0.07	-0.16
PR	-0.44*	-0.38*	0.04	-0.42*	-0.63*	-0.50*
RH	-0.08	-0.05	-0.02	0.12	-0.32*	-0.36*
WS	-0.27*	-0.1	-0.22*	-0.27*	-0.28*	-0.24*
PBLH	-0.61*	-0.43*	-0.32*	-0.61*	-0.60*	-0.55*

## Figure Captions

**Fig. 1.** The locations of EPA-AQS sites with measurements that meet the criteria described in Sect. 2.1 in the text.  $\text{PM}_{2.5}$  measurements are available for years of 1999–2013 (sites are marked by black dots) and speciated aerosol ( $\text{SO}_4^{2-}$ ,  $\text{NO}_3^-$ ,  $\text{NH}_4^+$ , BC, and OC) concentrations are available over years of 2000–2013 (sites are marked by red diamonds). The grey solid line defines the western United States (west of  $100^\circ\text{W}$ ) and eastern United States (east of  $100^\circ\text{W}$ ).

**Fig. 2.** (a) PNAI for years of 1986–2013 calculated using the NCEP-2 data (NCEP2-PNAI), with the PNA+ and PNA– months during 1999–2013 indicated. (b) PNAI for years of 1986–2013 calculated using the NCEP-2 data, with the PNA+ and PNA– months during 2000–2013 indicated. (c) PNAI for years of 1986–2006 calculated using the GEOS-4 data (GEOS4-PNAI), with the PNA+ and PNA– months over 1986–2006 indicated. Red circles are PNA+ months and blue circles PNA– months.

**Fig. 3.** The absolute ( $\mu\text{g m}^{-3}$ , left column) and relative differences (% , right column) in observed monthly mean aerosol concentrations between PNA+ and PNA– months (PNA+ minus PNA–). The measurements of  $\text{PM}_{2.5}$  were carried out over 1999–2013, in which there were 18 PNA+ months and 18 PNA– months as shown in Fig. 2a. The measurements of speciated aerosols were taken during 2000–2013, in which there were 17 PNA+ and 17 PNA– months (Fig. 2b). The sites with black dots were the differences that passed the two-tail t-test with 90% confidence level.

**Fig. 4.** (a) Simulated surface-layer concentrations ( $\mu\text{g m}^{-3}$ ) of  $\text{PM}_{2.5}$  (the sum of  $\text{SO}_4^{2-}$ ,  $\text{NO}_3^-$ ,  $\text{NH}_4^+$ , BC, and OC) and each aerosol species averaged over NDJFM of 1999–2006. (b) Scatter plots of the simulated concentrations ( $\mu\text{g m}^{-3}$ , vertical axis) versus the EPA-AQS observations ( $\mu\text{g m}^{-3}$ , horizontal axis). Also shown are the  $y=x$  line (black dash line), linear fit for whole U.S. (black line), linear fit for western U.S. (blue line), and linear fit for eastern U.S. (red line). The blue and red dots represent sites in the western and eastern U.S., respectively. (c) Comparisons of the deviation from the mean (DM) of observed concentration (black line) with that of simulated concentration (red line) in each winter month for each aerosol species, left axis. Also shown in the panel for OC (BC) the monthly variation in DM of biomass burning emission of OC (BC), blue line, right axis.

**Fig. 5.** (a) Simulated concentrations ( $\mu\text{g m}^{-3}$ ) of  $\text{PM}_{2.5}$  and each aerosols species averaged over the PNA– months of 1986–2006. (b) The absolute differences ( $\mu\text{g m}^{-3}$ ) in simulated aerosol concentrations between PNA+ and PNA– months (PNA+ minus PNA–). (c) The relative differences (%) in simulated aerosol concentrations between PNA+ and PNA– months. The white spaces in (C) indicate the areas that did not pass the two-tail student-t test with 90% significance level. The seasonal cycles of simulated aerosol concentrations were removed.

**Fig. 6.** (a) Horizontal winds at 700 hPa averaged over the winter months of NDJFM of 1986–2006, and (b) the corresponding differences between the PNA+ and PNA– months. Datasets are from the assimilated GEOS-4 meteorological fields. Also shown in (b) is the domain of (75–120°W, 28–49°N) for which transboundary mass fluxes of PM<sub>2.5</sub> are calculated.

**Fig. 7.** (a) The absolute and (b) relative differences in meteorological parameters between PNA+ and PNA– months. Datasets are from the assimilated GEOS-4 meteorological fields. The white spaces in indicate the areas that did not pass the two-tail student-t test with 90% significance level. The seasonal cycles of meteorological variables were removed, similar to the treatment for observations in Fig. 3.



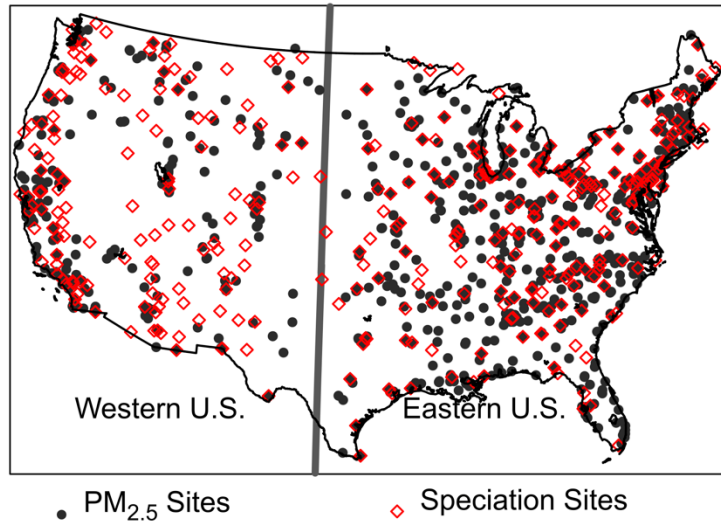


**Fig. 1.** The locations of EPA-AQS sites with measurements that meet the criteria described in Sect. 2.1 in the text. PM<sub>2.5</sub> measurements are available for years of 1999–2013 (sites are marked by black dots) and speciated aerosol (SO<sub>4</sub><sup>2-</sup>, NO<sub>3</sub><sup>-</sup>, NH<sub>4</sub><sup>+</sup>, BC, and OC) concentrations are available over years of 2000–2013 (sites are marked by red diamonds). The grey solid line defines the western United States (west of 100°W) and eastern United States (east of 100°W).

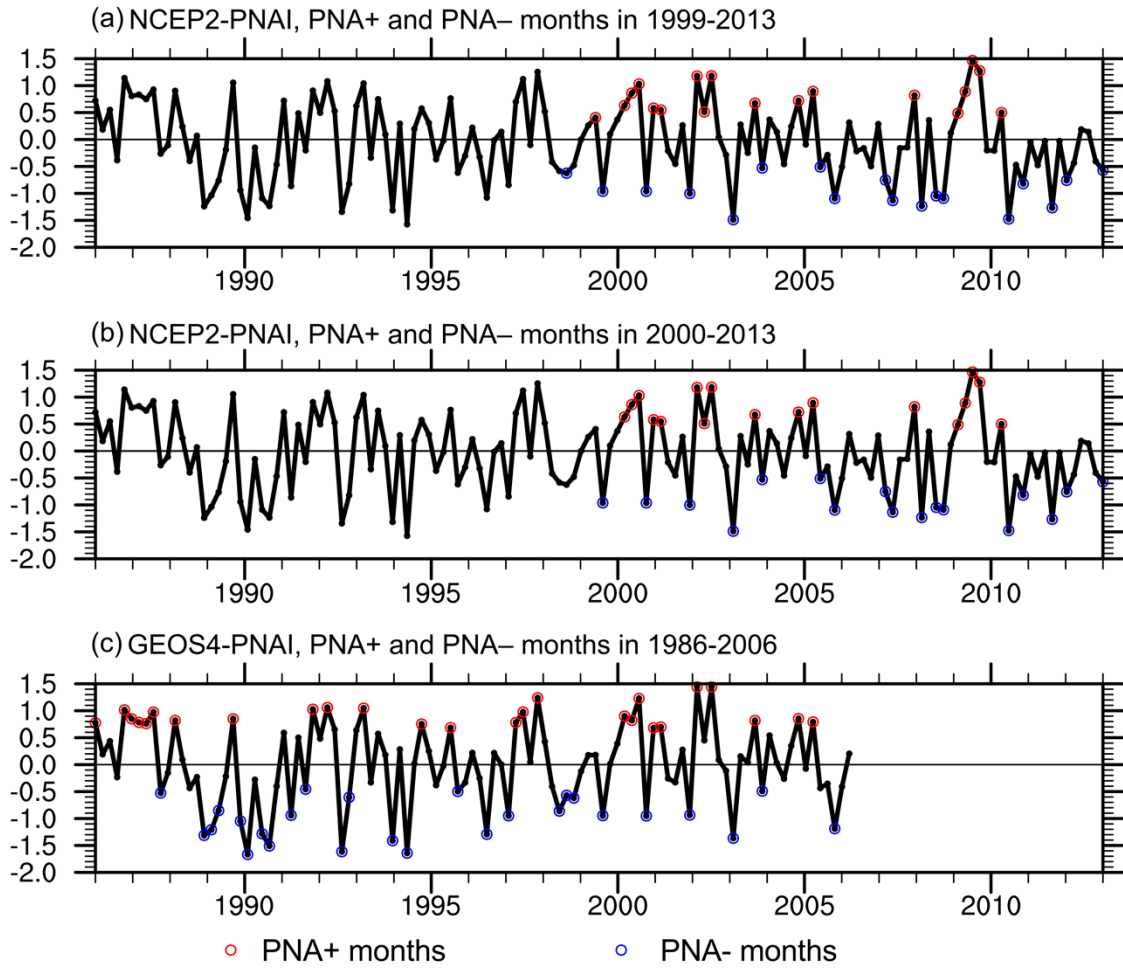


**Fig. 2.** (a) PNAI for years of 1986–2013 calculated using the NCEP-2 data (NCEP2-PNAI), with the PNA+ and PNA- months during 1999–2013 indicated. (b) PNAI for years of 1986–2013 calculated using the NCEP-2 data, with the PNA+ and PNA- months during 2000–2013 indicated. (c) PNAI for years of 1986–2006 calculated using the GEOS-4 data (GEOS4-PNAI), with the PNA+ and PNA- months over 1986–2006 indicated. Red circles are PNA+ months and blue circles PNA- months.

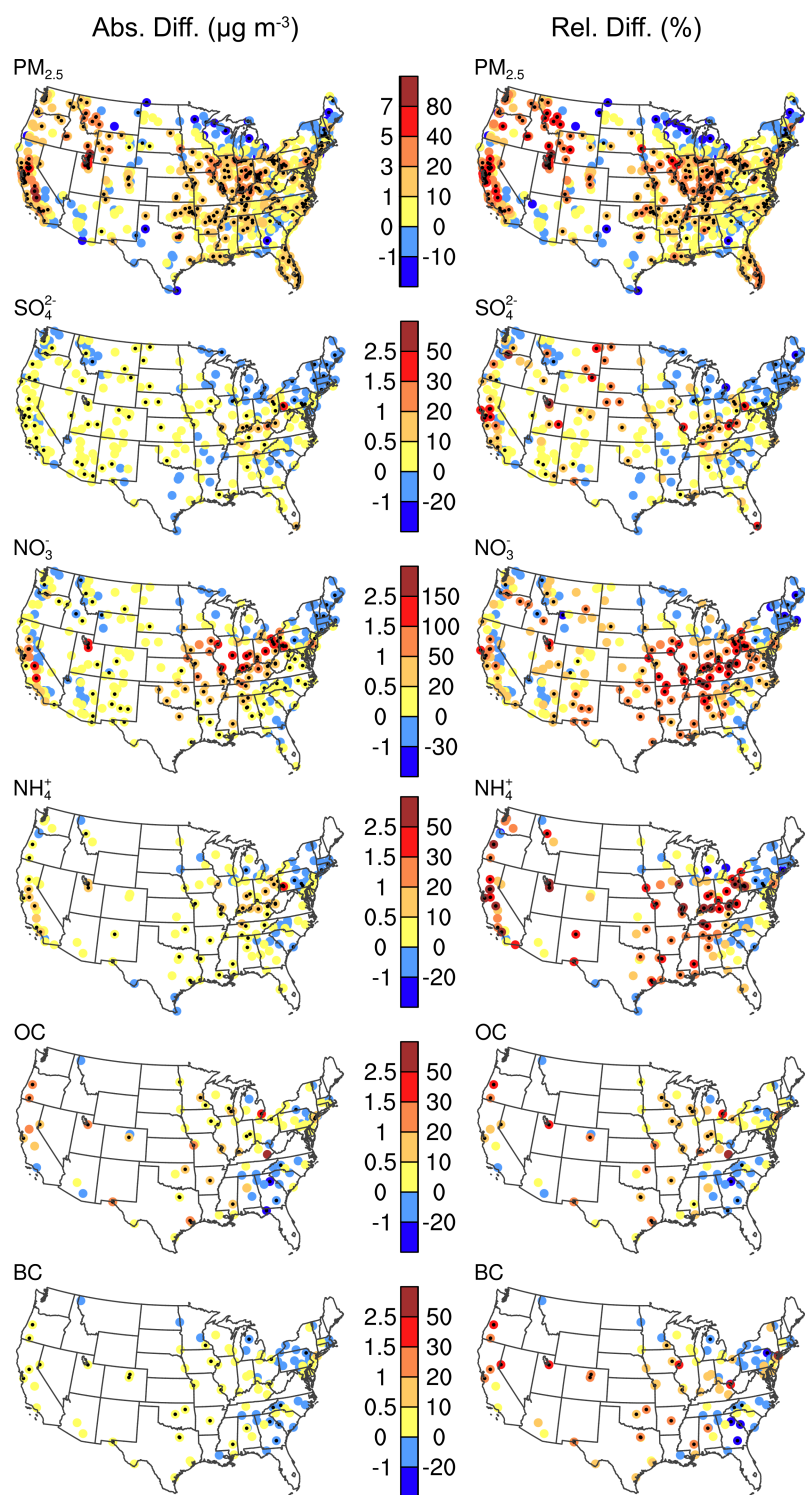


**Fig. 3.** The absolute ( $\mu g m^{-3}$ , left column) and relative differences (% , right column) in observed monthly mean aerosol concentrations between PNA+ and PNA- months (PNA+ minus PNA-). The measurements of  $PM_{2.5}$  were carried out over 1999–2013, in which there were 18 PNA+ months and 18 PNA- months as shown in Fig. 2a. The measurements of speciated aerosols were taken during 2000–2013, in which there were 17 PNA+ and 17 PNA- months (Fig. 2b). The sites with black dots were the differences that passed the two-tail t-test with 90% confidence level.

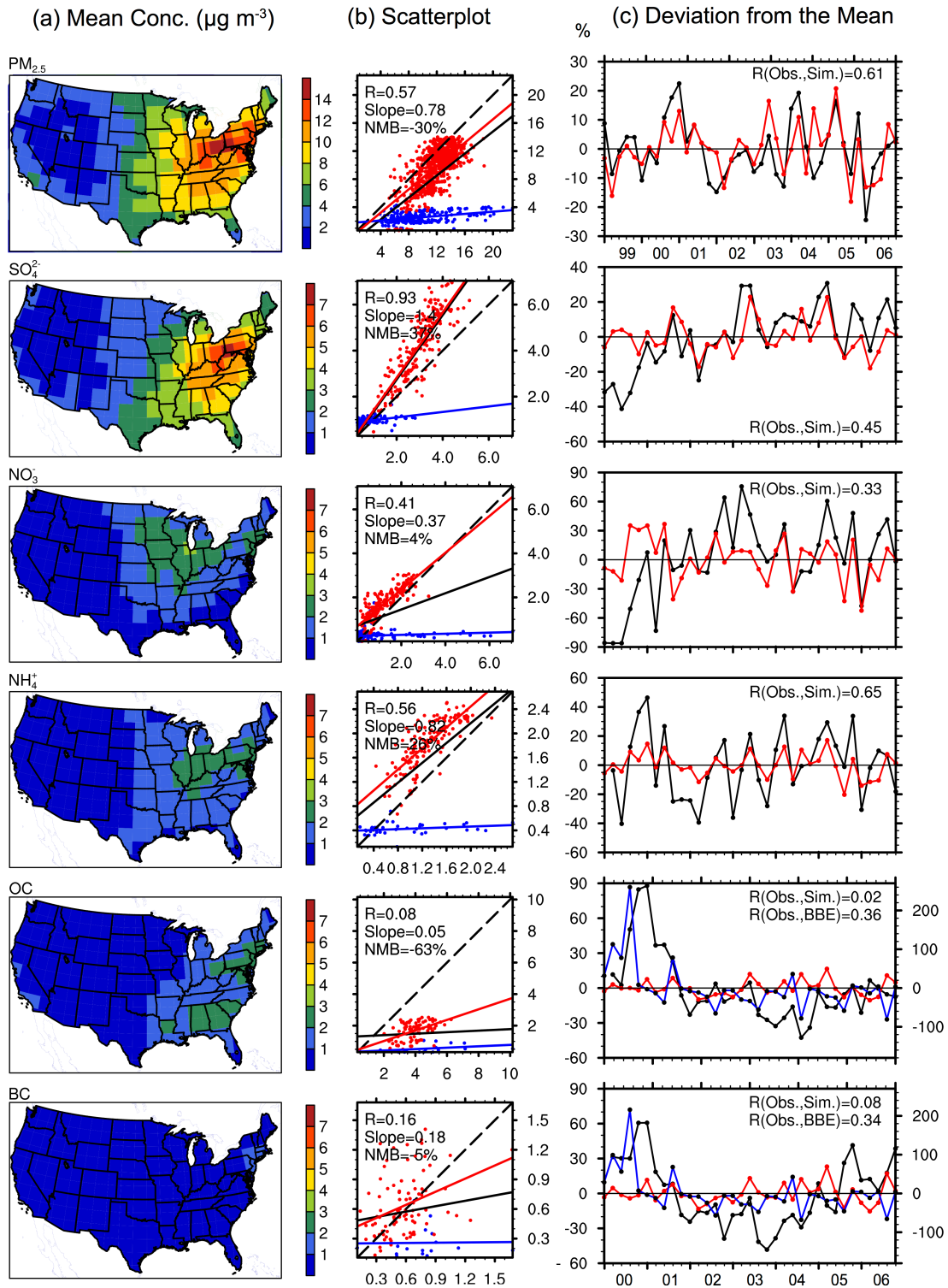


**Fig. 4.** (a) Simulated surface-layer concentrations ( $\mu\text{g m}^{-3}$ ) of  $\text{PM}_{2.5}$  (the sum of  $\text{SO}_4^{2-}$ ,  $\text{NO}_3^-$ ,  $\text{NH}_4^+$ , BC, and OC) and each aerosol species averaged over NDJFM of 1999–2006. (b) Scatter plots of the simulated concentrations ( $\mu\text{g m}^{-3}$ , vertical axis) versus the EPA-AQS observations ( $\mu\text{g m}^{-3}$ , horizontal axis). Also shown are the  $y=x$  line (black dash line), linear fit for whole U.S. (black line), linear fit for western U.S. (blue line), and linear fit for eastern U.S. (red line). The blue and red dots represent sites in the western and eastern U.S., respectively. (c) Comparisons of the deviation from the mean (DM) of observed concentration (black line) with that of simulated concentration (red line) in each winter month for each aerosol species, left axis. Also shown in the

1153 panel for OC (BC) the monthly variation in DM of biomass burning emission of OC  
1154 (BC), blue line, right axis.

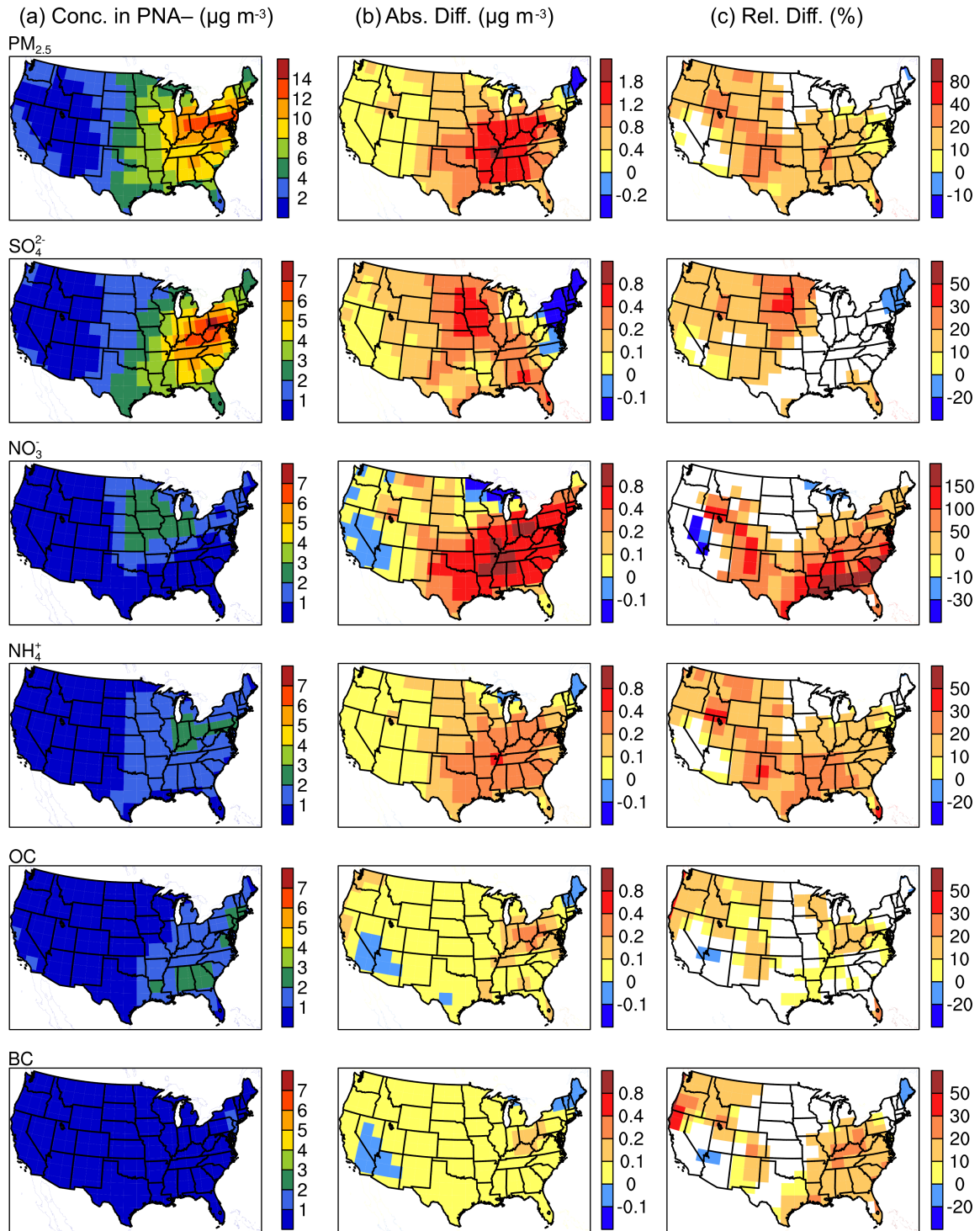
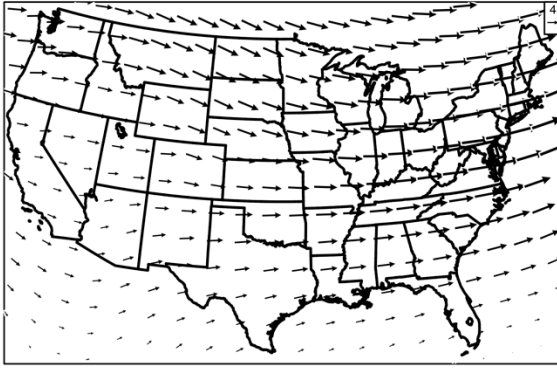


**Fig. 5.** (a) Simulated concentrations ( $\mu g m^{-3}$ ) of  $PM_{2.5}$  and each aerosols species averaged over the PNA- months of 1986–2006. (b) The absolute differences ( $\mu g m^{-3}$ ) in simulated aerosol concentrations between PNA+ and PNA- months (PNA+ minus PNA-). (c) The relative differences (%) in simulated aerosol concentrations between PNA+ and PNA- months. The white spaces in (C) indicate the areas that did not pass the two-tail student-t test with 90% significance level. The seasonal cycles of simulated aerosol concentrations were removed, similar to the treatment for observations in Fig. 3.



(a) UV ( $\text{m s}^{-1}$ ) at 700hPa



(b) UV ( $\text{m s}^{-1}$ ) Diff. at 700hPa

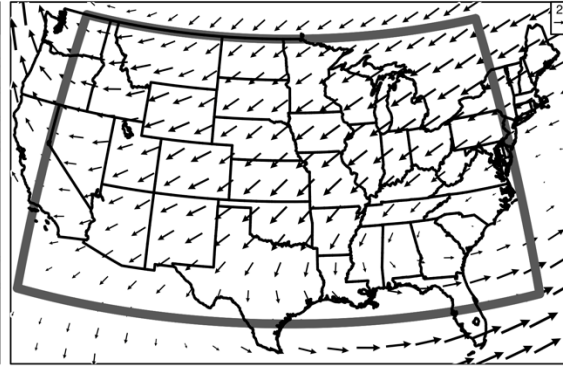


**Fig. 6.** (a) Horizontal winds at 700 hPa averaged over the winter months of NDJFM of 1986–2006, and (b) the corresponding differences between the PNA+ and PNA– months. Datasets are from the assimilated GEOS-4 meteorological fields. Also shown in (b) is the domain of (75–120°W, 28–49°N) for which transboundary mass fluxes of  $\text{PM}_{2.5}$  are calculated.



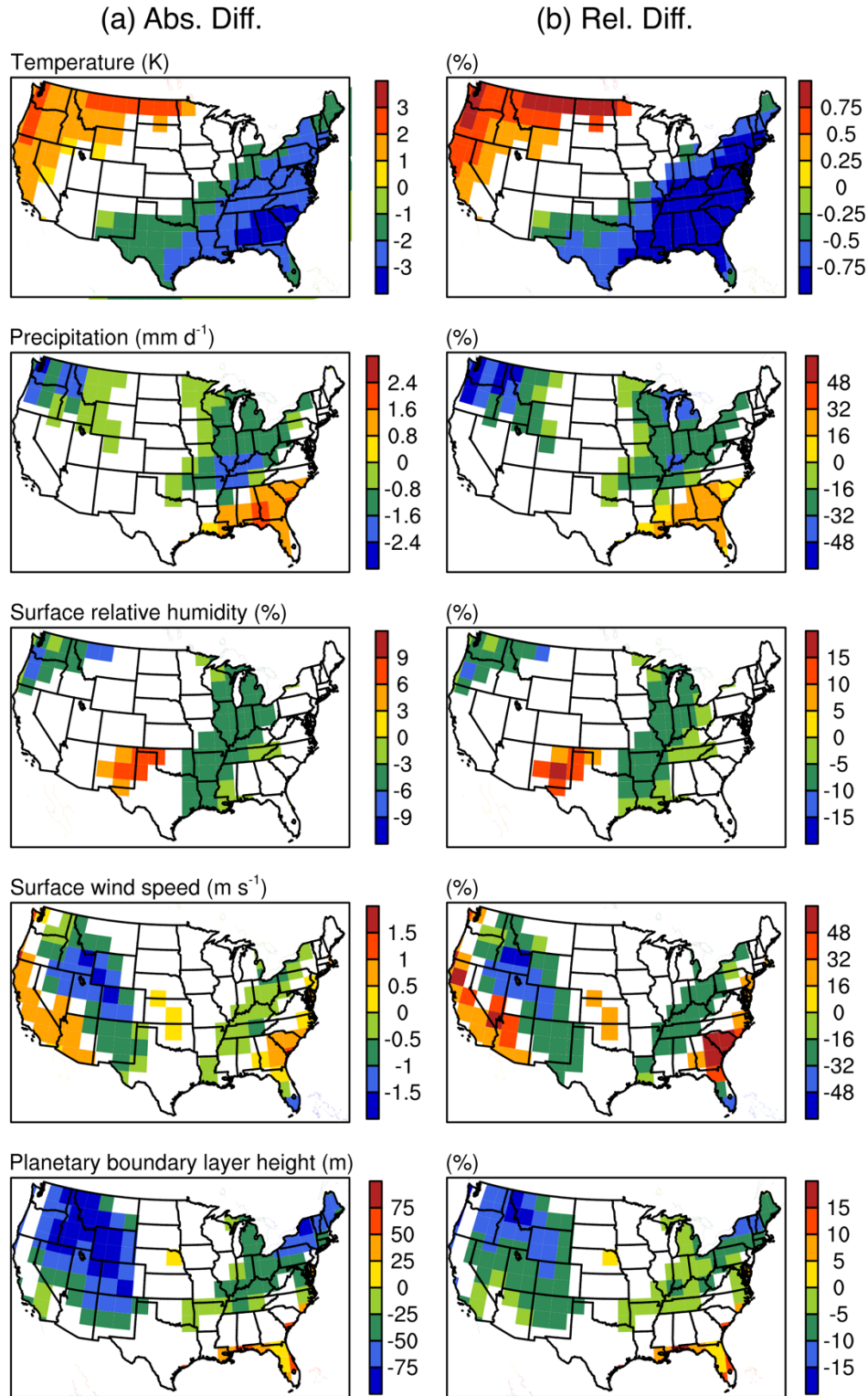


**Fig. 7.** (a) The absolute and (b) relative differences in meteorological parameters between PNA+ and PNA- months. Datasets are from the assimilated GEOS-4 meteorological fields. The white spaces in indicate the areas that did not pass the two-tail student-t test with 90% significance level. The seasonal cycles of meteorological variables were removed, similar to the treatment for observations in Fig. 3.